School of Chemical and Petroleum Engineering

Fuels and Energy Technology Institute

Transformation of Bio-oil during Pyrolysis and Reforming

Yi Wang

This thesis is presented for the Degree of
Doctor of Philosophy
of
Curtin University

September 2012

Declaration

To the best of my knowledge and belief this thesis contains no material previously published by any other person except where due acknowledgement has been made.

This thesis contains no material which has been accepted for the award of any other degree or diploma in any university.

Signature:……

Date:…….....

Abstract

The pyrolysis of biomass is a very effective means of energy densification. With the bio-char returned to the field as a soil conditioner and for carbon bio-sequestration, bio-oil can be used in many ways, including being upgraded into liquid transport biofuels or being used as a feedstock for gasifiers or conventional boilers. However, a number of technical challenges exist during bio-oil applications, such as formation of tar and coke. The fundamental understanding on the transformation of bio-oil under various thermal chemical conversion conditions is essential for the development of novel technologies for the clean utilisation of bio-oil.

Thermal decomposition (pyrolysis) is always the first step in all thermal chemical processes involving bio-oil. The pyrolysis of bio-oil and its separated fractions was carried out in a novel two-stage fluidised-bed/fixed-bed quartz reactor. The results indicated that bio-oil was exceedingly reactive and underwent drastic changes when it was further heated. The evolution of various complex aromatic ring systems was tightly related to the formation of coke and tar. The interactions among the different chemical groups of the bio-oil constituted a unique thermal behaviour of bio-oil.

The behaviour of bio-oil during reforming was studied. The non-catalytic/catalytic steam reforming of above feedstock was conducted respectively. Without catalysts, extra steam supply showed limited effects on tar reforming. Char-supported iron catalyst showed good performance on the reforming of tars produced from the thermal cracking of the bio-oil and its components with steam. The catalytic steam reforming showed obvious effects on the conversion of non-aromatics (e.g. sugars), particularly the large molecules at low temperatures (< 700 °C). With increasing temperature, the catalyst showed good performance on the reforming of aromatic ring systems. The interactions among the species degraded from lignin and cellulose/hemicellulose obviously affected the evolution of aromatic structures during the catalytic steam reforming of bio-oil. The main possible role played by cellulose/hemicellulose-derived species was the provision of additional radicals during the reforming of bio-oil.

Acknowledgements

I would like to give my sincere acknowledgements to my supervisor, Professor Chun-Zhu Li, who gave his expertise, understanding, and patience to my study. During the period of my PhD candidature, he has made numerous valuable comments on my studies. Without his guidance and encouragement, this work would not have been possible. More importantly, the knowledge and philosophy I learned from him will benefit me throughout my life.

My special thanks go to all members in our research institute for their support and advice throughout my candidature. In particular, I would like to thank Professor Hongwei Wu, Dr Zhenghua Min, Dr Shu Zhang, Dr Daniel Mourant, Dr Caroline Lievens and Dr Xun Hu for help and feedback on my studies.

I gratefully acknowledge the financial support for this study from the following sources:

- Australian Government funding through the Second Generation Biofuels Research and Development Grant Program,
- Australian Government funding through the International Science Linkages Program,
- Australian Research Council (DP110105514), and
- Government of Western Australia via the Centre for Research into Energy for Sustainable Transport (CREST).

I also thank Curtin University for awarding me a Curtin International Postgraduate Research Scholarship.

The help and support from all staffs in Fuel and Energy Technology Institute in Curtin University are gratefully acknowledged.

Lastly, I would like to dedicate this thesis to my dear parents, Weifu Wang and Xiaozhen Wang for all their love, support and encouragement in all that I set out to achieve.

Thank you all.

Yi Wang

Table of Content

List of Tables

CHAPTER 1

CHAPTER 2

CHAPTER 3

CHAPTER 5

List of Figures

CHAPTER 1

CHAPTER 2

CHAPTER 3

CHAPTER 4

CHAPTER 5

CHAPTER 6

Chapter 1

Introduction

1.1 Importance of bio-energy in the energy supply mix

1.1.1 Importance of biomass as an energy source

As a result of rapid growth in population and expectance in living standards (gross domestic product), energy and environmental concerns have become the most important global issues. According to the World Energy Outlook [1], the world energy consumption would increase by 53% between 2008 and 2035 at an average annual growth rate of 1.6% (Table 1-1). The fossil fuels (petroleum, coal and natural gas) remain the dominant sources of energy, contributing to the largest portion of the total energy supply in the next 20 years (Figure 1-1) [2].

It is well known that the use of fossil fuels has resulted in many adverse environmental impacts, including air pollution and greenhouse gas emissions. Therefore, the environmental impacts of the increased energy consumption have caused great public concerns. These concerns have promoted the active search for clean renewable energy sources.

Table 1-1. *World energy consumption by regions, 2008-2035* (quadrillion Btu) (based on the data in Ref.1)

Region	2008	2015	2020	2025	2030	2035	Average annual percentage change 2008-2035 (%)
Americas	150.6	157.1	165.2	173.9	184.2	195.5	1.0
Europe and Eurasia	132.7	135	139.2	143.7	147.8	152.2	0.5
Asia	177.1	228.8	257.7	290.6	319.7	345.5	2.6
Others	44.4	52.5	57.5	63.2	69.8	76.7	2.1
World	504.8	573.4	619.6	671.4	721.5	769.9	1.6

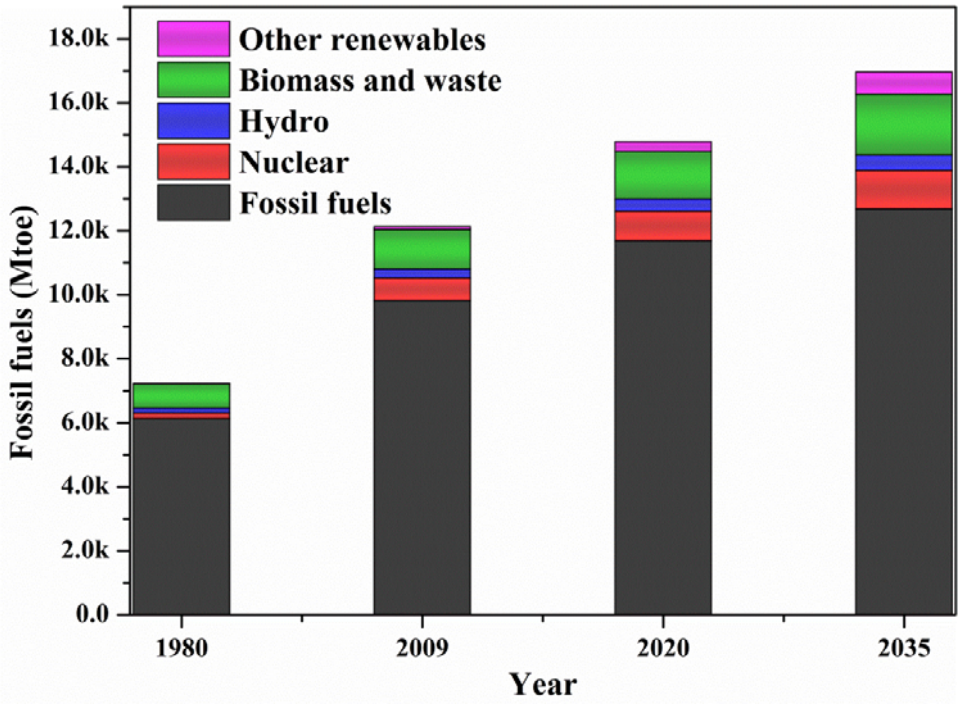

Figure 1-1. World primary energy demand by fuel. (based on the data in [2])

Among all renewable energy sources, biomass has many potential advantages and is currently and will continue to be the biggest contributor to global primary renewable energy market:

1. Compared with other renewable energy sources, biomass has great similarities to fossil fuels. This makes it suitable to be an alternative feedstock for existing fossil-fuel-based energy conversion processes.
2. In principle, biomass utilisation is carbon-free because the CO_2 emitted was previously captured by the biomass plants during the growth.
3. Using biomass could generate much lower emissions of SOx and NOx than fossil fuels.
4. The development of biomass utilisation value chain can spur rural/regional developments.

Therefore, the development of technologies to convert biomass into bio-energy products has the potential to reduce the dependence on fossil fuels and to produce positive environmental and economic benefits.

With this potential, bio-energy is expected to play an important role in the energy

mix. According to the IEA World Energy Outlook 2011 [2], the total world demand for bio-energy would rise from 1230 million tonnes of oil equivalent (Mtoe) in 2009 to about 1911 Mtoe in 2035 at an average annual growth rate of 1.7% (Figure 1-1).

1.1.2 Importance of non-food biomass as a feedstock for bio-energy

Among various type of biomass, many food crops have been arbitrarily used as biomass resources. For example, to produce so-called 1st generation or conventional biofuels (bio-alcohol, biodiesel, vegetable oil and biogas produced primarily from food crops) [3, 4], a large amount of corn and wheat have been converted into ethanol through fermentation. Vegetable oils such as rapeseeds were converted through trans-esterification to produce bio-diesel [4-6]. Consequently, the food-versus-fuel debate revealed: the increase in the production of these fuels was considered as one of the reasons for rising food prices [3, 4, 7]. Additionally, many studies have shown the limited ability for the 1st generation biofuels to achieve targets for significant substitution of petroleum-derived products, climate change mitigation, and economic growth [4, 5].

The cumulative impacts of these concerns have shifted the focus on bio-energy from non-food biomass. Feedstock from non-food biomass materials such as cereal straw, bagasse, forest residues, and purpose-grown energy crops could avoid many of the concerns facing the bio-energy from food crops [4, 5]. These biomass materials are all belonging to lignocellulosic biomass, a generic term referring to plant biomass composed of lignin, cellulose and hemicellulose. Lignocellulosic biomass is generally grouped into four main categories: agricultural residues, dedicated energy crops, wood residues, and paper waste. Many research results have shown the great potential of lignocellulosic biomass to be a renewable energy source [3, 4, 8-10].

In this study, as a non-food crop, mallee has been selected as a renewable energy source with many additional advantages:

1. Mallees can be planted to manage the dry-land salinity, because they are highly effective at using rainfalls and at drawing down groundwater table,

thus preventing salt rising to and accumulating in the lower landscape positions [11, 12].

2. Mallees can be planted in narrow belts, taking less than 10% of farmlands, while still achieving effective control of dry-land salinity spread. Additionally, the enhanced productivity of food crops over the whole farm will compensate for the land allocated to mallees. More importantly, the growth of mallee does not require supplemental water supply [11, 12].
3. Mallee trees can be first harvested about 5 to 6 years after establishment. They then re-grow as coppice from the cut stump for subsequent harvests on short cycles (3 to 5 years) [12].
4. Mallee can store more than 40 unit of energy for every unit of energy input (excluding solar energy), and has an energy productivity of 206.3 GJ/ha/year. This energy performance is greatly better than those achieved by other annual energy crops (e.g., canola, which have energy ratios typically less than 7.0 and energy productivity less than 40.0 GJ/ha/year) [8].

In short, lignocellulosic biomass has the great potential to produce renewable energy without impacting the food supply.

1.1.3 Conversion technologies for lignocellulosic biomass

Lignocellulosic biomass can be converted into energy products through two main pathways: biological or thermochemical, as is shown in Figure 1-2 [13-20]. In biochemical pathway, enzymes are used to convert cellulose and hemicellulose components of the feedstock to sugars which can be used to produce ethanol by fermentation [5]. Thermochemical process converts biomass into bio-energy by thermal decomposition and chemical reformation, involving heating biomass in the presence of different concentration of oxygen. The most important advantage of thermochemical process is that it can convert all the organic components of the biomass feedstock, while biological processes focus mostly on the sugar compounds. This thesis hereafter mainly focuses on the thermochemical conversion processes.

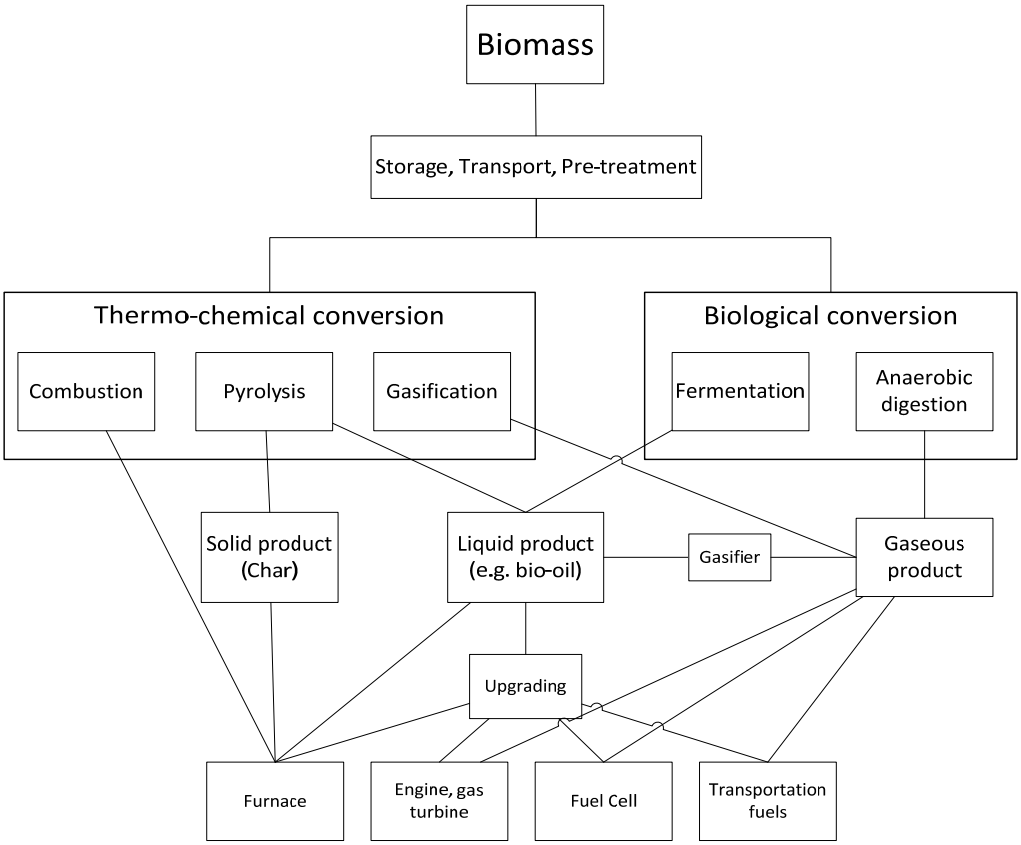

Figure 1-2. Common routes for the conversion of biomass [13-20].

Compared with other renewable energy sources, lignocellulosic biomass has great similarities to fossil fuels. Many existing fossil-fuel-based energy conversion processes are available for lignocellulosic biomass conversion with small modification. Thermochemical conversion process includes mainly combustion, pyrolysis and gasification [3]. These technologies are in varying stages of development. While combustion is most developed, gasification and pyrolysis are becoming more and more important.

1.1.3.1 Pyrolysis

Pyrolysis is the thermochemical decomposition of the feedstock by heating it in an inert atmosphere (without oxygen or a very limited amount of oxygen) up to a certain desired temperature. It is always the first step in gasification or combustion where partial or complete oxidation of the primary products follows [21]. Depending on the operating conditions, pyrolysis may be slow or fast pyrolysis [22]. However, the

terms “slow pyrolysis” and “fast pyrolysis” are slightly arbitrary and have no precise definition of the residence times or heating rates involved in each [23].

The pyrolysis of biomass takes place in a very complex set of physical processes (mass and heat transfer) and chemical reactions, resulting in the production of gases, vapour and solid (always is defined as “char”). A part of the vapour can be condensed to a liquid, which is normally termed as “bio-oil”. The observed product distribution depends strongly on many key factors of this process such as heating rate, final temperature, residence time of the vapours and condensing system [16, 18, 22, 24-26]. Some typical product distributions from different pyrolysis technologies are shown in Table 1-2.

Conventional or slow pyrolysis has been applied for thousands of years to produce charcoal [22, 23]. In slow pyrolysis, biomass is heated up to about 500 °C at a relatively slow heating rate (< 50 ℃/min). The vapour residence time varies from 5 min to 30 min. A higher yield of solid carbonaceous materials (char) can be obtained from slow pyrolysis than that from fast pyrolysis [22, 23, 27].

Fast pyrolysis is a process in which biomass is rapidly heated in the absence of oxygen. Biomass decomposes to generate vapours, non-condensable gases, and char. Bio-oil can be collected by cooling and condensation of the vapours. Generally, fast pyrolysis of biomass can produce 40-70 wt.% of liquid bio-oil, 15-35 wt.% of solid char, and 10-25 wt.% of non-condensable gases, depending on the feedstock used. Thus, fast pyrolysis is mostly used to produce high yield of bio-oil. There are four essential features of a fast pyrolysis process that need to be controlled carefully to give high liquid yields [16, 18, 22, 24-26, 28]:

Table 1-2. Product distribution from different pyrolysis technologies (based on the data in Refs.16, 18, 22, 24-26, 28)

Pyrolysis technology	Process conditions			Products		
	Residence time	Heating rate	Temperature	Char	Bio-oil	Gas
Slow pyrolysis	days	<10 ℃/min	~400 ℃	~35%	~30%	~35%
	5-30 min	<50 ℃/min	400-600 ℃	~20%	~50%	~30%
Fast pyrolysis	0.5~5 sec	~1000 ℃/s	400-600 ℃	~20%	~60%	~20%
	<0.5 sec	>1000 ℃/s	800-1000 ℃	~10%	~10%	~80%

1. Very high heating and heat transfer rates are needed, which are usually realised by a finely ground biomass feed.

2. A carefully controlled pyrolysis reaction temperature is used, often in the 425-550 °C range.

3. Short vapour residence times are used (typically < 2 s).

4. Pyrolysis vapours are rapidly cooled to give bio-oil.

To achieve these parameters, many reactors have been designed in different configurations, such as fluidised bed reactors, ablative reactors, vortex reactors and the rotating cones reactors [10, 16, 22, 24, 25, 29].

1.1.3.1.1Bubbling fluidised-bed reactors and circulating fluidised beds reactors

Bubbling fluidised bed pyrolysis is a well-understood technology [22]. In the reactor, sand is often used as the solid phase of the bed. With the high solid density in the bed, it has a potential to provide good temperature control and efficient heat transfer to biomass particles. The residence time of char and vapour is partly controlled by the fluidising gas flow rate. However, char has a higher residence time

than the vapour. Thus, char can be a possible vapour cracking catalyst at fast pyrolysis reaction temperatures. Mostly, char does not accumulate in the fluidised bed, but it is rapidly elutriated. Therefore, one or more cyclone separators are always used to separate char rapidly and effectively from ejection. To produce good quality bio-oil with a high liquid product yield from bubbling fluidised bed, a careful design of sand and biomass/char hydrodynamics in the reactor, including a precise selection of sand particle size, biomass particle size and gas velocity is needed [21-23, 27].

A circulating fluidised bed reactor is another variation of the fluidized bed reactor. Higher gas flow rates are used to entrain the bed material and char out of the reactor into a cyclone separator. Combustion of char mixed with the sand can supply heat to the sand which is then recirculated into the reactor. The vapour exits the cyclone and enters a condensation system. An advantage of circulating fluidised bed reactors is that they are suitable for very large throughputs. But, their heat transfer rates are not particularly high, because they are dependent primarily on gas-solid convective heat transfer [21-23, 27].

1.1.3.1.2 Ablative pyrolysis reactors

Ablative pyrolysis relies on a heated surface in which wood is pressed against and moved rapidly leaving an oily film which then evaporates. An important feature of ablative heat transfer is that when biomass comes into contact with the hot solid, ablation occurs and exposes fresh biomass to the hot surface. This allows for no limit on particle size in certain ablative reactors. The limiting factor is the rate of heat supplied to the reactor. With this feature, ablative pyrolysis reactors can be intensive (can process large amounts of biomass in little volume), compact, and do not require carrier gases. There are two main disadvantages. One is that it requires a surface area controlled system and operates with moving parts at high temperatures. Another one is that micro-chars are produced which are difficult to remove from the vapour phase, resulting in the contamination of the liquid product [21-23, 30].

1.1.3.1.3Vortex and cyclone reactors

Vortex and cyclone reactors use a flow of high velocity gas to suspend the particles of biomass. A tangential introduction of these gases into the reactor uses

centrifugal actions to force the particles against the heated walls of the reactor. Even though both of these reactors are inherently mechanically simple, they require motive gas in large volumes compared to the volume of the biomass feed [21-23, 30].

1.1.3.1.4 Rotating cone reactors

The rotating cone reactors are relatively a recent development and effectively operate as a transported bed reactor, but with transport effect by centrifugal forces in a rotating cone rather than gas. Wood particles fed to the bottom of the rotating cone together with an excess of inert heat carrier particles (e.g. sand) are converted while being transported spirally upwards along the hot cone wall. The most important advantages of the atmospheric rotating cone technology are its high selectivity towards bio-oil and absence of diluting gas. The bio-oil yield is comparable to the yields of other high bio-oil yield production technologies [21-23, 30].

1.1.3.2 Gasification

Gasification is basically a thermochemical process which converts carbonaceous materials into gas by a gasifying agent such as air, oxygen or steam [13]. The process of gasification has two main steps:

1. Pyrolysis/thermal decomposition of carbonaceous feedstock into gases, vaporised tars and solid char.

2. Gasification of these products by reacting with gasifying agent such as air, steam or oxygen.

Pyrolysis occurs firstly, the relative yields of gas, tar and char depend on the heating rate and final temperature. Generally, pyrolysis proceeds at a much more rapid rate than char gasification, which is the rate controlling step. At higher temperature (> 700 ℃), the products of pyrolysis then react with the gasifying agents (e.g. steam) to generate permanent gases (CO, CO_2, H_2 and other lesser quantities of hydrocarbon gases). The composition of product gas is influence by many factors, including the feed composition, water content, reaction temperature and residence time.

Biomass is particularly suitable for gasification due to its high volatile yield and low aromatic content. The result of biomass gasification is the syngas, containing carbon monoxide, hydrogen, methane and some other inert gases. Syngas can be used as a fuel for furnace or boiler to produce heat and electricity [17], and can be synthesised into liquid fuels (e.g. through Fischer-Tropsch synthesis) [21]. H_2 can be enriched by upgrading syngas through water-gas-shift reaction [31]. Overall, the energy conversion efficiency of gasification of biomass has been proved much higher than that of combustion [32].

However, many technical barriers need to be tackled before biomass gasification becoming a commercial renewable energy technology. The most significant one is the presence of tar in the product gas [33-35]. Tar is an undesirable product of biomass gasification, usually containing the condensable fraction of organic gasification products. The composition of tar varies with the feedstock and gasification conditions especially temperature. Tar can cause the plugging of downstream equipment and the poisoning of catalyst, resulting in a decline in efficiency as well as a rise in maintenance costs. Therefore, the aspect of tar cracking or removal in gas clean-up is one of the most important technical uncertainties in the implementation of biomass gasification [33].

Generally, tar can be removed from the gaseous products by physical separation (e.g. filtrations and scrubbing), thermal cracking and catalytic reforming processes [36]. Physical separation requires a cooling step until the gas reaches ambient temperature, resulting in large amounts of energy loss in the whole process. Additionally, scrubbing process produces large amounts of wastewater, which need additional treatments or recycle systems at downstream. Thermal cracking has low efficiency for tar removal unless the temperature is higher than 1000 ℃ which is much higher than common gasification temperature. It needs much energy supply and decrease the energy efficiency of the process. Catalytic reforming is the commonly accepted as an economical way to deal with tar, because it can convert tar into syngas at relative low temperature [32-35].

Many catalysts have been developed for tar reforming [34, 35, 37, 38]. Unfortunately, most of the catalysts were either not effective enough or not affordable. For example, dolomites were used for tar elimination with high activity

and low cost. However, as a result of fragility, they are very soft and quickly eroded in fluidised beds [39]. Although zeolites and olivine are also inexpensive, they can be deactivated easily by coke deposition [40, 41]. Nordgreen et al. [42, 43] used elemental and metallic iron as catalysts for tar reforming during gasification of biomass in a fluidised bed. However, iron can be deactivated rapidly by coke in the absence of hydrogen. With high activity for converting tar to syngas, Ni-based catalysts have been widely used in biomass gasification [37, 38]. Nevertheless, Ni-based catalysts are expensive and hardly regenerated, limiting the use for industrial application [37].

Among these catalysts, the char or char-supported iron catalyst have shown adequate catalytic activities and have highly economic feasibility used to reform tar during gasification of biomass/coal [34]. Hayashi et al.[44] reported that the tars from the pyrolysis of brown coal could be eliminated by using char inherently containing AAEM (alkali and alkaline earth metallic species) as a catalyst at the temperatures higher than 900 °C. The catalytic activity could be greatly improved if the char was loaded with some catalytically active species. Min et al.[34] investigated char-supported iron catalyst and ilmenite used for the steam reforming of biomass tar derived from the pyrolysis of mallee wood *in situ*. Their results indicated that the char-supported iron catalysts exhibited much higher activity for the reforming of tar than ilmenite and the H-form char catalysts.

1.1.3.3 Combustion

Combustion is the sequence of exothermic chemical reactions between a fuel and an oxidant accompanied by the production of heat and conversion of chemical species [3]. The combustion process essentially has three main steps: pyrolysis, gasification and combustion. In industry, the combustion of fossil fuels using a boiler to produce heat is a mature technology. With great similarities to fossil fuel, biomass can be used as a feedstock for combustion. Biomass has many clear advantages over fossil fuels for combustion. The most important one is that the carbon dioxide emitted from biomass combustion was previously captured by the biomass plants during their growth through photosynthesis. Additionally, biomass combustion could generate much lower emissions of pollutants (e.g. NOx, SOx and particulates) than fossil fuels. However, fuel quality and consistency can vary significantly by using

biomass as a feedstock, which is a serious drawback for biomass combustion.

Amongst the conversion technologies discussed in this section, fast pyrolysis has attracted particular interest as it is a very effective way of energy densification. While the bio-char is returned to the field as a soil conditioner and for carbon bio-sequestration, bio-oil can be transported and stored more easily than bulky biomass. Subsequently, it can be used in many ways, including being upgraded into liquid transport biofuels or being used as a feedstock for gasifiers or conventional boilers [15, 19, 20, 45, 46].

1.2 The importance of bio-oil in the thermal chemical conversion

1.2.1 Advantages of bio-oil

As discussed in the last section, bio-oil can be produced from the fast pyrolysis of biomass. As an intermediate energy carrier, bio-oil has many advantages compared to the use of biomass directly:

1. Bio-oil is a liquid product from the pyrolysis of biomass. During pyrolysis, part of chemical energy contained in bulky biomass can be concentrated into a denser liquid form. Thus, the volumetric energy density is increased about four times after this transformation [47]. This makes the transportation of bio-oil much more effective and economical than that of biomass.

2. Bio-oil is stable against biological decomposition and cannot ignite at ambient temperature, simplifying the storage requirement.

3. Bio-oil is easier than original biomass for further applications, particularly when high pressure processes are designed.

With these advantages, bio-oil produced from distributed pyrolysis units can be

transported to a centralised bio-refinery. Subsequently, it can be converted into many types of fuels or chemicals.

1.2.2 Bio-oil physical and chemical characteristics

Bio-oil, also known as pyrolysis oil, pyrolysis liquid, is usually dark brown, free flowing and has a distinctive smoky odour [22, 48, 49]. The basic chemical and physical properties of bio-oils originated from different biomass feedstock are well documented in the literature [18, 22, 48, 49]. Some typical physical properties of bio-oil are summarised in Table 1-3.

Bio-oil contains a high content of oxygen, resulting in a high polarity and immiscibility with hydrocarbons. The high oxygen content also affords the bio-oil a lower heating value than conventional fuel oils.

Water in the bio-oil is not only from original water in the biomass but also from the dehydration of biomass components, during its pyrolysis. With additional water, bio-oil can be separated into two phases: an aqueous phase and a heavy organic phase [26, 48, 50, 51].

Table 1-3. Bio-oils properties [16, 26, 47, 52, 53]

Properties		Typical values	Mallee wood oil, used in this study [47, 53]
Water content (wt %)		15-30	19.0
pH		2.0-3.8	2.5
Elemental Composition (wt %)	C	48.0-63.5	48.4
	H	5.2-7.2	6.3
	N	0.07-0.39	0.1
	O	32-46	45.2
HHV (MJ/Kg)		15-24.3	19.03
Viscosity (cp, at 20 ^{o}C)		50-672	Not determined
Ash yield (wt%)		0.03-0.3	0.09
Density (kg/dm^3)		~1.2	1.18

The molecular weights of the compounds in the bio-oil vary over a wide range, from values as low as 18 g/mol for water to values as high as a few thousands g/mol for oligomers [54].

Bio-oil has a very complicated chemical composition, containing hundreds or thousands of compounds with a wide range of functionalities such as carboxylic acids, hydroxyl aldehydes, hydroxyl ketones, alcohols, esters, furan/pyran ring derivatives, sugars/anhydro sugars, phenolic compounds and lignin derived oligomeric compounds. (Table 1-4) [48, 55]. These species in bio-oil have originated from the thermal decomposition of biomass components such as lignin, cellulose and hemicelluloses as well as the interactions among the intermediates from these biomass components. Therefore, the identification and quantification of these compounds, particularly with high molecular masses, are very difficult missions by using current analytical techniques.

Many researchers have been studying the bio-oil compositions using various

methods and analytical instruments [10, 54-60]. Gas Chromatography-Mass Spectrometry (GC-MS) analysis has often been used to identify various compounds present in bio-oil; however this technique is limited to the compounds that have sufficient volatility. Along with GC-MS, Fourier Transform Infrared (FTIR) spectroscopy, Nuclear Magnetic Resonance (NMR) spectroscopy, High Performance Liquid Chromatography (HPLC) including Gel Permeation Chromatography (GPC) has also been used for qualitative characterization of bio-oil.

Generally, as shown in Figure 1-3, only 40 % of the bio-oil can be detected by gas chromatographic (GC) analysis. About 15 % of the bio-oil, containing polar and non-volatile compounds, is only accessible by HPLC analysis. A significant amount (about 20 %) of the bio-oil is the high molecular fraction. This fraction is often obtained by introducing additional water. The characterization of this fraction has been extensively studied via various analytical methods [50, 56-59]. These studies have revealed that this fraction contains various oligomers mainly originating from degradation of lignin [9].

The lignin-derived oligomers constitute an important part of bio-oils, and they have negative effects on bio-oils physical and chemical properties, such as viscosity and stability. In addition, these compounds show responsibility for many operating problems during the thermal conversion of bio-oil. For example, due to their longer burn-out time, the formation of soot and high NOx-emission can occur as a result of incomplete combustion [56].

Table 1-4. Main chemical compounds of raw bio-oil (used in this study) determined by GC-MS [51]

No.	Compounds	No.	Compounds
1	Water	11	2-Methoxy-4-(2-propenyl) phenol (Eugenol)
2	1,3,5 Trioxane	12	2,6-Dimethoxy phenol (Syringol)
3	1-Hydroxy-2-propanone	13	4-Methoxy-3-(methoxymethyl) phenol
4	Acetic acid	14	2,6-Dimethoxy-4-(2-propenyl) phenol
5	Furfural	15	2-acetate-1,3-dimethoxy-5-(1-propenyl)-Benzen
6	2(5H)-Furanone	16	4-Hydroxy-3,5-dimethoxy benzaldehyde (Syringaldehyde)
7	1,2-Cyclopentanedione	17	1-(4-Hydroxy, 3,5-dimethoxyphenyl) ethanone
8	2-Hydroxy-3-methyl-2 -cyclopenten-1-one	18	Desaspidinol
9	2-Methoxy phenol (Guaiacol)	19	1,6-Anhydro-β-d-glocopyranose (Levoglucosan)
10	2-Methoxy-4-methyl phenol	20	3,5-Dimethoxy-4-hydroxycinnamalde

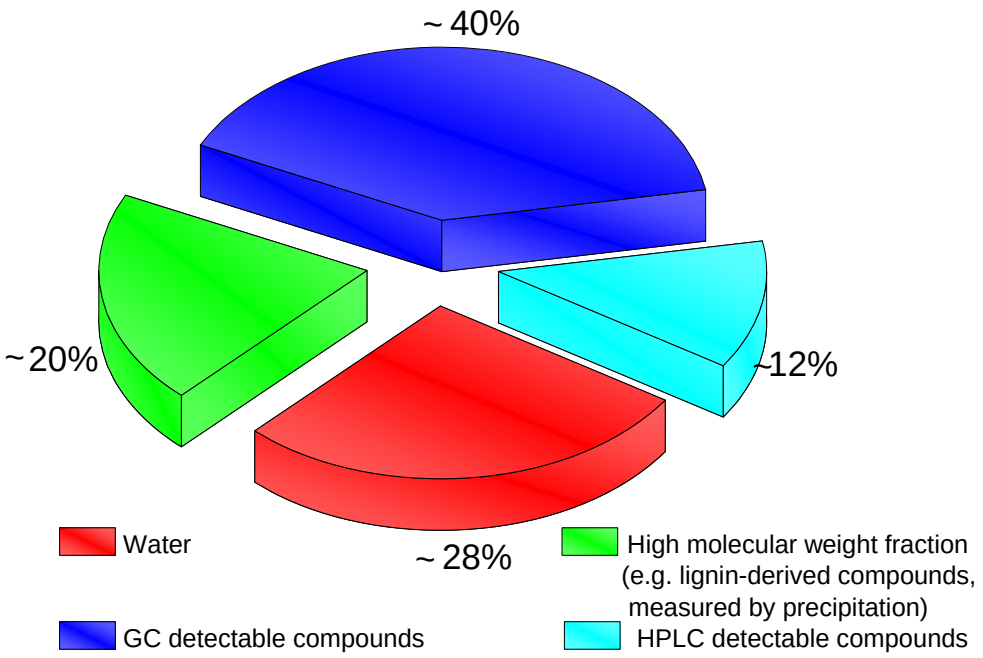

Figure 1-3. Typical portions of fractions in bio-oil [22, 56, 60].

1.2.3 Production of bio-oil

The principles of pyrolysis and various fast pyrolysis reactors have been reviewed in Section 1.1.3.1. It is clear that the fast pyrolysis of biomass is an effective way to produce bio-oil. Many studies [16, 22, 24-26, 29] have been conducted to maximise the yield of bio-oil. Regardless of the type of original biomass, a high heating rate, a short residence time of vapour and moderate temperatures (400-600°C) are considered as the essential parameters to obtain a high liquid yield in a range of 60-70 wt % from the pyrolysis of biomass.

Instead of pursuing high bio-oil yields alone, to ensure the profitability and reliability of bio-oil refinery, the bio-oil quality has attracted increasingly more attention recently [18, 48, 61]. The quality of bio-oil is determined by its physicochemical properties and therefore its chemical composition. Hence, many studies have been done to study the effects of intricate factors influencing on the the chemical composition of product bio-oil.

For example, Garcia-Perez, Shen, Mourant, Min and co-workers pyrolysed mallee biomass by using a fluidised-bed reactor and reported the effects of various factors on the properties of the bio-oil [16, 24-26, 62]. Many analytical techniques such as GC-MS, Karl Fischer titration, solvent extraction, thermogravimetric analyses (TGA), FTIR spectroscopy and UV-fluorescence spectroscopy, were used to follow the evolution of bio-oil chemical composition.

Garcia-Perez and co-workers reported the configuration of this pyrolysis system and the effect of temperature on the yield and composition of the bio-oil from the pyrolysis of mallee wood [16, 26]. From this study, it is learned that the increases in bio-oil yield with increasing temperature from 350 to 500 °C were mainly due to the increases in the production of lignin-derived oligomers insoluble in water but soluble in CH_2Cl_2. The maximum bio-oil yield could be obtained at about 475 °C. The bio-oil produced at this temperature had almost the highest content of oligomers and, consequently, the highest viscosity. The bio-oil samples were characterised with TGA. The DTG curve was then curve-fitted with six Gaussian peaks to represent six families/groups of chemical compounds in the bio-oil. The effects of pyrolysis

temperature on the evolution of each family have been studied by comparing the DTG curves of bio-oils produced at different temperatures.

Shen and co-workers reported the effects of particle size on the yield and composition of the bio-oil [25]. Eight mallee woody biomass samples with different particle sizes (0.18–5.6 mm) were pyrolysed in a fluidised-bed reactor at 500 °C. From this study, it is learned that the actual heating rates experienced by biomass, which decrease with increasing particle size, were a major factor contributing to the decreases in the yield of lignin-derived oligomers, resulting in decreases in the yield of bio-oil with increasing average biomass particle size from 0.3 to about 1.5 mm. By comparing the DTG curves of oil samples, the pyrolysis of small biomass particles gave lower yields of light bio-oil components and higher yields of heavy components than the pyrolysis of large biomass particles.

Mourant and co-workers reported the effects of alkali and alkaline earth metallic species on the yield and composition of bio-oil [24]. The mallee wood sample was washed with water and a dilute acid before pyrolysis. By this pre-treatment, AAEM species in the wood were differentiated into two forms: water-soluble and water-insoluble but acid-soluble. By different periods of washing, the concentrations of AAEM species were different. From this study, the effect of this pre-treatment on the yield of bio-oil is not significant. However, the composition of bio-oil was drastically affected by the removal of AAEM species, especially the water-insoluble but acid-soluble AAEM species (especially Ca). For example, compared with the bio-oil from raw mallee wood, the yields of sugars and lignin-derived oligomers increased significantly at the expenses of the yields of water and light organic compounds in the bio-oil from pre-treated biomass.

Min and co-workers studied the pyrolysis behaviour of mallee leaves in the same fluidized-bed reactor at temperatures ranging from 300 to 580 °C [62]. The composition of wood and leaf is shown in Table 1-5. As expected, the yields and composition/properties of bio-oils from leaves were quite different from those obtained from the pyrolysis of the woody fraction of the same mallee tree species. Comparing with the wood bio-oil, the bio-oils from the leaves contained less compounds [(e.g. levoglucosan, acids (especially acetic acid) and aldehydes] originated from thermal degradation of cellulose and hemicelluloses, due to the low

contents of these components in leaves (compared with wood). Eucalyptol was the most abundant simple compound identified in the liquid product, resulting in a much higher concentration of water-insoluble compounds in leaf bio-oils than in wood bio-oils. Although similar contents of lignin existed in leaves and wood, the composition of phenolic compounds were not identical in their bio-oils. The different structure of the lignin in leaves and wood might be the reason.

In short, it is evident that several factors such as lignocellulosic composition of biomass, the presence of minerals, reaction temperature, heating rate and residence time have effects not only on the yield but also the chemical composition of bio-oil [63-65].

Base on the better understanding of effects of abovementioned factors, many new processes and operational strategies [chemical, physical and physicochemical pre-treatments of biomass prior to the pyrolysis, changing pyrolysis conditions and catalytic pyrolysis (can be considered as in-situ upgrading)] for biomass pyrolysis have been developed to manage the quality of the product bio-oils by controlling the concentrations of target species in bio-oils [18, 21, 22, 66].

Table 1-5. Contents of lignin, hemicellulose, cellulose and extractives in mallee wood and leaves [62]

	Wood	Leaf
Lignin (wt.%)	24.9	25.9
Hemicellulose (wt.%)	40.7	14.8
Cellulose (wt.%)	22.2	14.6
Extractives (wt.%)	12.2	44.7

1.2.4 Bio-oil applications and their problems

Bio-oil has the potential to be a substitute for fuel oil in many conventional applications, such as boiler, gasifier, engines and turbines. Bio-oil also contains various chemical compounds, making it possible to produce chemicals. The applications for bio-oil have been well reviewed in the literatures, and are depicted generally in Figure 1-4.

However, during these applications of bio-oil, many operating problems have been reported.

Although bio-oil is combustible, its chemical and physical properties adversely affect its combustion, resulting in a series of operating challenges [18, 67, 68]. Bio-oil, containing high water, oxygen contents and aromatics, is very reactive. Once it is heated up, polymerization may occur, resulting in the formation of large molecules [9, 18, 51, 54]. The formation of these large molecules can increase the ignition temperature and decrease the volatility of bio-oil. As a result of its decreased volatility, the incomplete combustion may occur, which can cause many problems such as soot formation and pollutant emissions [18, 67, 68].

Besides its direct use for combustion, bio-oil has the potential to be upgraded to suitable fuels for transportation. Attempts have been made to upgrade bio-oils in fluid catalytic cracking reactors at low pressure or in hydrotreating reactors at a higher pressure [10]. In these upgrading processes, one of the most important problems is the deactivation of the catalyst by coke deposition [69, 70]. However, there are a series of reactions leading to the formation of carbonaceous deposits. The understanding of these reaction mechanisms is still insufficient.

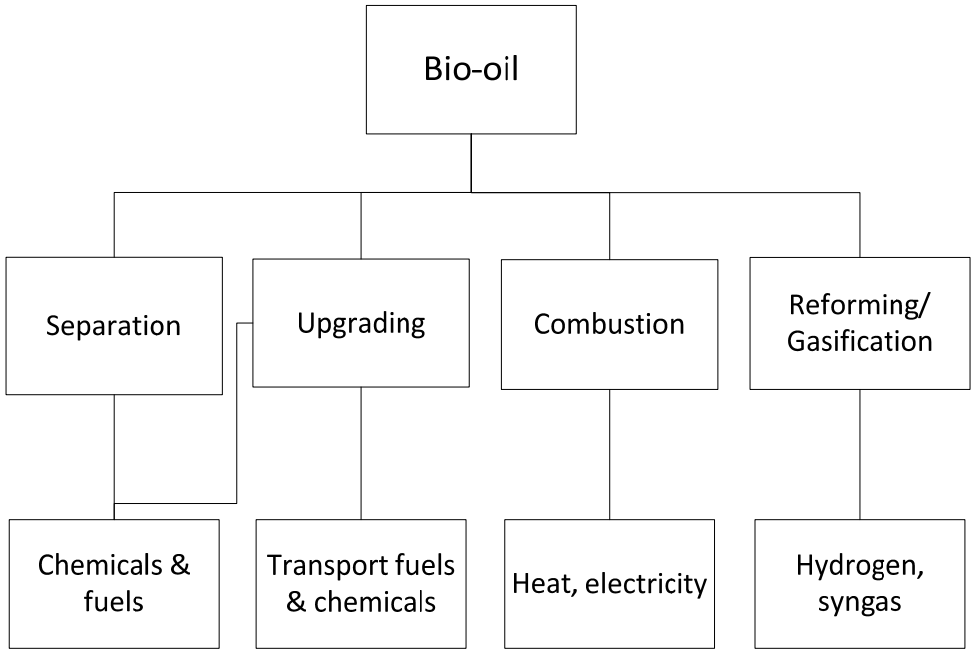

Figure 1-4. Applications for bio-oil (adapted from [18]).

Similar to the gasification of biomass, the catalytic steam reforming of bio-oil is a promising process to produce hydrogen or syngas [14, 31, 71]. To avoid the complexity of the bio-oil, its model compounds, including mixture of model compounds, have been used to study the process parameters and the selection of catalysts for steam reforming of bio-oil [31, 72]. The results indicate the importance of interactions by comparing the reforming of model compounds with that of their mixture under similar conditions. For example, coke formation was observed to occur to a higher extent from the reforming of a mixture of bio-oil model compounds (including acetic acid, ethylene glycol and acetone) than from the individual compounds (e.g. ethylene glycol) [72]. Besides the coke formation issues, the formation of tar is another major problem in this process [33-35, 73]. Particularly, bio-oil contains high concentrations of heavy compounds, which are prone to form tar.

As is discussed in Section 1.1.3.2, char-supported catalysts have shown adequate catalytic activities and have highly economic feasibility used to reform tar during gasification of biomass/coal. Therefore, a char-supported iron catalyst is selected to

reform bio-oil in this study. However, due to the exceeding complexity of bio-oil, the reaction involved particularly the interactions among different components, still remain largely unclear. In particular, little is known about how these interactions might affect the notorious coke formation on catalyst surface, which could deactivate the catalyst [34, 35].

1.3 Purpose of this study

From what have been discussed above, it is clear that bio-oil has great potential to be used directly or be upgraded to high grade fuels. However, there are many challenges in its thermal application or conversion processes due to its exceeding complexity and the high reactivity. To overcome these challenges, a full understanding of related reactions occurring in the thermal applications of bio-oil is essential. This should be the long term goal of research in this area.

No matter if bio-oil is chemically upgraded, combusted or gasified/reformed, bio-oil will have to be heated up first. As bio-oil is heated up, it will undergo thermal decomposition reactions, resulting in the formation of many radicals. After that, the recombination of them often results in the formation of large molecular mass compounds such as tar and coke. The formation of these compounds is a particularly serious problem for the upgrading or processing of bio-oil. To limit the negative effects or to suppress the formation of these compounds, a fundamental understanding of the related reactions is primary. Particularly, bio-oil contains a large portion of oligomers. Most of these oligomers have complex aromatic ring systems and are prone to form undesired by-products with rising temperature. Thus, the evolution of various large/complex aromatic ring systems is a key clue to understand the formation of large molecules.

Therefore, this study aims to investigate the evolution of bio-oil during the thermal decomposition (pyrolysis) at temperatures in a wide range, including the temperatures required by different bio-oil thermal application. The reaction mechanisms for the formation of heavy molecules need particular attention due to the

abovementioned reasons. The interactions among different bio-oil components during this process also need to be revealed to gain further understanding about the overall reactions.

Although biomass gasification is considered as a highly efficient way to produce gaseous components, many technical challenges still exist and block the way to commercialise this technology. The problem of tar is the most important one that needs to be solved. The formation of tar during biomass gasification is complicated, which is always related with heavy molecules. Bio-oil contains the main part of heavy compounds from the thermal decomposition of biomass except from the char. To understand the evolution of bio-oil under biomass gasification conditions is an effect way to investigate the mechanism of tar formation. Thus, this study aims to trace the evolution of bio-oil during its gasification.

Char-supported iron catalysts have been proved to be a class of suitable catalysts for the steam reforming of biomass tar [34]. As part of our ongoing efforts to fully understand the catalytic reforming mechanism, the char-supported iron catalyst is selected in this study to reform bio-oil with steam. The evolution of chemical compositions, especially with complex aromatic structures, during the bio-oil reforming process needs to be studied. Understanding the interactions among different bio-oil components is important to gain further understanding of the abovementioned reactions.

1.4 Scope of thesis

Chapter 2 will describe the details of the set-up of the experimental systems. The procedures for carrying out the pyrolysis and steam reforming experiments of the bio-oil and bio-oil components will be depicted. This will also include the procedures and techniques to characterise the reaction products.

Chapters 3-7 will present the experimental results and discussions. Each of these chapters contains a review of relevant literature as an introduction to the chapter.

Chapter 3 and ***Chapter 4*** will present the thermal behaviour of the bio-oil during it is pyrolysed over a wide range of temperature. ***Chapter 3*** will focus on the formation of aromatic structures during the pyrolysis of bio-oil and its key family of components such as cellulose- and lignin-derived compounds. The possible interactions between these components and their effects on the formation of aromatics will be discussed. In ***Chapter 4***, the yield of solid carbonaceous materials (coke) will be quantified during the pyrolysis of the bio-oil and bio-oil components. The possible reactions involved to the coke formation, including the interactions between different components of the bio-oil, will be discussed.

Chapter 5 and ***Chapter 6*** will present the behaviour of bio-oil and bio-oil key components during the catalytic and non-catalytic reforming of bio-oil in steam. ***Chapter 5*** will show the results of the steam reforming of cellulose-derived compounds derived from the pyrolysis of cellulose *in situ*. The tar yield will be quantified, and its chemical composition will be investigated. The effect of the char-supported iron as a catalyst will be also investigated. By comparing the results from the reforming of bio-oil and key components, the possible effects of the interactions among bio-oil components during the catalytic reforming of the bio-oil will be discussed in detail in ***Chapter 6***.

The conclusions of this study and the recommendations for future work are summarised in ***Chapter 7***.

Figure 1-5 summarises the flow diagram for the main content of each chapter to illustrate the relation between each chapter.

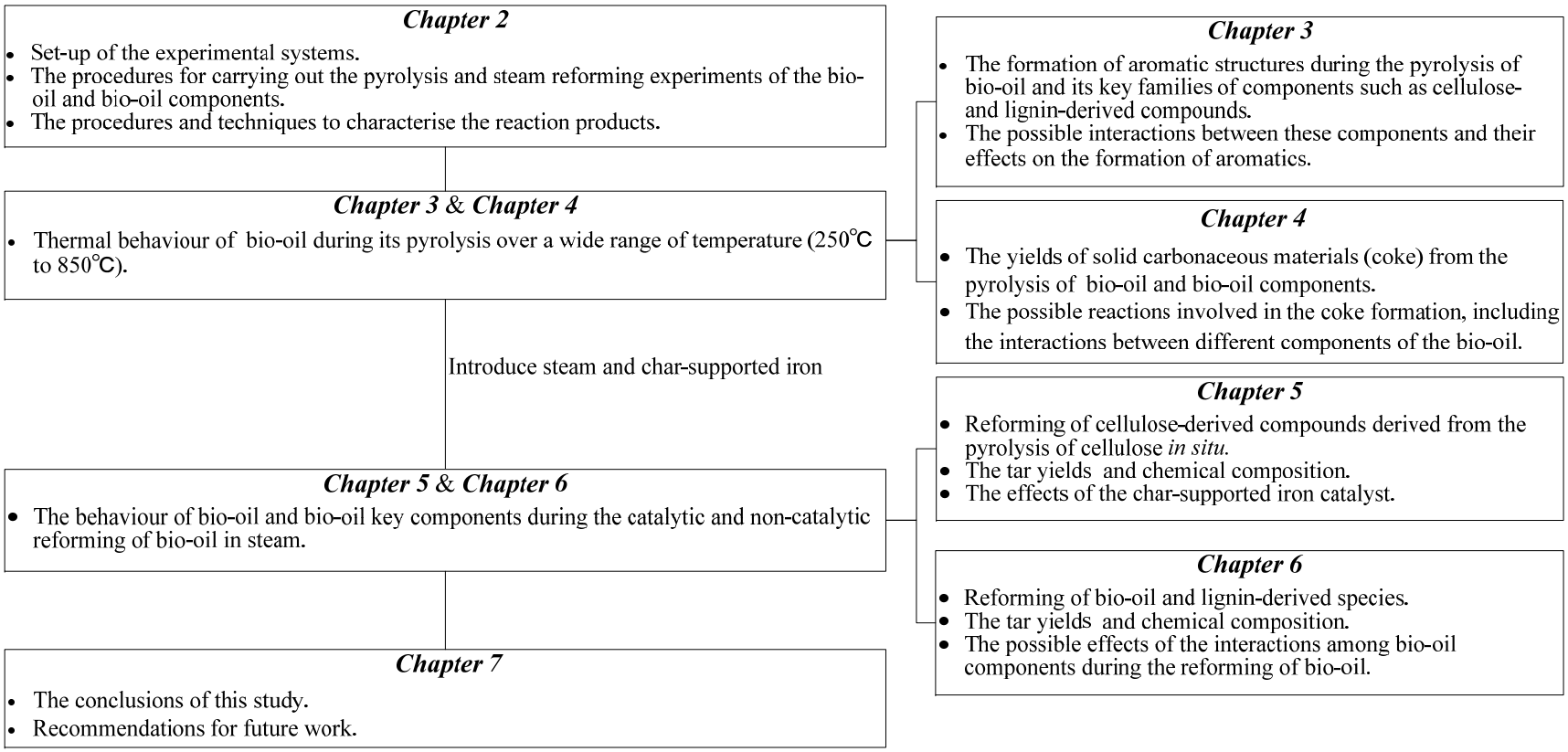

Figure 1-5. A flow chart of the scope of this thesis.

1.5 References

[1] EIA, International Energy Outlook 2011, U.S. Energy Information Administration, Washington, DC, 2011.

[2] IEA, World Energy Outlook 2011, OECD Publishing, 2011.

[3] S.N. Naik, V.V. Goud, P.K. Rout, A.K. Dalai, Production of first and second generation biofuels: A comprehensive review, Renewable and Sustainable Energy Reviews, 14 (2010) 578-597.

[4] IEA, From 1st - to 2nd-generation biofuel technologies – an overview of current industry and RD&D activities, in, International Energy Agency, IEA/OECD, Paris., 2008, pp. 120.

[5] R.E.H. Sims, W. Mabee, J.N. Saddler, M. Taylor, An overview of second generation biofuel technologies, Bioresource Technology, 101 (2010) 1570-1580.

[6] J. Fargione, J. Hill, D. Tilman, S. Polasky, P. Hawthorne, Land clearing and the biofuel carbon debt, Science, 319 (2008) 1235-1238.

[7] Fresco L O, Dijk D, Ridder W. Biomass, food and sustainability: Is there a dilemma? Utrecht, Netherlands, Rabobank. 2007.

[8] H. Wu, Q. Fu, R. Giles, J. Bartle, Production of mallee biomass in western australia: energy balance analysis, Energy & Fuels, 22 (2007) 190-198.

[9] D.S.T.A.G. Radlein, J. Piskorz, D.S. Scott, Lignin derived oils from the fast pyrolysis of poplar wood, Journal of Analytical and Applied Pyrolysis, 12 (1987) 51-59.

[10] D. Meier, O. Faix, State of the art of applied fast pyrolysis of lignocellulosic materials — a review, Bioresource Technology, 68 (1999) 71-77.

[11] D. Cooper, G. Olsen, J. Bartle, Capture of agricultural surplus water determines the productivity and scale of new low-rainfall woody crop industries, Australian Journal of Experimental Agriculture, 45 (2005) 1369-1388.

[12] J. Bartle, G. Olsen, D. Cooper, T. Hobbs, Scale of biomass production from new woody crops for salinity control in dryland agriculture in Australia, International Journal of Global Energy Issues, 27 (2007) 115-137.

[13] P. McKendry, Energy production from biomass (part 1): Overview of biomass, Bioresource Technology, 83 (2002) 37-46.

[14] S. Czernik, R. French, C. Feik, E. Chornet, Hydrogen by catalytic steam reforming of liquid byproducts from biomass thermoconversion processes, Industrial and Engineering Chemistry Research, 41 (2002) 4209-4215.

[15] S. Iborra, G. Huber, Synthesis of transportation fuels from biomass: Chemistry, catalysts, and engineering, Chemical reviews, 106 (2006) 4044-4098.

[16] M. Garcia-Perez, X.S. Wang, J. Shen, M.J. Rhodes, F. Tian, W.-J. Lee, H. Wu, C.-Z. Li, Fast pyrolysis of oil mallee woody biomass: Effect of temperature on the yield and quality of pyrolysis products, Industrial & Engineering Chemistry Research, 47 (2008) 1846-1854.

[17] A.V. Bridgwater, The technical and economic feasibility of biomass gasification for power generation, Fuel, 74 (1995) 631-653.

[18] S. Czernik, A.V. Bridgwater, Overview of applications of biomass fast pyrolysis oil, Energy & Fuels, 18 (2004) 590-598.

[19] D. Chiaramonti, A. Oasmaa, Y. Solantausta, Power generation using fast pyrolysis liquids from biomass, Renewable and Sustainable Energy Reviews, 11 (2007) 1056-1086.

[20] A. Demirbas, Progress and recent trends in biodiesel fuels, Energy Conversion and Management, 50 (2009) 14-34.

[21] A.V. Bridgwater, Renewable fuels and chemicals by thermal processing of biomass, Chemical Engineering Journal, 91 (2003) 87-102.

[22] D. Mohan, C.U. Pittman, P.H. Steele, Pyrolysis of wood/biomass for bio-oil: a critical review, Energy & Fuels, 20 (2006) 848-889.

[23] Bridgwater, Fast pyrolysis of biomass : a handbook / A. Bridgwater ... [et al.].

[24] D. Mourant, Z. Wang, M. He, X.S. Wang, M. Garcia-Perez, K. Ling, C.-Z. Li, Mallee wood fast pyrolysis: Effects of alkali and alkaline earth metallic species on the yield and composition of bio-oil, Fuel, 90 (2011) 2915-2922.

[25] J. Shen, X.-S. Wang, M. Garcia-Perez, D. Mourant, M.J. Rhodes, C.-Z. Li, Effects of particle size on the fast pyrolysis of oil mallee woody biomass, Fuel, 88 (2009) 1810-1817.

[26] M. Garcia-Perez, S. Wang, J. Shen, M. Rhodes, W.J. Lee, C.-Z. Li, Effects of temperature on the formation of lignin-derived oligomers during the fast pyrolysis of mallee woody biomass, Energy & Fuels, 22 (2008) 2022-2032.

[27] A.V. Bridgwater, Pyrolysis and gasification of biomass and waste: Proceedings of an Expert Meeting : Strasbourg, France, 30 September - 1 October 2002, Cpl Press, 2003.

[28] J.A. Libra, K.S. Ro, C. Kammann, A. Funke, N.D. Berge, Y. Neubauer, M.-M. Titirici, C. Fühner, O. Bens, J. Kern, K.-H. Emmerich, Hydrothermal carbonization of biomass residuals: A comparative review of the chemistry, processes and applications of wet and dry pyrolysis, Biofuels, 2 (2010) 71-106.

[29] G.V.C. Peacocke, E.S. Madrali, C.Z. Li, A.J. GUELL, F. Wu, R. Kandiyoti, A.V. Bridgwater, Effect of reactor configuration on the yields and structures of pine-wood derived pyrolysis liquids: A comparison between ablative and wire-mesh pyrolysis, Biomass and Bioenergy, 7 (1994) 155-167.

[30] A. Bridgewater, Biomass fast pyrolysis, Thermal science, 8 (2004) 21-50.

[31] D. Wang, S. Czernik, D. Montané, M. Mann, E. Chornet, Biomass to hydrogen via fast pyrolysis and catalytic steam reforming of the pyrolysis oil or its fractions, Industrial and Engineering Chemistry Research, 36 (1997) 1507-1518.

[32] M.M. Yung, W.S. Jablonski, K.A. Magrini-Bair, Review of catalytic conditioning of biomass-derived syngas, Energy & Fuels, 23 (2009) 1874-1887.

[33] T.A. Milne, N. Abatzoglou, R.J. Evans, Biomass gasifier “tars”: their nature,

formation, and conversion, in, NERL, Golden, CO, USA, 1998.

[34] Z. Min, P. Yimsiri, M. Asadullah, S. Zhang, C.Z. Li, Catalytic reforming of tar during gasification. Part II. Char as a catalyst or as a catalyst support for tar reforming, Fuel, 90 (2011) 2545-2552.

[35] Z. Min, M. Asadullah, P. Yimsiri, S. Zhang, H. Wu, C.-Z. Li, Catalytic reforming of tar during gasification. Part I. Steam reforming of biomass tar using ilmenite as a catalyst, Fuel, 90 (2011) 1847-1854.

[36] J. Han, The reduction and control technology of tar during biomass gasification/pyrolysis: An overview, Renewable & Sustainable Energy Reviews, 12 (2008) 397-416.

[37] Z. Abu El-Rub, E.A. Bramer, G. Brem, Review of catalysts for tar elimination in biomass gasification processes, Industrial & Engineering Chemistry Research, 43 (2004) 6911-6919.

[38] M.A. Caballero, J. Corella, M.P. Aznar, J. Gil, Biomass gasification with air in fluidized bed. Hot gas cleanup with selected commercial and full-size nickel-based catalysts, Industrial and Engineering Chemistry Research, 39 (2000) 1143-1154.

[39] J. Delgado, M.P. Aznar, J. Corella, Calcined dolomite, magnesite, and calcite for cleaning hot gas from a fluidized bed biomass gasifier with steam: Life and usefulness, Industrial & Engineering Chemistry Research, 35 (1996) 3637-3643.

[40] K.S. Seshadri, A. Shamsi, Effects of temperature, pressure, and carrier gas on the cracking of coal tar over a char−dolomite mixture and calcined dolomite in a fixed-bed reactor, Industrial & Engineering Chemistry Research, 37 (1998) 3830-3837.

[41] S. Rapagnà, N. Jand, A. Kiennemann, P.U. Foscolo, Steam-gasification of biomass in a fluidised-bed of olivine particles, Biomass and Bioenergy, 19 (2000) 187-197.

[42] T. Nordgreen, T. Liliedahl, K. Sjöström, Elemental iron as a tar breakdown

catalyst in conjunction with atmospheric fluidized bed gasification of biomass: A thermodynamic study, Energy & Fuels, 20 (2006) 890-895.

[43] T. Nordgreen, T. Liliedahl, K. Sjöström, Metallic iron as a tar breakdown catalyst related to atmospheric, fluidised bed gasification of biomass, Fuel, 85 (2006) 689-694.

[44] J.-I. Hayashi, M. Iwatsuki, K. Morishita, A. Tsutsumi, C.-Z. Li, T. Chiba, Roles of inherent metallic species in secondary reactions of tar and char during rapid pyrolysis of brown coals in a drop-tube reactor, Fuel, 81 (2002) 1977-1987.

[45] D.C. Elliott, A. Oasmaa, Catalytic hydrotreating of black liquor oils, Energy & Fuels, 5 (1991) 102-109.

[46] X. Li, R. Gunawan, C. Lievens, Y. Wang, D. Mourant, S. Wang, H. Wu, M. Garcia-Perez, C.-Z. Li, Simultaneous catalytic esterification of carboxylic acids and acetalisation of aldehydes in a fast pyrolysis bio-oil from mallee biomass, Fuel, 90 (2011) 2530-2537.

[47] H. Abdullah, H. Wu, Bioslurry as a fuel. 4. Preparation of bioslurry fuels from biochar and the bio-oil-rich fractions after bio-oil/biodiesel extraction, Energy & Fuels, 25 (2011) 1759-1771.

[48] M. Garcia-Perez, A. Chaala, H. Pakdel, D. Kretschmer, C. Roy, Characterization of bio-oils in chemical families, Biomass and Bioenergy, 31 (2007) 222-242.

[49] E.L. A. Oasmaa, P. Koponen, I Levander and E. Tapola, Physical characterisation off biomass-based pyrolysis liquids., Application of standard fuel oil analyses. VTT Publications 3 06. VTT Energy, Espoo, (1997).

[50] C.A. Mullen, A.A. Boateng, Characterization of water insoluble solids isolated from various biomass fast pyrolysis oils, Journal of Analytical and Applied Pyrolysis, 90 (2011) 197-203.

[51] Y. Wang, X. Li, D. Mourant, R. Gunawan, S. Zhang, C.-Z. Li, Formation of aromatic structures during the pyrolysis of bio-oil, Energy & Fuels, 26 (2012) 241-247.

[52] M. Garcìa-Pèrez, A. Chaala, C. Roy, Vacuum pyrolysis of sugarcane bagasse, Journal of Analytical and Applied Pyrolysis, 65 (2002) 111-136.

[53] H. Abdullah, D. Mourant, C.-Z. Li, H. Wu, Bioslurry as a fuel. 3. Fuel and rheological properties of bioslurry prepared from the bio-oil and biochar of mallee biomass fast pyrolysis, Energy & Fuels, 24 (2010) 5669-5676.

[54] A. Oasmaa, S. Czernik, Fuel oil quality of biomass pyrolysis oilsstate of the art for the end users, Energy & Fuels, 13 (1999) 914-921.

[55] C. Lievens, D. Mourant, M. He, R. Gunawan, X. Li, C.-Z. Li, An FT-IR spectroscopic study of carbonyl functionalities in bio-oils, Fuel, 90 (2011) 3417-3423.

[56] R. Bayerbach, D. Meier, Characterization of the water-insoluble fraction from fast pyrolysis liquids (pyrolytic lignin). Part IV: Structure elucidation of oligomeric molecules, Journal of Analytical and Applied Pyrolysis, 85 (2009) 98-107.

[57] R. Bayerbach, V.D. Nguyen, U. Schurr, D. Meier, Characterization of the water-insoluble fraction from fast pyrolysis liquids (pyrolytic lignin): Part III. Molar mass characteristics by SEC, MALDI-TOF-MS, LDI-TOF-MS, and Py-FIMS, Journal of Analytical and Applied Pyrolysis, 77 (2006) 95-101.

[58] B. Scholze, C. Hanser, D. Meier, Characterization of the water-insoluble fraction from fast pyrolysis liquids (pyrolytic lignin): Part II. GPC, carbonyl goups, and 13C-NMR, Journal of Analytical and Applied Pyrolysis, 58-59 (2001) 387-400.

[59] B. Scholze, D. Meier, Characterization of the water-insoluble fraction from pyrolysis oil (pyrolytic lignin). Part I. PY-GC/MS, FTIR, and functional groups, Journal of Analytical and Applied Pyrolysis, 60 (2001) 41-54.

[60] C. Gerdes, C.M. Simon, T. Ollesch, D. Meier, W. Kaminsky, Design, construction, and operation of a fast pyrolysis plant for biomass, Engineering in Life Sciences, 2 (2002) 167-174.

[61] S. Fernando, S. Adhikari, C. Chandrapal, N. Murali, Biorefineries: Current

status, challenges, and future direction, Energy and Fuels, 20 (2006) 1727-1737.

[62] M. He, D. Mourant, R. Gunawan, C. Lievens, X.S. Wang, K. Ling, J. Bartle, C.-Z. Li, Yield and properties of bio-oil from the pyrolysis of mallee leaves in a fluidised-bed reactor, Fuel. In Press.

[63] C. Di Blasi, C. Branca, A. Galgano, Thermal and catalytic decomposition of wood impregnated with sulfur- and phosphorus-containing ammonium salts, Polymer Degradation and Stability, 93 (2008) 335-346.

[64] G. Dobele, T. Dizhbite, G. Rossinskaja, G. Telysheva, D. Meier, S. Radtke, O. Faix, Pre-treatment of biomass with phosphoric acid prior to fast pyrolysis: A promising method for obtaining 1,6-anhydrosaccharides in high yields, Journal of Analytical and Applied Pyrolysis, 68–69 (2003) 197-211.

[65] A. Demirbas, The influence of temperature on the yields of compounds existing in bio-oils obtained from biomass samples via pyrolysis, Fuel Processing Technology, 88 (2007) 591-597.

[66] S. Zhou, D. Mourant, C. Lievens, Y. Wang, C.-Z. Li, M. Garcia-Perez, Effect of sulfuric acid concentration on the yield and properties of the bio-oils obtained from the auger and fast pyrolysis of Douglas Fir, Fuel.

[67] M.J. Wornat, B.G. Porter, N.Y.C. Yang, Single droplet combustion of biomass pyrolysis oils, Energy & Fuels, 8 (1994) 1131-1142.

[68] V. Stamatov, D. Honnery, J. Soria, Combustion properties of slow pyrolysis bio-oil produced from indigenous Australian species, Renewable Energy, 31 (2006) 2108-2121.

[69] J.D. Adjaye, N.N. Bakhshi, Production of hydrocarbons by catalytic upgrading of a fast pyrolysis bio-oil. Part II: Comparative catalyst performance and reaction pathways, Fuel Processing Technology, 45 (1995) 185-202.

[70] E. Butler, G. Devlin, D. Meier, K. McDonnell, A review of recent laboratory research and commercial developments in fast pyrolysis and upgrading, Renewable and Sustainable Energy Reviews, 15 (2011) 4171-4186.

[71] J.R. Galdámez, L. García, R. Bilbao, Hydrogen production by steam reforming of bio-oil using coprecipitated ni−al catalysts: Acetic acid as a model compound, Energy & Fuels, 19 (2005) 1133-1142.

[72] P.N. Kechagiopoulos, S.S. Voutetakis, A.A. Lemonidou, I.A. Vasalos, Hydrogen production via steam reforming of the aqueous phase of bio-oil in a fixed bed reactor, Energy & Fuels, 20 (2006) 2155-2163.

[73] D.M. Quyn, H. Wu, J.-i. Hayashi, C.-Z. Li, Volatilisation and catalytic effects of alkali and alkaline earth metallic species during the pyrolysis and gasification of Victorian brown coal. Part IV. Catalytic effects of NaCl and ion-exchangeable Na in coal on char reactivity, Fuel, 82 (2003) 587-593.

Chapter 2

Experimental methods

2.1 Introduction

The reactor designs and operating procedures used to carry out this study are detailed in this chapter. The methods of tar sample analysis and the characterization of fresh and spent catalysts are also detailed in this chapter.

2.2 Sample preparation

The bio-oil sample was prepared by Dr Daniel Mourant. It is produced from the pyrolysis of mallee eucalypts (E. loxopheba ssp. lissophloia) wood at fast heating rates in a fluidised-bed reactor (nominally 1 kg/hr) at 500 °C [1-3]. Briefly, preheated nitrogen was used as the fluidisation gas to fluidise the bed solids (silica sand) at a velocity about twice the minimum fluidisation velocity. The auger feeder speed was controlled to achieve a feeding rate of about 1 kg/hr. About 1.0 kg of biomass was fed per run. The pyrolysis was conducted at 500 °C. Heating tapes were installed outside the walls of the reactor, cyclones, and pipes to supply heat. Two cyclones were maintained at 420 °C. The bio-oil vapours were condensed by a series of condensers. The first condenser was cooled by water, reducing the temperature from 420 °C to ~23 °C, while the second condenser relied on dry ice to further reduce the temperature down to about −10 °C. Most of the remaining aerosols, representing between 8 and 20 mass % of the total oil, were trapped by an aerosol filter (a 240 mm Advantec Quantitative filter paper no. 1). The total yield of bio-oil is about 62.0 wt% of biomass. The bio-oil was only one liquid phase and stored in a freezer (about -10 °C) until required in further experiments described herein.

To study the interactions among different bio-oil components during the pyrolysis of bio-oil, the bio-oil was separated into water-soluble and water-insoluble fractions through the cold water precipitation [4, 5]. Briefly, 10 g of bio-oil was added drop-wise to 1L of ice-cold deionised water, under strong agitation. The mixture was then filtered using a Whatman #42 paper. More deionised water was used to wash the flask and the agitator until the filtrate was clear. The aqueous solution in the Erlenmeyer was removed and CH_2Cl_2 was then used to rinse the filter paper. More

CH_2Cl_2 was used to rinse the flask and the agitator until the filtrate was clear. The CH_2Cl_2 solution was then evaporated using a rotary evaporator at 40 °C, with the remains being quantified as the water-insoluble-CH_2Cl_2-soluble fraction. After drying at 105 °C for 1 hour, the content left on the filter paper was weighed as the water insoluble CH_2Cl_2 insoluble fraction. The yields of water insoluble CH_2Cl_2 soluble fraction and water insoluble CH_2Cl_2 insoluble fraction are ~18.0 wt% and ~3.6 wt% of bio-oil, respectively [6]. This process was repeated to prepare a significant amount of these two fractions for further experiments.

The pure cellulose powder (α-cellulose, Sigma-Aldrich) was dried in the oven at 105 °C for 24 hours prior to use in experiment.

2.3 Pyrolysis experiment

The pyrolysis of bio-oil, its separated fractions and cellulose was carried out in a novel two-stage fluidised-bed/fixed-bed quartz reactor (Figure 2-1) [7, 8]. 60 grams of silica sand ranging from 0.21 to 0.30 mm in particle size was used as a bed material in the bottom stage of the reactor, which was fluidised with argon fed into the reactor from the bottom. The bio-oil was fed into the reactor via an air-cooled injection probe, with the help of argon carrier gas (0.21 L/min), at a rate of 100 mg/min using a syringe pump (KD Scientific 410CE) equipped with a 20 ml stainless steel syringe. The weights of the syringe and the injection probe were recorded before and after an experiment to determine the exact amount of bio-oil fed into the reactor. The solid feedstock (water-insoluble fractions and cellulose) particles were entrained in a feeder with argon (1 L/min) and fed into the fluidised bed at 100 mg/min via a cold water-cooled injection probe injection probe.

The reactor (Figure 2-1) was operated with two different temperature profiles. For the pyrolysis of bio-oil and water-insoluble soluble fractions, both the top and bottom stages of the reactor were maintained at the same temperature. The gas residence time in the reactor was about 2.4 s: the residence time in the top stage was much longer (about 1.6 times) than that in the bottom stage.

Bio-oil contains many compounds from thermal degradation of cellulose during pyrolysis of woody biomass. To study the thermal behaviour of cellulose-derived compounds alone, cellulose was pyrolysed in the bottom stage of the reactor at 500°C (the same temperature as that used to produce the bio-oil from the pyrolysis of wood in the larger pyrolysis facility). The volatiles produced from the pyrolysis of cellulose in the bottom stage directly entered (i.e. *in-situ*) the top stage where the temperature was controlled at a pre-set level between 500 and 850°C to investigate the pyrolysis of the nascent volatiles produced from the bottom stage.

The flow rate of fluidising gas was adjusted so that the actual total flow rate and therefore the gas residence time inside the top stage of the reactor remained roughly constant even when the reactor temperature was increased.

The produced gas exiting the reactor passed through a series of three tar traps containing a High Performance Liquid Chromatography (HPLC) grade $CHCl_3$:CH_3OH mixture (80:20 by volume) cooled respectively with ice-water (the first trap) and dry ice (the second and third traps) baths as outlined previously [7-10]. The tarry materials would be dissolved and trapped in the solvent mixture.

Tar is experimentally defined as the material that dissolves in the mixture solvent but does not evaporate at 35 °C within 4 hours and was determined following the procedure developed by Dr Zhenhua Min [11]. Briefly, the aluminium tray was dried in oven at 35 °C before using. It was taken out for 20 minutes to equilibrate with atmospheric conditions and recorded the weigh by using a 5-digital balance. About 2 ml tar solution was suck out from the storing vial, and put onto a weighed aluminium tray and dried at 35 °C for 4 hours to evaporate all solvents and water. The time of drying process was determined by the experiments of evaporating tar solution at 35 °C from 2 to 24 hours. No visible liquor can be found in the aluminium tray after 4 hours. Additionally, the weight loss was similar to the results after drying for 5 hours. Thus, 4 hours was chosen to measure the tar yield.

The amount of tar solution was calculated accurately by weighing the storing vial before and after removing tar solution. After drying process, the aluminium tray was taken out for 20 minutes to equilibrate with atmospheric conditions and weighed accurately using a 5-digital balance. The residues in the solvents themselves were

determined following the same procedure and considered in the calculation of the tar concentration (Equation 2-1).

$$C = \frac{C_2 - C_1}{1 - C_1} \times 100\,\% \qquad (2\text{-}1)$$

C: the actual tar concentration in the solution;

C_1: the residues concentration in the solvent, blank experiment;

C_2: the residues concentration in the tar solution.

In this study, the solid residual produced from the pyrolysis experiment which cannot be dissolved into the $CHCl_3$:CH_3OH mixture is experimentally defined as "coke". The reactor after an experiment was washed and then dried at 105°C for 30 mins with air supply to evaporate the solvent used for tar washing. The coke was then burned with air. The coke was measured as the weight difference before and after the coke was burned.

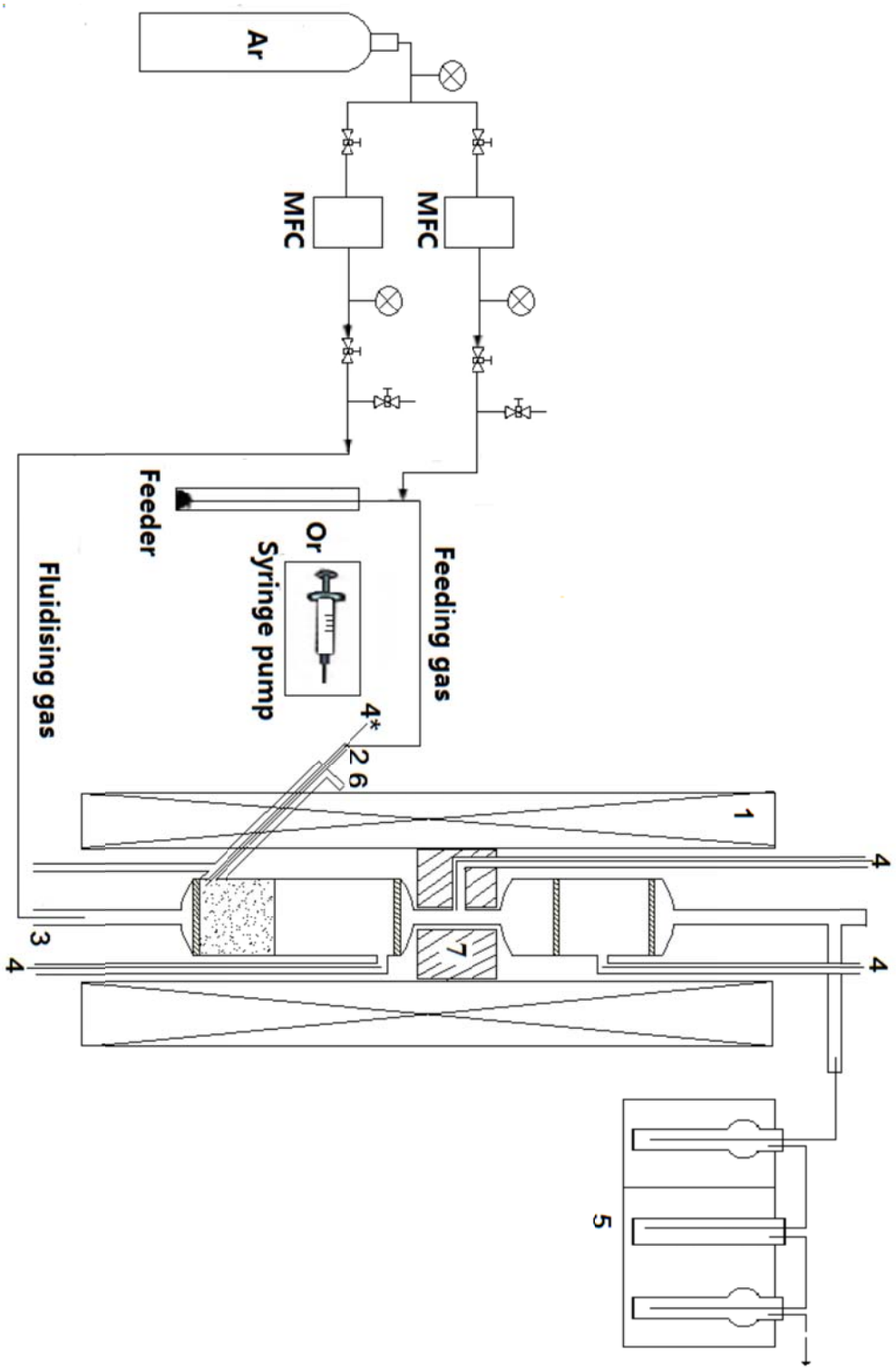

Figure 2-1. A schematic diagram of the experimental set-up for pyrolysis process. 1, furnace; 2, feeding tube; 3, fluidising gas inlet 4, thermocouples; 5, tar trap system. 6, cold water cooling tube; 7, insulation materials (kaowool). (*) This thermocouple was used to measure the temperature in the fluidised bed, and it would be replaced by a feeding probe after target temperature was reached.

2.4 Preparation of catalyst for steam reforming experiment

Char-supported iron catalyst has been proved to be a suitable catalyst for steam reforming of biomass tar [7, 8]. Continuing the previous study in this group [7, 8], char-supported iron catalyst is selected in this study to reform bio-oil with steam. The catalysts were prepared with the assistance from Dr Shu Zhang. A description of preparation procedure follows.

Loy Yang brown coal (Victoria, Australia) was pulverised and sieved into different size particles. The size ranging from 106 to 150 μm was chosen as the precursor of the catalyst. The properties of the coal are as follows: C, 70.4; H, 5.4; N, 0.62; S, 0.28; Cl, 0.1; O, 23.2 and VM, 52.2 wt% (daf basis) together with an ash yield of 1.1 wt% (db) [12].

The raw coal was mixed in an aqueous solution of 0.2M H_2SO_4 with a ratio of the acid solution to coal of 30:1 by mass and stirred in an argon atmosphere for 24 hour. The slurry was then filtered and washed with de-ionized water until the pH value of the filtrates was constant (4.5–5.0). After drying, the acid-washed coal contains a negligible amount of inorganic species because all carboxylates (-COOM) have been turned into acids (-COOH), and it is termed as the H-form coal. The H-from coal was then impregnated with 1 wt% Fe by ion-exchanging with corresponding $FeCl_3$ solution respectively. The treated coal is termed as the Fe-loaded coal.

A one-stage fluidised-bed/fixed-bed reactor (Figure 2-2) [12, 13], heated with a furnace was used to prepare the catalysts at 800 °C. In each experiment, about 25 grams of iron-loaded coal were firstly loaded into the quartz reactor followed by 15 min argon purging before it was heated at about 10 °C/min to the desired temperature with 0.5 L/min of argon flow. The reactor was then held for 15 min at the peak temperature with the additional supply of gasification agents (30 vol.% steam). At the end of 15 min, the reactor was lifted out of the furnace to be cooled down to room temperature with the continuous argon flow. The fresh char-supported iron catalysts were then collected and stored in a freezer (about -10 °C) until required for the reforming experiments.

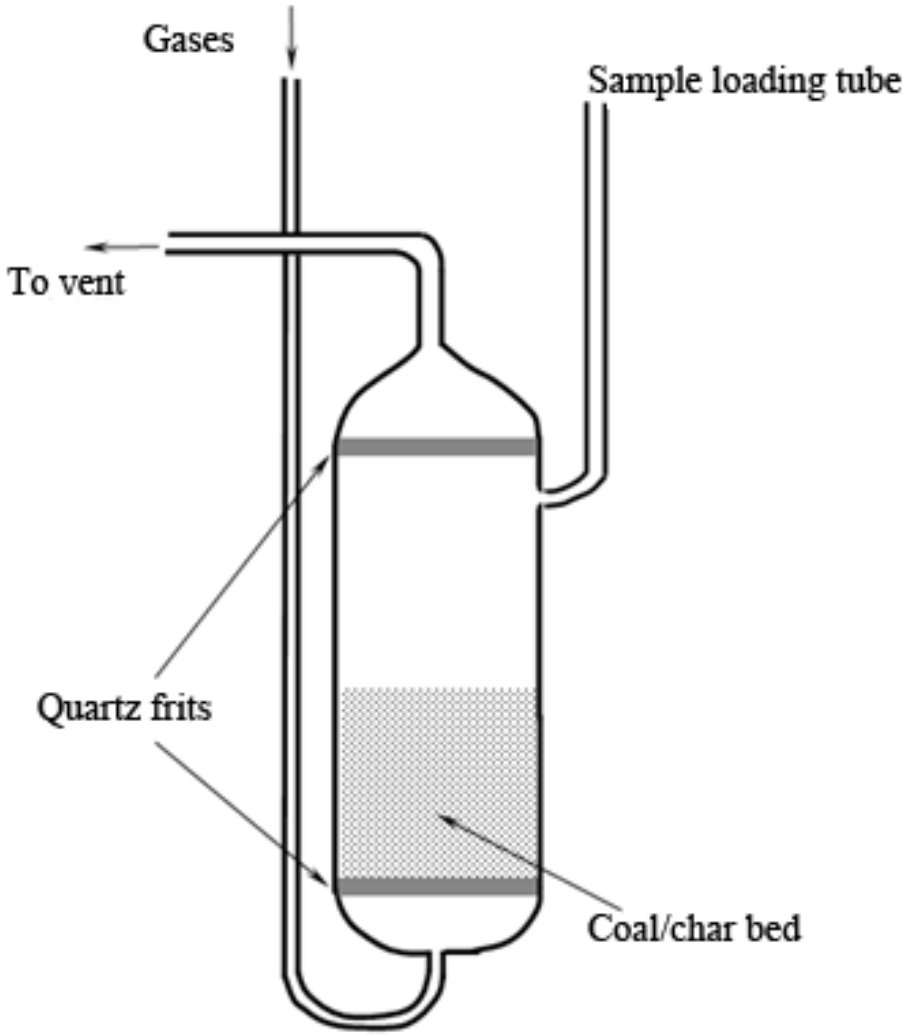

Figure 2-2. A schematic diagram of the fluidised-bed/fixed-bed reactor used for preparing the catalysts from iron-loaded brown coal [12, 13].

2.5 Steam reforming experiment

The reforming experiments were conducted using the quartz reactor system. The reactor was the same one used for pyrolysis experiment. The only difference for reforming is the introduction of catalyst and steam (Figure 2-3). Briefly, the bottom part of the reactor acted as a fluidised-bed pyrolyser while the top part was used as a catalytic fixed-bed reformer. The syringe pump was used to control the feeding of oil

into the fluidised sand bed. The solid feedstock (water-insoluble fractions and cellulose) particles were entrained in a feeder with argon (1 L/min) and fed into the fluidised bed at 100 mg/min via a cool water-cooled injection probe.

Similar to the pyrolysis experiments, the reactor (Figure 2-3) was operated with two different temperature profiles in reforming experiments.

For the reforming of bio-oil and water-insoluble soluble fractions, both the top and bottom stages of the reactor were operated at the same temperature. Experiments would be carried out in a temperature range of 500 °C to 850 °C. Steam was injected from the bottom part of the reactor, which was controlled by a HPLC pump.

For the reforming of cellulose-derived compounds, cellulose was pyrolysed in the bottom stage of the reactor at 500 °C (the same temperature as that used to produce the bio-oil from the pyrolysis of wood in the larger pyrolysis facility). The volatiles produced from the pyrolysis of cellulose in the bottom stage directly entered (i.e. in-situ) the top stage where the temperature was controlled at a pre-set level between 500 and 850°C to investigate the reforming of the nascent volatiles produced from the bottom stage in steam. Therefore, Steam was injected from the middle part of the reactor.

The flow rate of steam/water was 15 vol.% of the total gas flow rate. It would be adjusted to correspond to the change of total gas flow rate, therefore the gas residence time inside the top stage of the reactor remained roughly constant even when the reactor temperature was increased.

In any catalytic reforming experiment, about 1 gram of catalyst was pre-loaded into the top zone of the reactor.

In reforming and pyrolysis experiments, the identical solvent trap system was used to dissolve and trap the tarry materials from the gas products exiting the reactor.

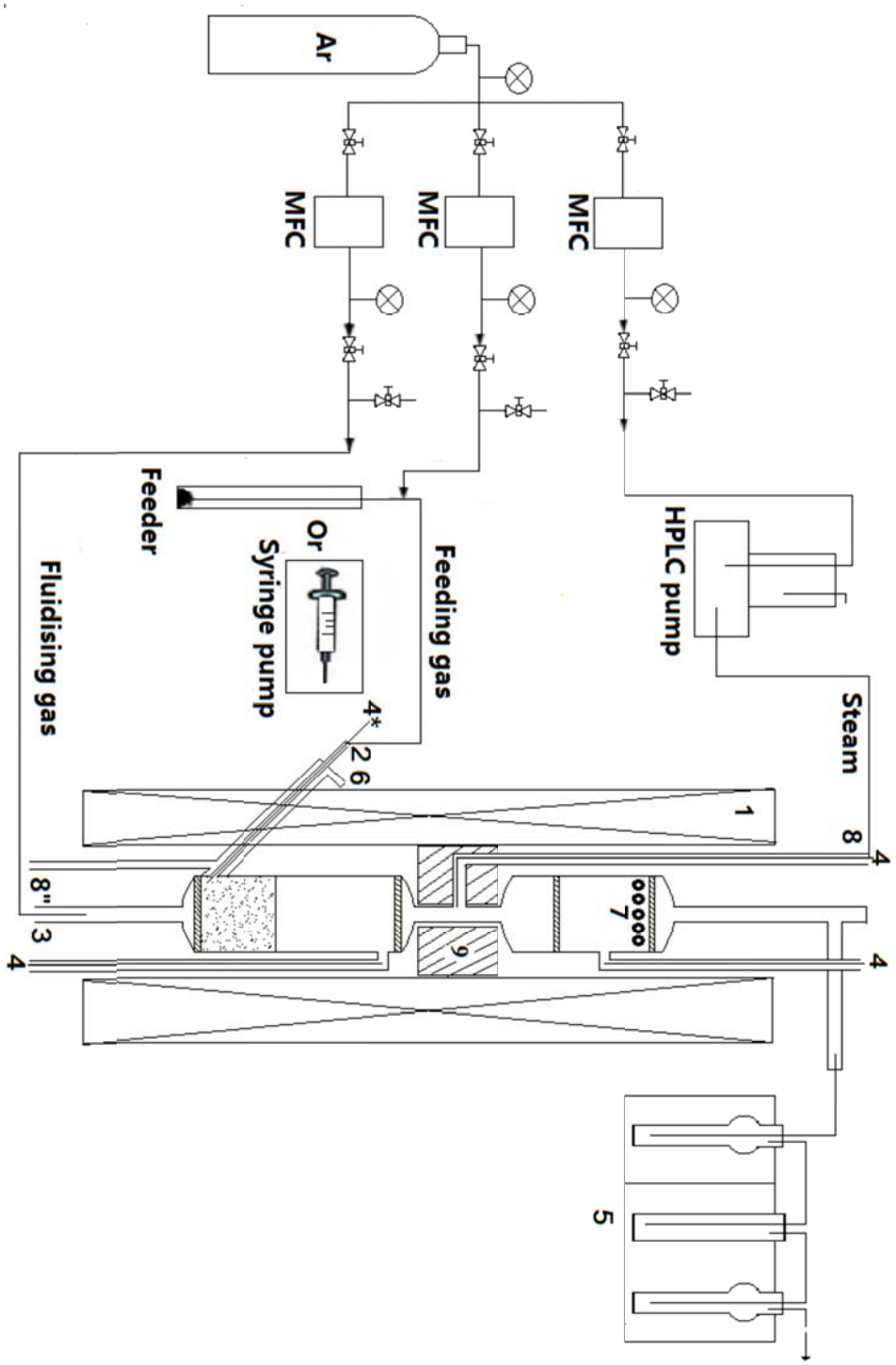

Figure 2-3. A schematic diagram of the experimental set-up for steam reforming process. 1, furnace; 2, feeding tube; 3, fluidising gas inlet 4, thermocouples; 5, tar trap system; 6, air or cold water cooling tube; 7, catalyst (catalytic reforming process); 8, steam injection tube; 9, insulation materials (kaowool). (″) the steam injection point was at bottom during the steam reforming of bio-oil and its lignin-derived oligomers. (*) This thermocouple was used to measure the temperature in the fluidised bed, and it would be replaced by a feeding probe after target temperature was reached.

2.6 Characterization of tar

2.6.1 UV-Fluorescence spectroscopy

UV-fluorescence spectroscopy has been widely used to characterise the structural features of "liquid" (such as bio-oil or tar) derived from coal and biomass, giving information about the relative size and concentration of aromatic ring systems in the sample [14-17].

In this study, the UV-fluorescence spectra of tars were recorded using a Perkin-Elmer LS50B spectrometer. The bio-oil/tar solution was diluted with methanol [Uvasol for spectroscopy; purity (GC): ≥ 99.9%] to 4 ppm (wt). The synchronous spectra were recorded with a constant energy difference of -2800 cm^{-1}. The slit widths were 2.5 nm and the scan speed was 200 nm/min. The "wavelength" shown for each spectrum refers to that of the excitation monochromator. Wavelength is a brief indication of the aromatic ring sizes (e.g. < 290 nm for mono-rings, 290-320 nm for aromatic ring systems containing 2 fused benzene rings, etc) although a clear delineation about ring sizes and wavelength ranges is impossible.

At the same concentration, the fluorescence intensity was multiplied by the bio-oil/tar yield in order to facilitate comparison of the signals of different tars on the basis of "per gram of feedstock" [18].

2.6.2 GC-MS analysis

Samples were analysed using an Agilent GC-MS (6890 series GC with an 5973 MS detector) with a capillary column (INNOWax) (length, 30 m; internal diameter, 0.25 mm; film thickness, 0.25 μm). 1 μL of sample was injected into the injection port set at 250 °C in a splitless configuration. The column was operated in a constant flow mode using helium as the carrier gas. The column temperature was initially maintained at 40 °C for 3 min before increasing to 260 °C at a heating rate of 10 °C/min. The MS acquisition occurred after 5 min solvent delay. The identification of the peaks in the chromatogram was based on the comparison with the standard spectra of compounds in the NIST library and/or on the retention times/spectra of

known species injected.

2.7 Char structural features of catalysts

The Fourier transformed Raman (FT-Raman) spectra of catalyst were recorded with a Perkin-Elmer Spectrum GX FT-Raman spectrometer following the procedures outlined previously [19-21]. An InGaAs detector operated at room temperature was used to collect Raman scattering using a back-scattering configuration. The excitation Nd:YAG laser wavelength was 1064 nm. A laser power of 150 mW was used. Each spectrum represents the average of 50 scans. The spectral resolution was 4 cm^{-1}. A curved baseline was considered for each spectrum, and the baseline correction was carried out with the software provided by Perkin-Elmer with the spectrometer.

To reduce the heat up of the sample by the laser, the sample was mixed with spectroscopic grade KBr (0.5% char in KBr) and ground manually.

The Raman spectra in the range between 800 and 1800 cm^{-1} were curve-fitted using the GRAMS/32 AI software with 10 Gaussian bands (Table 2-1) representing the typical structural features .

The assignment of the main bands (G, G_R, V_L, V_R, D and S) will be outlined here briefly. The G band at 1590 cm^{-1} mainly represents aromatic ring quadrant E_{2g}^2 breathing and the graphite vibration. The graphite structures are not expected to be present in char, and even if they were, they have been shown to have extremely low Raman intensities [21]. So the observed G band is mainly due to the aromatic ring systems. The D (1300 cm^{-1}) band represents defect structures in the highly ordered carbonaceous materials and, more importantly, aromatics with not less than 6 fused rings. The "overlap" between the D and G bands has been deconvoluted into three bands: G_R (1540 cm^{-1}), V_L (1465 cm^{-1}) and V_R (1380 cm^{-1}). These three bands represent typical structures in amorphous carbon (especially smaller aromatic ring systems) as well as the semi-circle breathing of aromatic rings.

The S (1185 cm^{-1}) band mainly represents $C_{aromatic}$-C_{alkyl}, aromatic (aliphatic) ethers, C-C on hydroaromatic rings, hexagonal diamond carbon sp3 and C-H on aromatic rings.

Table 2-1. A summary of peak/band assignments [19]

Band name	Band position cm^{-1}	Description	Bond type
G_l	1700	Carbonyl group C=O	sp^2
G	1590	Graphite E_{2g}^2 ; aromatic ring quadrant breathing; alkene C=C	sp^2
G_r	1540	Aromatics with 3~5 rings; amorphous carbon structures	sp^2
V_l	1465	Methylene or methyl; semicircle breathing of aromatic rings; amorphous carbon structures	sp^2, sp^3
V_r	1380	Methyl group; semicircle breathing of aromatic rings; amorphous carbon structures	sp^2, sp^3
D	1300	D band on highly ordered carbonaceous materials; C-C between aromatic rings and aromatics with not less than 6 rings	sp^2
S_l	1230	Aryl-alkyl ether; para-aromatics	sp^2, sp^3
S	1185	$C_{aromatic}$-C_{alkyl}; aromatic (aliphatic) ethers; C-C on hydroaromatic rings; hexagonal diamond carbon sp^3; C-H on aromatic rings	sp^2, sp^3
S_r	1060	C-H on aromatic rings; benzene (ortho-di-substituted) ring	sp^2
R	960-800	C-C on alkanes and cyclic alkanes; C-H on aromatic rings	sp^2, sp^3

2.8 References

[1] M. Garcia-Perez, X.S. Wang, J. Shen, M.J. Rhodes, F. Tian, W.-J. Lee, H. Wu, C.-Z. Li, Fast Pyrolysis of Oil Mallee Woody Biomass: Effect of Temperature on the Yield and Quality of Pyrolysis Products, Industrial & Engineering Chemistry Research, 47 (2008) 1846-1854.

[2] J. Shen, X.-S. Wang, M. Garcia-Perez, D. Mourant, M.J. Rhodes, C.-Z. Li, Effects of particle size on the fast pyrolysis of oil mallee woody biomass, Fuel, 88 (2009) 1810-1817.

[3] D. Mourant, Z. Wang, M. He, X.S. Wang, M. Garcia-Perez, K. Ling, C.-Z. Li, Mallee wood fast pyrolysis: Effects of alkali and alkaline earth metallic species on the yield and composition of bio-oil, Fuel, 90 (2011) 2915-2922.

[4] E.L. A. Oasmaa, P. Koponen, I Levander and E. Tapola, Physical characterisation off biomass-based pyrolysis liquids., Application of standard fuel oil analyses. VTT Publications 3 06. VTT Energy, Espoo, (1997).

[5] M. Garcia-Perez, A. Chaala, H. Pakdel, D. Kretschmer, C. Roy, Characterization of bio-oils in chemical families, Biomass and Bioenergy, 31 (2007) 222-242.

[6] Y. Wang, X. Li, D. Mourant, R. Gunawan, S. Zhang, C.-Z. Li, Formation of Aromatic Structures during the Pyrolysis of Bio-oil, Energy & Fuels, 26 (2012) 241-247.

[7] Z. Min, M. Asadullah, P. Yimsiri, S. Zhang, H. Wu, C.-Z. Li, Catalytic reforming of tar during gasification. Part I. Steam reforming of biomass tar using ilmenite as a catalyst, Fuel, 90 (2011) 1847-1854.

[8] Z. Min, P. Yimsiri, M. Asadullah, S. Zhang, C.Z. Li, Catalytic reforming of tar during gasification. Part II. Char as a catalyst or as a catalyst support for tar reforming, Fuel, 90 (2011) 2545-2552.

[9] C.-Z. Li, K.D. Bartle, R. Kandiyoti, Vacuum pyrolysis of maceral concentrates in a wire-mesh reactor, Fuel, 72 (1993) 1459-1468.

[10] C.-Z. Li, K.D. Bartle, R. Kandiyoti, Characterization of tars from variable heating rate pyrolysis of maceral concentrates, fuel, 72 (1993) 3-11.

[11] C. Sathe, Y. Pang, C.-Z. Li, Effects of Heating Rate and Ion-Exchangeable Cations on the Pyrolysis Yields from a Victorian Brown Coal, Energy & Fuels, 13 (1999) 748-755.

[12] D.M. Quyn, H. Wu, C.-Z. Li, Volatilisation and catalytic effects of alkali and alkaline earth metallic species during the pyrolysis and gasification of Victorian brown coal. Part I. Volatilisation of Na and Cl from a set of NaCl-loaded samples, fuel, 81 (2002) 143-149.

[13] D.M. Quyn, H. Wu, J.-i. Hayashi, C.-Z. Li, Volatilisation and catalytic effects of alkali and alkaline earth metallic species during the pyrolysis and gasification of Victorian brown coal. Part IV. Catalytic effects of NaCl and ion-exchangeable Na in coal on char reactivity, Fuel, 82 (2003) 587-593.

[14] C.-Z. Li, F. Wu, H.-Y. Cai, R. Kandiyoti, UV-Fluorescence Spectroscopy of Coal Pyrolysis Tars, Energy & Fuels, 8 (1994) 1039-1048.

[15] C. Zeng, G. Favas, H. Wu, A.L. Chaffee, J.-i. Hayashi, C.-Z. Li, Effects of Pretreatment in Steam on the Pyrolysis Behavior of Loy Yang Brown Coal, Energy & Fuels, 20 (2005) 281-286.

[16] G.V.C. Peacocke, E.S. Madrali, C.Z. Li, A.J. GUELL, F. Wu, R. Kandiyoti, A.V. Bridgwater, Effect of reactor configuration on the yields and structures of pine-wood derived pyrolysis liquids: A comparison between ablative and wire-mesh pyrolysis, Biomass and Bioenergy, 7 (1994) 155-167.

[17] M. Garcia-Perez, S. Wang, J. Shen, M. Rhodes, W.J. Lee, C.-Z. Li, Effects of Temperature on the Formation of Lignin-Derived Oligomers during the Fast Pyrolysis of Mallee Woody Biomass, Energy & Fuels, 22 (2008) 2022-2032.

[18] C.-Z. Li, C. Sathe, J.R. Kershaw, Y. Pang, Fates and roles of alkali and alkaline earth metals during the pyrolysis of a Victorian brown coal, Fuel, 79 (2000) 427-438.

[19] X. Li, J.-i. Hayashi, C.-Z. Li, FT-Raman spectroscopic study of the evolution of char structure during the pyrolysis of a Victorian brown coal, Fuel, 85 (2006) 1700-1707.

[20] X. Li, J.-i. Hayashi, C.-Z. Li, Volatilisation and catalytic effects of alkali and alkaline earth metallic species during the pyrolysis and gasification of Victorian brown coal. Part VII. Raman spectroscopic study on the changes in char structure during the catalytic gasification in air, Fuel, 85 (2006) 1509-1517.

[21] X. Li, C.-Z. Li, Volatilisation and catalytic effects of alkali and alkaline earth metallic species during the pyrolysis and gasification of Victorian brown coal. Part VIII. Catalysis and changes in char structure during gasification in steam, Fuel, 85 (2006) 1518-1525.

Chapter 3

Formation of Aromatic Structures during the Pyrolysis of Bio-oil

3.1 Introduction

The pyrolysis of biomass is a very effective means of energy densification. With the bio-char returned to the field as a soil conditioner and for carbon bio-sequestration, bio-oil is a complex chemical mixture that can be used in many ways, including being upgraded into liquid transport biofuels or being used as a feedstock for gasifiers or conventional boilers (e.g. co-fired with coal) [1-5].

However, bio-oil is exceedingly reactive and would undergo drastic changes when it is further heated up, which could impact on its utilisation [6, 7]. The formation of various large/complex aromatic ring systems is especially important. For example, coke formation during the upgrading of bio-oil can deactivate catalysts and is a major operating problem. Tar formation in a gasifier is a major problem for the utilisation of the gasification product gas [8, 9].

Insufficient knowledge exists about the formation of various aromatic ring systems during the pyrolysis of biomass and the subsequent utilisation of bio-oil. Lignin, cellulose and hemicellulose are the most important cellular components of woody biomass in the production of bio-oil. While lignin contains abundant mono-aromatic structures, the woody biomass generally contains little polycyclic aromatic ring structures [10]. Even the mono-aromatic ring structures in lignin could lead to the formation of aromatic ring systems containing more than one benzene ring during pyrolysis.

As part of our ongoing efforts to understand the formation of aromatic ring systems during the pyrolysis of biomass and the further utilisation of bio-oil, this study aims to investigate the evolution of aromatic ring structures during the thermal decomposition (pyrolysis) of bio-oil between 350 and 850 °C. To gain further insight into the reactions involved, cellulose- and lignin-derived oligomers separated from bio-oil were also pyrolysed under similar conditions. While relatively simple aromatic compounds were quantified with gas chromatography – mass spectrometry (GC-MS), UV-fluorescence spectroscopy was used to trace the overall development of aromatic ring systems during pyrolysis.

3.2 Experimental section

3.2.1 Preparation of bio-oil and bio-oil fractions

The bio-oil used in this study was produced from the pyrolysis of mallee eucalypts (E. loxopheba ssp. lissophloia) wood at fast heating rates in a fluidised-bed reactor (nominally 1 kg/hr) at 500 °C. A detailed description of the reactor system and the experimental procedure can be found in Section 2.2, ***Chapter 2***. The bio-oil was stored in a freezer (about -10 °C) until required in further experiments described herein.

The bio-oil was separated into water-soluble and water-insoluble fractions through the cold water precipitation (Section 2.2, ***Chapter 2***). The water-insoluble fraction (filter cake) was further washed with CH_2Cl_2 to produce CH_2Cl_2-soluble (~18.0 wt% of bio-oil) and CH_2Cl_2-insoluble (~3.6 wt% of bio-oil) fractions. This process was repeated to prepare a significant amount of water-insoluble but CH_2Cl_2-soluble fraction for the pyrolysis experiments described below. The water-insoluble-CH_2Cl_2-soluble fraction is mainly the lignin-derived oligomers in the bio-oil [11, 12]. Again, the sample was dried and stored in a freezer until required.

The pure cellulose powder (α-cellulose, Sigma-Aldrich) was dried in the oven at 105 °C for 24 hours prior to use in experiment.

3.2.2 Pyrolysis experiment

The pyrolysis of bio-oil, cellulose and lignin-derived oligomers was carried out in a novel two-stage fluidised-bed/fixed-bed quartz reactor (Figure 3-1). A detailed description of the reactor system and the experimental procedure can be found in Section 2.3, ***Chapter 2***.

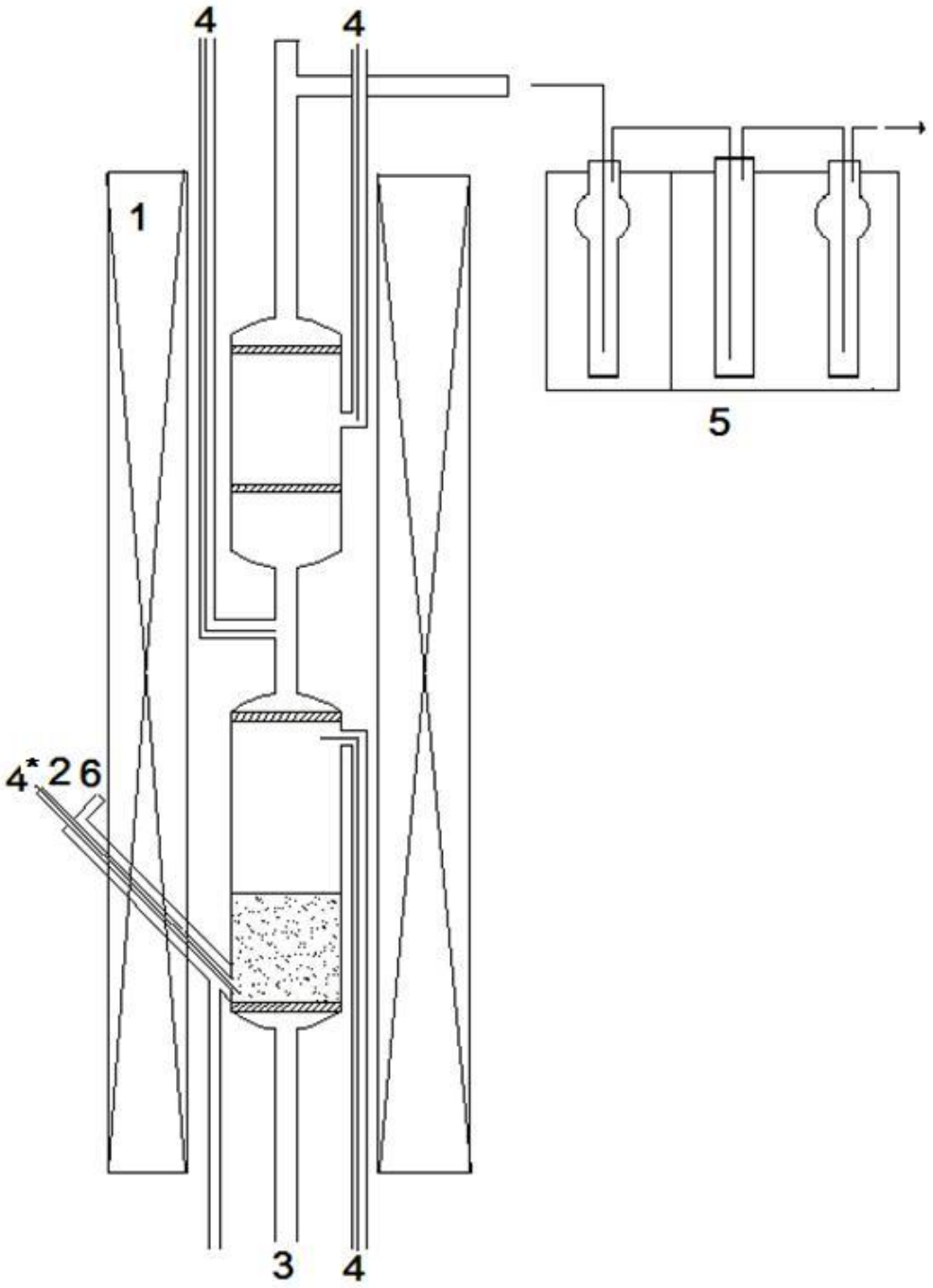

Figure 3-1. A schematic diagram of the two-stage fluidised-bed/fixed-bed reactor system. 1, furnace; 2, feeding tube; 3, fluidising gas inlet 4, thermocouples; 5, tar trap system; 6, air cooling tube. *: This thermocouple was used to measure the temperature in the fluidized bed, and it would be replaced by a feeding probe after target temperature was reached.

Briefly, 60 grams of silica sand were used as a bed material in the bottom stage of the reactor, which was fluidised with argon fed into the reactor from the bottom. The bio-oil was fed into the reactor via an air-cooled injection probe, with the help of argon carrier gas (0.21 L/min), at a rate of 100 mg/min using a syringe pump equipped with a 20 ml stainless steel syringe. The weights of the syringe and the injection probe were recorded before and after an experiment to calculate the amount of bio-oil fed into the reactor. The solid feedstock (water-insoluble-CH_2Cl_2-soluble fraction and cellulose) particles were entrained in a feeder with argon (1 L/min) and fed into the fluidised bed at 100 mg/min via a cold-water cooled injection probe.

The reactor was operated with two different temperature profiles. For the pyrolysis of bio-oil and water-insoluble-CH_2Cl_2-soluble fraction, both the top and bottom stages of the reactor were maintained at the same temperature. For the pyrolysis of cellulose, the bottom stage of the reactor was maintained at 500 °C, which was the same temperature as that used to produce the bio-oil from the pyrolysis of wood in the larger pyrolysis facility. The volatiles produced from the pyrolysis of cellulose in the bottom stage directly entered (i.e. in-situ) the top stage where the temperature was controlled at a level between 500 to 850 °C to investigate the pyrolysis of the nascent volatiles produced from the bottom stage.

The flow rate of fluidising gas was adjusted so that the actual total flow rate and therefore the gas residence time inside the top stage of the reactor remained roughly constant even when the reactor temperature was increased.

The produced gas exiting the reactor passed through a series of three tar traps containing HPLC grade $CHCl_3$:CH_3OH mixture (80:20 by volume) cooled respectively with ice-water (the first trap) and dry ice (the second and third traps) baths as outlined in Section 2.3, ***Chapter 2***. The tarry materials would be dissolved and trapped in the solvent mixture. Tar is experimentally defined as the material that dissolves in the mixture solvent but does not evaporate at 35 °C within 4 hours and was determined following the procedure outlined previously.

Depending on the pyrolysis temperature, two types of tar were determined. "Trapped tar" refers to the tar trapped in the $CHCl_3$:CH_3OH mixture in the traps described above. In addition, the solvent mixture was used to wash the sand bed and the reactor to collect the residual tar, which is termed as "washed tar". The yield of "washed tar" became negligible once the temperature reached 500 °C or higher. The total tar is the sum of the trapped tar and the washed tar.

3.2.3 Characterization of tar

3.2.3.1 UV-Fluorescence Spectroscopy

In this study, the UV-fluorescence spectra of tars were recorded using a Perkin-Elmer LS50B spectrometer. The detail procedure can be found Section 2.6.1, ***Chapter 2***. At the same concentration, the fluorescence intensity was multiplied by the bio-oil/tar yield to express the fluorescence intensity on the basis of "per gram of feedstock".

3.2.3.2 GC-MS analysis

Samples were analysed using an Agilent GC-MS with a capillary column (INNOWax). The details of the instrument and procedures can be found in 2.6.2, ***Chapter 2.***

3.3 Results and discussion

3.3.1 Aromatic ring systems in the original bio-oil

Figure 3-2 shows the synchronous spectra of bio-oil and its fractions. The fluorescence intensity was multiplied by the yield of each fraction to express the fluorescence intensity on the basis of "per gram of bio-oil". The water-insoluble-CH_2Cl_2-soluble fraction gave the strongest fluoresce intensity among all the fractions of bio-oil. Comparing the intensity and the shape of peaks between the raw bio-oil and the water-insoluble-CH_2Cl_2-soluble fraction, it can be concluded that the aromatic structures, especially the larger aromatic ring systems (intensities at wavelengths between 310 nm and 370 nm), of bio-oil are in this fraction. This fraction contains mainly lignin-derived materials particularly oligomers. Therefore in this paper this fraction is termed as lignin-derived oligomers fraction [11, 13]. This observation is in good agreement with the previous studies on the identification of the different fractions of bio-oil [11, 12, 14-17].

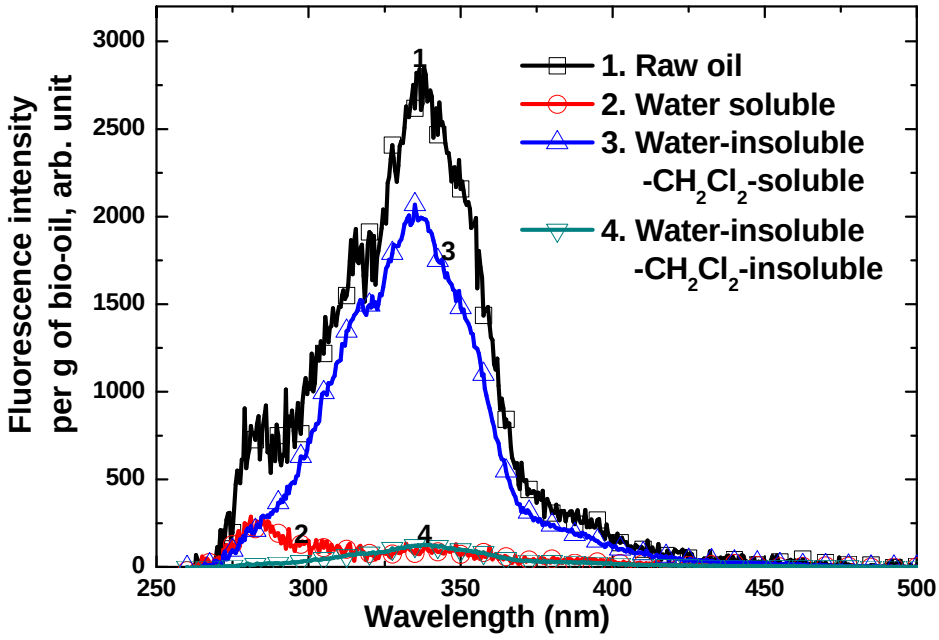

Figure 3-2. Constant energy (-2800 cm^{-1}) synchronous spectra of different fractions produced from the precipitation of bio-oil in cold water and the subsequent washing of the filter cake with CH_2Cl_2. The fluorescence intensity is expressed on the basis of per g of bio-oil.

UV-fluorescence spectra shown in Figure 3-2 are strongly biased towards larger (with two or more fused benzene rings or equivalent) aromatic ring systems. GC-MS was used to analyse the light components in the bio-oil. Figure 3-3 and Table 3-1 show that similar types of mono-ring aromatic structures are present in the raw bio-oil and its water-insoluble-CH_2Cl_2-soluble fraction. However, the lighter compounds with retention time shorter than 15 min (Figure 3-3) were present in the bio-oil but only at much lower concentration (or not all) in the water-insoluble-CH_2Cl_2-soluble fraction. These compounds must have been dissolved in the water during the precipitation of bio-oil in cold water.

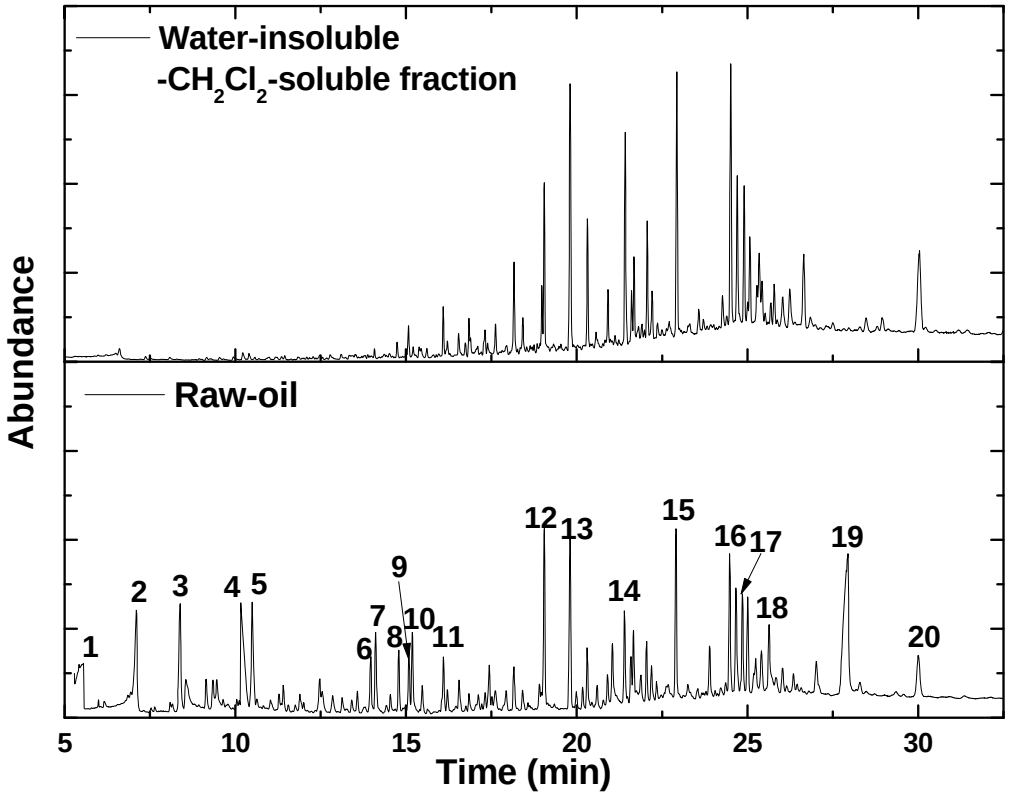

Figure 3-3. GC-MS total ion chromatograms of the raw bio-oil and its water-insoluble-CH_2Cl_2-soluble fraction. See Table 3-1 for the tentative identification of the peaks numbered.

Table 3-1. Tentative identification of peaks in raw bio-oil determined by GC-MS

No.	*Compound*	*No.*	*Compound*
1	Water 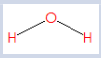	**11***	2-Methoxy-4-(2-propenyl) phenol (Eugenol) 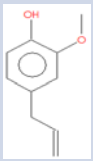
2	Methoxy methanol 	**12***	2,6-Dimethoxy phenol (Syringol) 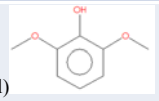
3	1-hydroxy-2-Propanone 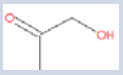	**13***	4-Methoxy-3-(methoxymethyl) phenol 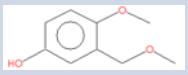
4	Acetic Acid 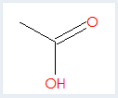	**14***	2,6-Dimethoxy-4-(2-propenyl) phenol 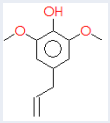
5	Furfural 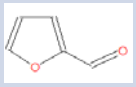	**15***	2-acetate-1,3-dimethoxy-5-(1-propenyl)- Benzen 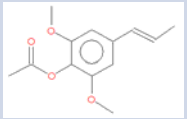
6	2(5H)-Furanone 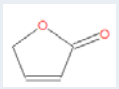	**16***	4-hydroxy-3,5-Dimethoxy benzaldehyde (Syringaldehyde) 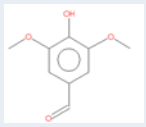
7	1,2-Cyclopentanedione 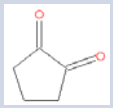	**17***	1-(4-hydroxy, 3,5-dimethoxyphenyl) Ethanone 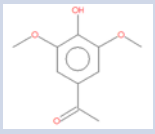
8	2-Hydroxy-3-methyl-2-cyclopenten-1-one 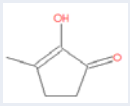	**18***	Desaspidinol 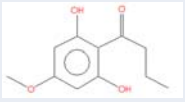
9*	2-Methoxyphenol (Guaiacol) 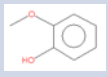	**19**	1,6-Anhydro-β-d-glucopyranose (Levoglucosan) 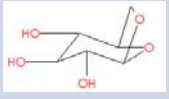
10*	2-Methoxy-4-methylphenol 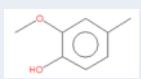	**20***	3,5-Dimethoxy-4-hydroxycinnamaldehyde 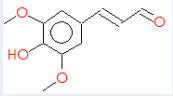

*: Compounds with aromatic structures.

3.3.2 Formation and evolution of aromatic structures during the pyrolysis of cellulose, bio-oil and its lignin-derived oligomers

3.3.2.1 Pyrolysis of cellulose

Figure 3-4 shows the tar yield from cellulose as a function of pyrolysis temperature in the top stage when the bottom stage was kept at 500 °C. As expected, the tar yield decreased with increasing temperature due to the intensified decomposition of tar molecules with increasing temperature.

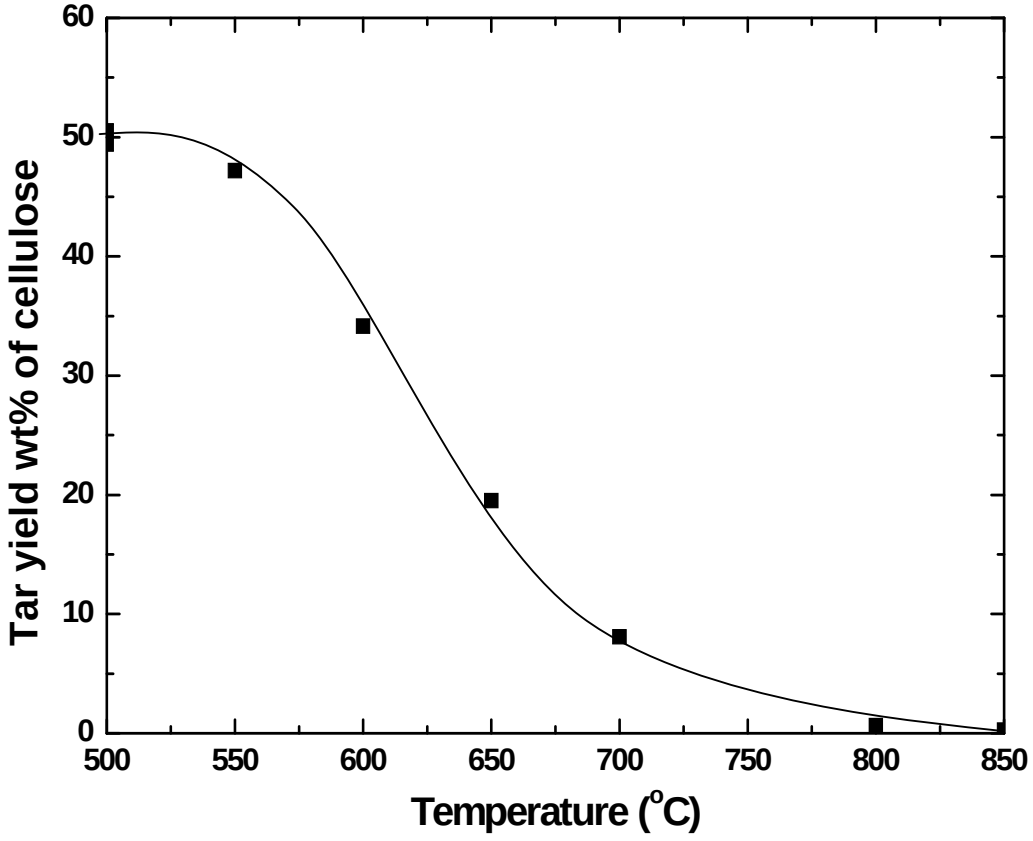

Figure 3-4. Total tar yield from cellulose as a function of pyrolysis temperature (500 to 850 °C).

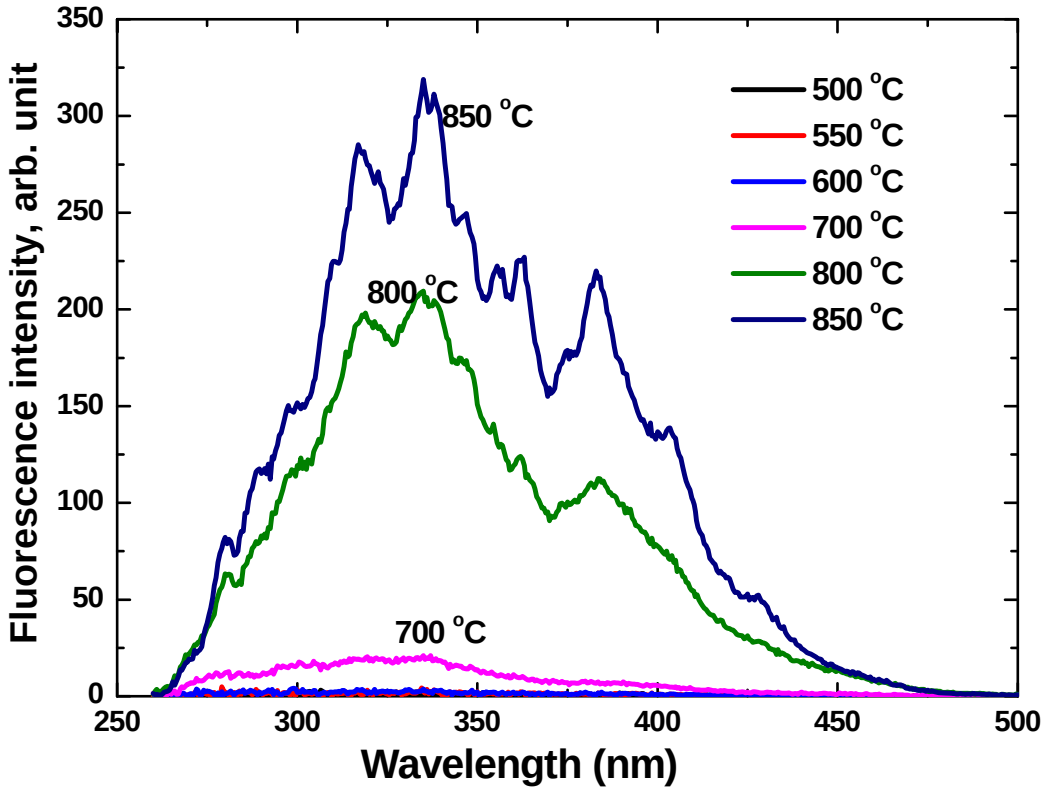

Figure 3-5. Constant energy (-2800 cm^{-1}) synchronous spectra of the tars produced from the pyrolysis of cellulose at temperatures between 500 and 850 °C. The fluorescence intensity is expressed on the basis of the same tar concentration.

The fluorescence synchronous spectra of these tars are shown in Figure 3-5. There was negligible fluorescence intensity until the temperature of the top stage reactor was raised up to 700 °C. At 600 °C or lower, little larger aromatic ring systems (with 2 or more fused benzene rings or equivalent) were formed in the tar. At 700 °C or higher, the pyrolysis reactions generated high concentrations of radicals that would form larger aromatic ring systems, for example, via the Diels-Alder type reactions [18]. However, because the tar yield became very small (< 10 wt%) at 700 °C and almost negligible (< 1 wt%) at 800 and 850 °C, the actual yields of larger aromatic ring systems were very low.

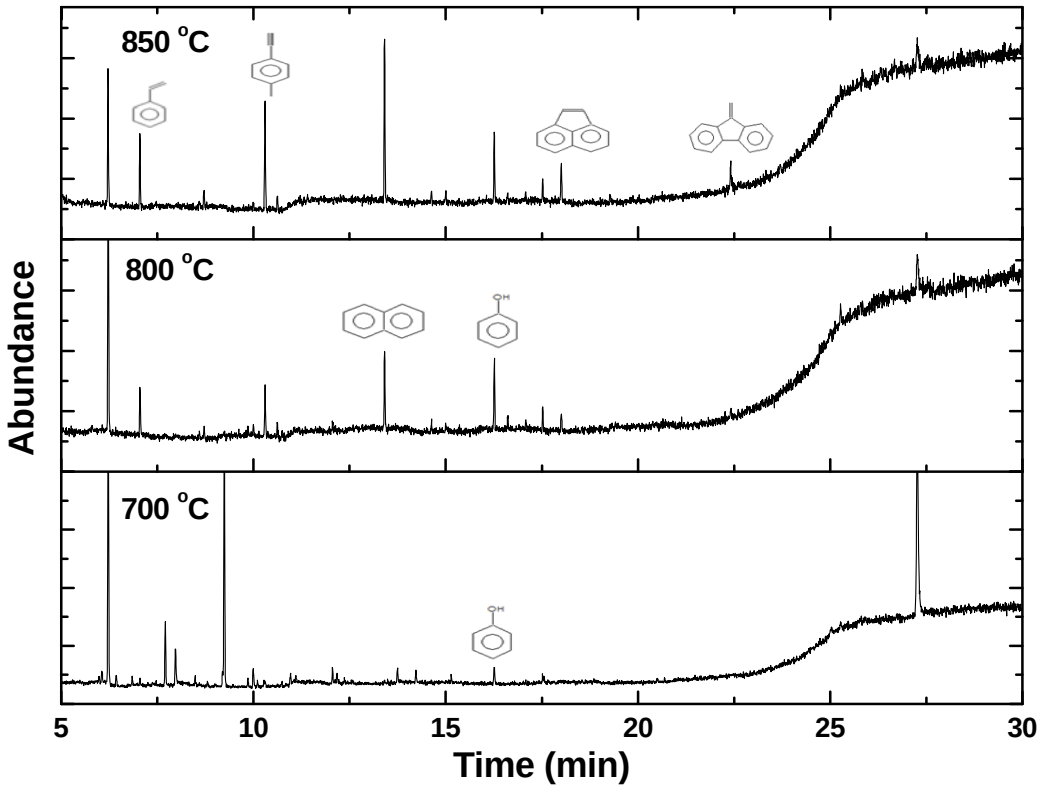

Figure 3-6. GC-MS total ion chromatograms of the tars produced from the pyrolysis of cellulose at different temperatures (700 to 850 °C).

The fluorescence data in Figure 3-5 would indicate the presence of ring systems containing 2 or more fused benzene rings (or equivalent). This was further confirmed by the analysis of tar samples with GC-MS, as is shown in Figure 3-6. It should be emphasised that some larger aromatic ring systems may exist in a large molecule that cannot be eluted out of the GC column and thus Figure 3-6 is only a brief indication (lower estimates) of the aromatic ring systems in the tar.

3.3.2.2 Pyrolysis of lignin-derived oligomers

Figure 3-7 presents the tar yield from the pyrolysis of lignin-derived oligomers in the bio-oil as a function of pyrolysis temperature (with both the bottom and top stages of reactor set at the same temperatures) between 350 and 800 °C. As expected, the total tar yield decreased with increasing pyrolysis temperature. However, the yield of trapped tar increased to a maximum at around 500 °C and then decreased with increasing temperature. The difference between the yield of "trapped tar" and total tar, which is the yield of "washed tar", diminished rapidly with increasing temperature from 350 °C to 500 °C. Taken together, these data indicate that a substantial portion, up to 50 wt% at 350 °C, of the lignin-derived oligomers could simply not evaporate at low temperature and thus stayed in the fluidised bed of sand. Further increases in temperature resulted in the breakdown of these large molecules and simultaneously enhanced their evaporation (due to increased vapour pressure) to result in negligible amounts of materials in the fluidised bed of sand that can be washed away with the solvent mixture of $CHCl_3$ and CH_3OH.

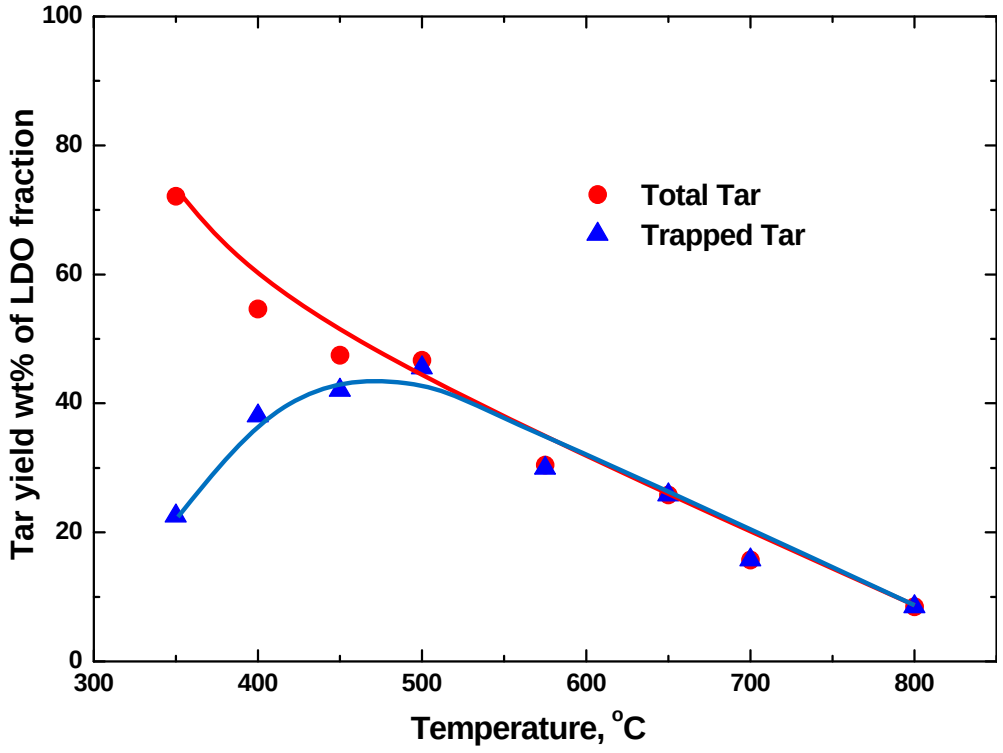

Figure 3-7. Tar yield from the lignin-derived oligomers as a function of pyrolysis temperature (350 to 800 °C).

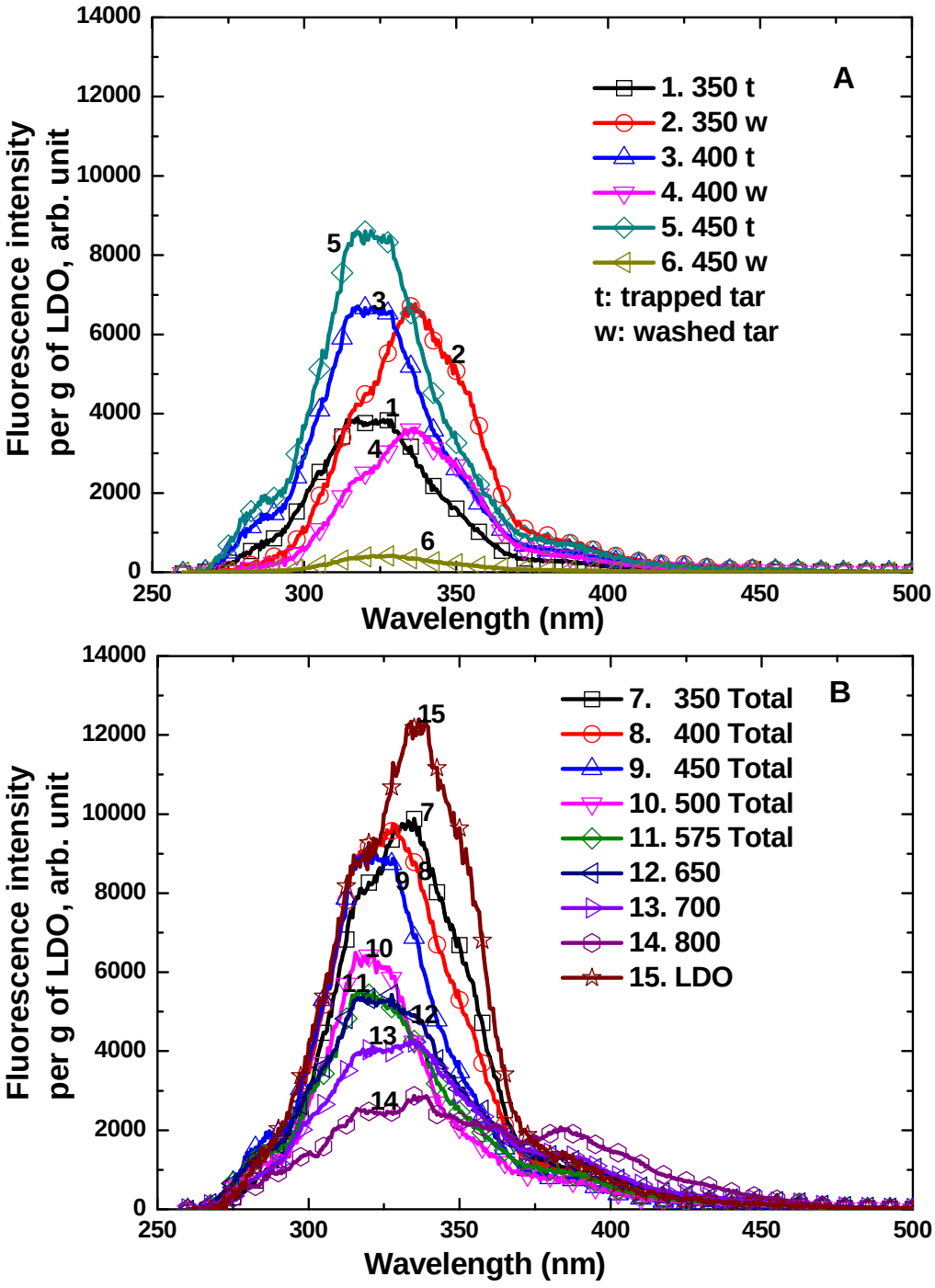

Figure 3-8. Constant energy (-2800 cm^{-1}) synchronous spectra of the tars produced from the pyrolysis of lignin-derived oligomers at temperatures between 350 and 800 °C. "LDO" denotes the lignin-derived oligomers and "Total" refers to the sum of the "trapped tar" and the "washed tar".

Figure 3-8 presents the synchronous spectra of the lignin-derived oligomer fraction of bio-oil and the tars produced from pyrolysis of the lignin-derived oligomers. The fluorescence intensity is expressed on the basis of feedstock – the lignin-derived oligomers fraction itself and thus is a reflection of the "yields" of larger aromatic ring systems. It is interesting to note the differences between the spectra of "trapped tar" and "washed tar" produced at the same temperature (e.g. 350 °C). The aromatic ring size distribution, as is qualitatively reflected by the shape of the synchronous spectra, tended to shift to larger ones (longer wavelength) going from the "trapped tar" to the "washed tar". In other words, the heavier "washed tar" also tended to have larger aromatic ring systems than the lighter "trapped tar" (Figure 3-8A). The "yields" of larger aromatic ring systems in the "washed tar" decreased drastically with increasing temperature; while those in the corresponding "trapped tar" increased.

However, the data in Figure 3-8B indicate that the sum of the fluorescence intensities (especially between 310 and 375 nm) of "trapped tar" and "washed tar" was smaller than that of the original feedstock – the lignin-derived oligomers in the bio-oil. Because the non-condensable gases would not contain larger aromatic ring systems, it then appears that significant portions of the larger aromatic ring systems have turned into solid (i.e. coke) insoluble in $CHCl_3$-CH_3OH mixture. Even the formation of additional larger aromatic ring systems at elevated pyrolysis temperature (e.g. 700 °C) was not sufficient to account for the loss of larger aromatic systems due to coke formation. It is only at 800 °C that the formation of additional very large aromatic ring systems (> 375 nm) have resulted in the fluorescence intensity of tar to exceed that of the feedstock lignin-derived oligomers at wavelengths longer than 375 nm.

3.3.2.3 Pyrolysis of bio-oil

Figure 3-9 shows the total yields of tar from the pyrolysis of bio-oil at temperatures between 350 and 800 °C. The first datum point refers to the raw bio-oil. About 65 wt% of the bio-oil was determined as "tar" under our conditions of tar determination. In other words, about 35 wt% of bio-oil evaporated due to the presence of a whole array of light components in the bio-oil, including water and organic volatile components.

The tar yield from the pyrolysis of bio-oil showed a relatively weak maximum at around 500 °C. As the tar yields shown in Figure 3-9 already include both "washed tar" and "trapped tar", it would appear that some components in bio-oil that was produced at 500 °C turned into solids insoluble in $CHCl_3$-CH_3OH mixture when it was re-heated to 350 °C. With increasing temperature beyond 500 °C, the thermal cracking of bio-oil resulted in decreases in the tar yield.

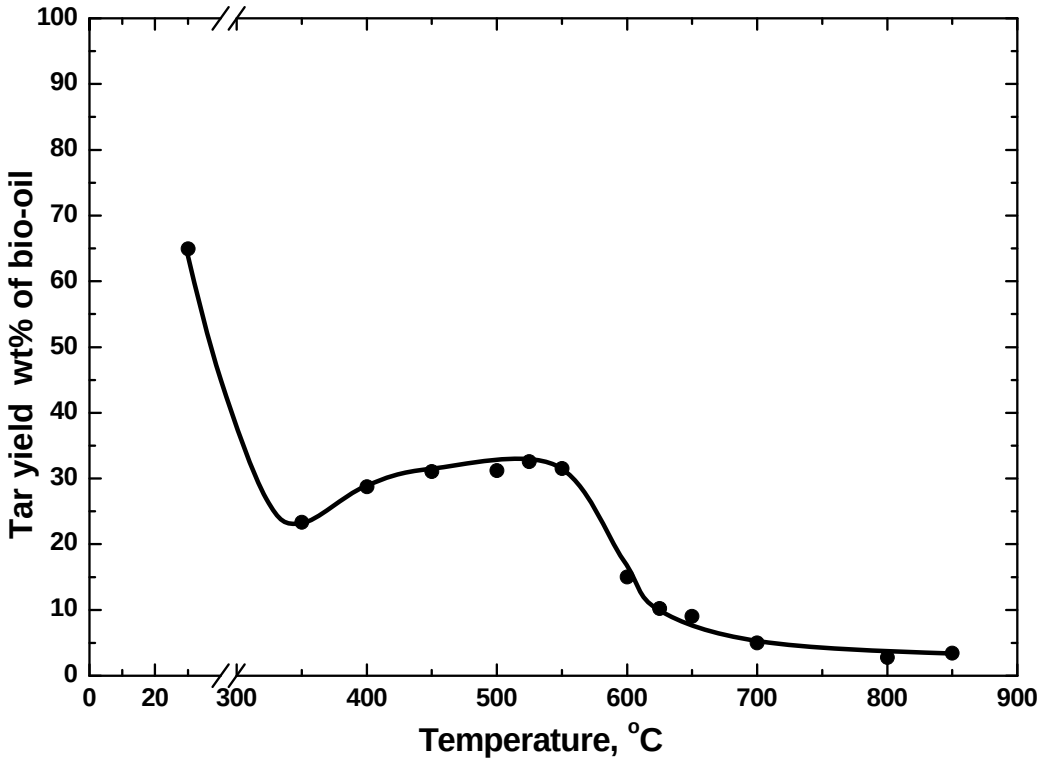

Figure 3-9. Total tar yield from the pyrolysis of bio-oil as a function of pyrolysis temperature (350 to 850 °C).

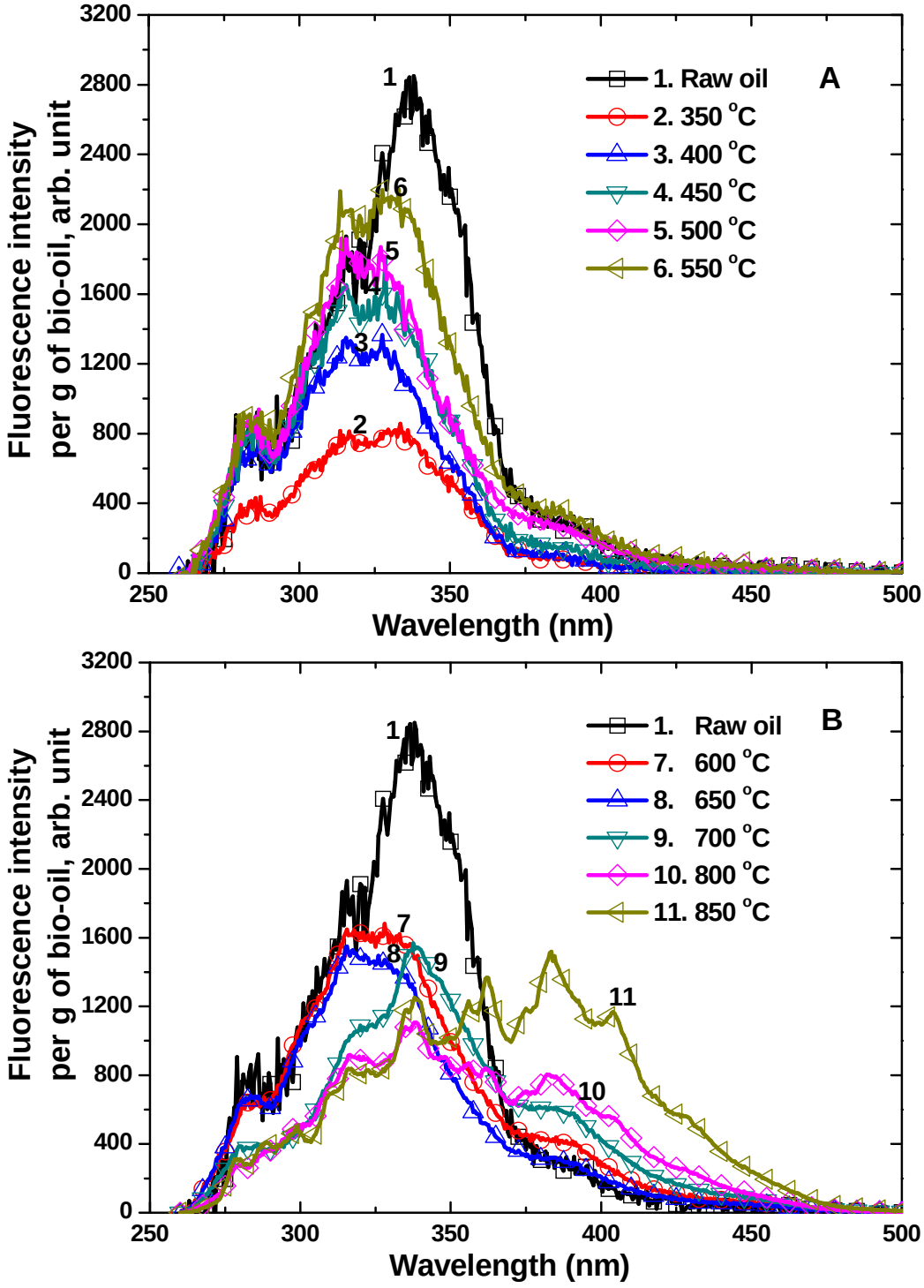

Figure 3-10. Constant energy (-2800 cm^{-1}) synchronous spectra of the total tars produced from the pyrolysis of bio-oil at temperatures between 350 and 850 °C.

Further evidence about the formation of solid material that is insoluble in $CHCl_3$ and CH_3OH mixture, which is often termed as "coke", is shown in Figure 3-10 when the raw bio-oil and its tars produced after pyrolysis were examined with UV-fluorescence spectroscopy. Because the synchronous fluorescence intensity has been expressed on the basis of "per g of bio-oil", the fluorescence intensity becomes a semi-quantitative reflection of the "yields" of the larger aromatic ring systems during pyrolysis. Similar to the pyrolysis of cellulose and the lignin-derived oligomers, the fluorescence data could be divided into two groups for pyrolysis at lower (Figure 3-10A) and higher (Figure 3-10B) temperatures. Compared with the spectrum of raw bio-oil, the spectral intensities of its tars (Figure 3-10A) decreased, especially at wavelengths longer than about 325 nm, indicating that some larger aromatic ring systems in the raw bio-oil were not recovered as tar. Increasing temperature from 350 to 550 °C (Figure 3-10A) resulted in large increases in the "yields" of larger aromatic ring systems, but still lower than the original bio-oil. Further increases in pyrolysis temperature from 600 to 850 °C (Figure 3-10B) resulted in decreases in the fluorescence intensity at wavelengths < 340 nm but increases at wavelengths > 370 nm, indicating the formation of additional very large aromatic ring systems that might not have existed in the raw bio-oil.

The data in Figure 3-10 indicate that the polymerisation reactions took place significantly when the bio-oil was reheated. The changes in the fluorescence intensity (Figure 3-10A, reflecting aromatic ring systems) with increasing temperature were a lot more drastic than the corresponding changes in the tar yields (Figure 3-9, reflecting both aromatic and non-aromatic materials), especially in the pyrolysis temperature range of 350 to 550 °C. This is believed to indicate that the polymerisation reactions were particularly effective involving larger aromatic ring systems. Clearly, the UV-fluorescence spectroscopy is a lot more sensitive than tar yield measurement in detecting changes in the yields of larger aromatic ring systems [11].

Furthermore, the thermal cracking reactions at temperatures > 550 °C have decreased the tar yield (Figure 3-9) and the "yields" of some smaller aromatic ring systems (275 to 340 nm, Figure 3-10B) but increased the yields of very large (> 370 nm, Figure 3-10B) aromatic ring systems. The GC-MS analysis indeed detected

some new aromatic compounds (such as fluorene and pyrene) after pyrolysis at high temperatures. Some large aromatic ring systems may be present in large tar molecules and have thus not been detected by GC-MS. Because the bio-oil contained a significant amount (~19 wt%) [11, 19, 20] of water and the thermal cracking reactions would also have produced more water, it then becomes clear that the self-reforming of bio-oil with steam under our experimental conditions were insufficient to suppress the formation of aromatic ring systems. This is in agreement with our earlier studies on the reforming of biomass volatiles [21, 22].

3.3.3 Comparison between the pyrolysis of bio-oil and that of lignin-derived oligomers

The data in Figure 3-2 indicate that the fluorescence properties of the raw bio-oil are dominated largely by its lignin-derived oligomers, in agreement with our previous study [11]. However, the pyrolysis behaviour of the lignin-derived oligomers (Figures 3-7 and 3-8) and that of the raw bio-oil (Figures 3-9 and 3-10) are not completely similar although they do have great similarities. In particular, more aromatic ring structures during the pyrolysis of bio-oil at 350 and 400 °C (Figure 3-10) have turned into solid, i.e. not detected as tar, than during the pyrolysis of lignin-derived oligomers (Figure 3-8) which had been separated from the same bio-oil. The amount of aromatic structures turning into solid decreased drastically with increasing pyrolysis temperature (Figure 3-10).

The exact reasons for the differences in pyrolysis behaviour between the bio-oil and lignin-derived oligomers remain unclear. However, it is believed that the differences originate from the differences in their composition. Bio-oil is an exceedingly complex mixture. In particular, bio-oil contains a lot of reactive, often O-containing, species such as acids, aldehydes and sugars formed from the breakdown of cellulose/hemicellulose [11, 22, 23]. These reactive species would dissociate to form radicals at relatively low temperatures e.g. 350 °C or lower. In comparison, the lignin-derived species, particularly larger aromatic ring systems (likely containing various substitutional groups) are relatively stable. When bio-oil is

heated up to 350 °C or higher (Figure 3-10), the radicals generated from the decomposition of these reactive species would attack and activate the structures containing larger aromatic ring systems, which in turn would combine/polymerise to become insoluble in the $CHCl_3$+CH_3OH solvent mixture. This would include the combination not only among lignin-derived species but also among cellulose-derived species and lignin-derived species. At low temperatures around 350 °C, the radical combination reactions (including polymerisation) dominates over the decomposition reactions. This appears to provide a plausible explanation for the transformation of large portion of larger aromatic ring systems in the bio-oil into solids (coke) at 350 and 400 °C (Figure 3-10) that is insoluble in $CHCl_3$+CH_3OH.

With increasing temperature, the decomposition reactions became significant. Even if some solid has been formed involving larger aromatic ring systems due to the enhanced polymerisation by the cellulose/hemicellulose-derived species, the solid would appears to be unstable and thus would decompose. This would seem to explain why the "yields" of larger aromatic ring systems increased with increasing temperature (Figure 3-10) during the pyrolysis of bio-oil.

In the case of the pyrolysis of lignin-derived oligomers, in the absence of cellulose/hemicellulose-derived reactive species, any radicals required for the combination (polymerisation) involving larger aromatic ring systems would have to come from the bond-breakage of the lignin-derived oligomers, which is relatively stable at low temperature. This explains the relatively high "yields" of larger aromatic ring systems in the lignin-derived oligomers remained as soluble in $CHCl_3$+CH_3OH after pyrolysis at low temperature.

Another distinct difference in the pyrolysis behaviour between bio-oil and its lignin-derive oligomers at high temperatures (> 700 °C) is the presence of very large (> 375 nm) aromatic ring systems in the tar of the bio-oil (Figure 3-10) but not so much in the tar of the lignin-derived oligomers (Figure 3-8). These very large aromatic ring systems appear to have origin in the cellulose-derived products. The pyrolysis of cellulose did generate these very large aromatic systems (Figure 3-5).

The bio-oil also contains some small amounts (~3.6 wt%) of water-insoluble-CH_2Cl_2-insoluble materials, which are mainly the high molecular

mass materials. The pyrolysis behaviour of this fraction remains unknown because the preparation of a significant amount of this fraction for the pyrolysis experiments was difficult due to its low concentration in the bio-oil.

3.4 Conclusions

The bio-oil produced from the pyrolysis of mallee wood at 500 °C at fast heating rates in a 1 kg/hr fluidised-bed reactor has been pyrolysed again in a bench-scale novel two-stage fluidised-bed/fixed-bed reactor at temperatures between 350 and 850 °C. The majority of larger (≥ 2 rings) aromatic ring systems as detected by UV-fluorescence spectroscopy are in the lignin-derived oligomers. To gain insights into the reactions responsible for the formation and evolution of aromatic ring systems during the re-pyrolysis of bio-oil, the lignin-derived oligomers were separated from the bio-oil and pyrolysed under the same conditions. The pyrolysis of cellulose (especially the volatiles formed in situ in the bottom reactor) has given further information about the formation of aromatic systems from the cellulose-derived species during the pyrolysis of bio-oil. The results from this study indicate that significant portions of aromatic ring systems in the bio-oil could turn/polymerise into solids not soluble in $CHCl_3$+CH_3OH during the pyrolysis at relatively low temperatures e.g. 350-400 °C. This process can be enhanced by the presence of cellulose/hemicellulose-derived species in the bio-oil, which are reactive and produce radicals to enhance the polymerisation reactions. The pyrolysis of cellulose-derived species in the bio-oil at high temperatures (e.g. > 700 °C) tended to form additional very large aromatic ring systems.

3.5 References

[1] D. Chiaramonti, A. Oasmaa, Y. Solantausta, Power generation using fast pyrolysis liquids from biomass, Renewable and Sustainable Energy Reviews, 11 (2007) 1056-1086.

[2] A. Demirbas, Progress and recent trends in biodiesel fuels, Energy Conversion and Management, 50 (2009) 14-34.

[3] S. Iborra, G. Huber, Synthesis of transportation fuels from biomass: chemistry, catalysts, and engineering, Chemical reviews, 106 (2006) 4044-4098.

[4] D.C. Elliott, A. Oasmaa, Catalytic hydrotreating of black liquor oils, Energy & Fuels, 5 (1991) 102-109.

[5] X. Li, R. Gunawan, C. Lievens, Y. Wang, D. Mourant, S. Wang, H. Wu, M. Garcia-Perez, C.-Z. Li, Simultaneous catalytic esterification of carboxylic acids and acetalisation of aldehydes in a fast pyrolysis bio-oil from mallee biomass, Fuel, 90 (2011) 2530-2537.

[6] S. Czernik, A.V. Bridgwater, Overview of applications of biomass fast pyrolysis oil, Energy & Fuels, 18 (2004) 590-598.

[7] A.V. Bridgwater, The technical and economic feasibility of biomass gasification for power generation, Fuel, 74 (1995) 631-653.

[8] A.G. Gayubo, B. Valle, A.T. Aguayo, M. Olazar, J. Bilbao, Pyrolytic lignin removal for the valorization of biomass pyrolysis crude bio-oil by catalytic transformation, Journal of Chemical Technology & Biotechnology, 85 (2010) 132-144.

[9] T.A. Milne, N. Abatzoglou, R.J. Evans, Biomass gasifier “tars”: their nature, formation, and conversion, NERL, Golden, CO, USA, 1998.

[10] J. Zakzeski, P.C.A. Bruijnincx, A.L. Jongerius, B.M. Weckhuysen, The catalytic valorization of lignin for the production of renewable chemicals, Chemical

Reviews, 110 (2010) 3552-3599.

[11] M. Garcia-Perez, S. Wang, J. Shen, M. Rhodes, W.J. Lee, C.-Z. Li, Effects of temperature on the formation of lignin-derived oligomers during the fast pyrolysis of mallee woody biomass, Energy & Fuels, 22 (2008) 2022-2032.

[12] B. Scholze, D. Meier, Characterization of the water-insoluble fraction from pyrolysis oil (pyrolytic lignin). Part I. PY-GC/MS, FTIR, and functional groups, Journal of Analytical and Applied Pyrolysis, 60 (2001) 41-54.

[13] M. Garcia-Perez, A. Chaala, H. Pakdel, D. Kretschmer, C. Roy, Characterization of bio-oils in chemical families, Biomass and Bioenergy, 31 (2007) 222-242.

[14] C.A. Mullen, A.A. Boateng, Characterization of water insoluble solids isolated from various biomass fast pyrolysis oils, Journal of Analytical and Applied Pyrolysis, 90 (2010) 197-203.

[15] B. Scholze, C. Hanser, D. Meier, Characterization of the water-insoluble fraction from fast pyrolysis liquids (pyrolytic lignin): Part II. GPC, carbonyl goups, and 13C-NMR, Journal of Analytical and Applied Pyrolysis, 58-59 (2001) 387-400.

[16] R. Bayerbach, V.D. Nguyen, U. Schurr, D. Meier, Characterization of the water-insoluble fraction from fast pyrolysis liquids (pyrolytic lignin): Part III. Molar mass characteristics by SEC, MALDI-TOF-MS, LDI-TOF-MS, and Py-FIMS, Journal of Analytical and Applied Pyrolysis, 77 (2006) 95-101.

[17] R. Bayerbach, D. Meier, Characterization of the water-insoluble fraction from fast pyrolysis liquids (pyrolytic lignin). Part IV: Structure elucidation of oligomeric molecules, Journal of Analytical and Applied Pyrolysis, 85 (2009) 98-107.

[18] H. Richter, J.B. Howard, Formation of polycyclic aromatic hydrocarbons and their growth to soot--a review of chemical reaction pathways, Progress In Energy And Combustion Science, 26 (2000) 565-608.

[19] M. Garcia-Perez, X.S. Wang, J. Shen, M.J. Rhodes, F. Tian, W.-J. Lee, H. Wu, C.-Z. Li, Fast pyrolysis of oil mallee woody biomass: Effect of temperature on

the Yield and quality of pyrolysis products, Industrial & Engineering Chemistry Research, 47 (2008) 1846-1854.

[20] D. Mourant, Z. Wang, M. He, X.S. Wang, M. Garcia-Perez, K. Ling, C.-Z. Li, Mallee wood fast pyrolysis: Effects of alkali and alkaline earth metallic species on the yield and composition of bio-oil, Fuel, 90 (2011) 2915-2922.

[21] Z. Min, M. Asadullah, P. Yimsiri, S. Zhang, H. Wu, C.-Z. Li, Catalytic reforming of tar during gasification. Part I. Steam reforming of biomass tar using ilmenite as a catalyst, Fuel, 90 (2011) 1847-1854.

[22] C. Lievens, D. Mourant, M. He, R. Gunawan, X. Li, C.-Z. Li, An FT-IR spectroscopic study of carbonyl functionalities in bio-oils, fuel, In Press, Corrected Proof (2011).

[23] J. Shen, X.-S. Wang, M. Garcia-Perez, D. Mourant, M.J. Rhodes, C.-Z. Li, Effects of particle size on the fast pyrolysis of oil mallee woody biomass, Fuel, 88 (2009) 1810-1817.

Chapter 4

Formation of Coke during the Pyrolysis of Bio-oil

4.1 Introduction

Pyrolysis is an important route of biomass utilisation. In particular, the pyrolysis of biomass produces bio-oil that can be used in many ways, including being upgraded into liquid transport bio-fuels or being used directly as fuels for conventional boilers or modern gasifiers [1-4].

Regardless if bio-oil is chemically upgraded, combusted or gasified/reformed, bio-oil will have to be heated up first. As bio-oil is heated up, it will undergo thermal decomposition reactions, which often result in the formation of solid carbonaceous materials (coke) [5-7]. The formation of coke is a particularly serious problem for the upgrading or processing of bio-oil. For example, the coke can foul/deactivate the catalyst for bio-oil upgrading [8, 9]. The coke deposit may also plug the downstream equipment of a gasification system.

Bio-oil has a very complicated chemical composition, having hundreds or thousands of compounds with a wide range of functionalities [10, 11]. These species in bio-oil have originated from the thermal decomposition of biomass components such as lignin, cellulose and hemicelluloses as well as the interactions among the intermediates from these biomass components. Many species in bio-oil, having reactive functionalities, such as carboxylic acids, aldehydes and sugars, are exceedingly reactive even at room temperature. As bio-oil is heated up, these species in bio-oil become even more reactive. Bio-oil species will therefore continue to decompose and interact with each other. The reactions responsible for coke formation are thus exceedingly complex, forming a reaction network, involving both decomposition and polymerization reactions. The mechanism of coke formation during the thermal decomposition of bio-oil remains poorly understood. In particular, little is known about the importance of the interactions among various bio-oil species from different biomass components as bio-oil is heated up. While separating a bio-oil into its constituent species is impossible, a bio-oil can be separated into various fractions having distinctly different properties. Investigating the formation of coke from each fraction as well as that from the whole bio-oil will gain significant insight into the complicated mechanism of coke formation from the pyrolysis of bio-oil.

This study aims to investigate the coke formation during the thermal decomposition (pyrolysis) of bio-oil when the bio-oil is heated up to elevated temperatures (250 to 800 °C). To gain further insight into the reactions involved, the lignin-derived oligomers separated from bio-oil were also pyrolysed under similar conditions. In addition to the quantification of coke yield as a function of temperature, UV-fluorescence spectroscopy was used to trace the formation and evolution of aromatic ring systems in bio-oil during pyrolysis.

4.2 Experimental section

4.2.1. Preparation of bio-oil and bio-oil fractions and pyrolysis experiment

The bio-oil used in this study was produced from the pyrolysis of mallee eucalypt (E. loxopheba ssp. lissophloia) wood at fast heating rates in a fluidised-bed reactor (nominally 1 kg/hr) at 500 °C (Section 2.2, ***Chapter 2***). The bio-oil was separated into water-soluble and water-insoluble fractions through the cold water precipitation. The water-insoluble fraction was further washed with CH_2Cl_2 to produce CH_2Cl_2-soluble (~18.0 wt% of bio-oil) and CH_2Cl_2-insoluble (~3.6 wt% of bio-oil) fractions. The water-insoluble-CH_2Cl_2-soluble fraction and water-insoluble-CH_2Cl_2-insoluble fraction together contain most of aromatic structure systems (especially the larger aromatic ring systems) in the bio-oil [12]. These two fractions contain mainly lignin-derived materials, especially lignin-derived oligomers [13-15]. Therefore, in this paper, these two fractions are termed as light lignin-derived oligomers fraction and heavy lignin-derived oligomers fraction, respectively. This terminology of lignin-derived oligomers is only used to facilitate the ease in discussion and does not imply that all species in the lignin-derived oligomers have their origin in lignin.

The pyrolysis of bio-oil and lignin-derived oligomers was carried out in a two-stage fluidised-bed/fixed-bed quartz reactor (Figure 2-1). The details of the pyrolysis system and operating procedures can be found in Section 2.3, ***Chapter 2***.

Three tar traps containing HPLC grade $CHCl_3$:CH_3OH mixture (80:20 by volume)

cooled respectively with ice-water (the first trap) and dry ice (the second and third traps) baths were used to trap the tar (Section 2.3, ***Chapter 2***).

In this study, the solid residual generated from pyrolysis experiment which cannot be dissolved into $CHCl_3$:CH_3OH mixture is experimentally defined as "coke". The reactor after an experiment was washed and then dried at 105 °C for 30 mins with air supply to evaporate the solvent used for tar washing. The coke was then burned with air. The coke was measured as the weight difference before and after the coke was burned.

The preparation of water-soluble and water-insoluble fractions from bio-oil based on the cold water precipitation method necessitated the use of a large amount of water. This presented a practical difficulty to concentrate the bio-oil organic species dissolved in the water (i.e. water-soluble fraction) into a form that can be easily fed into the pyrolysis reactor to determine the coke yield from the pyrolysis of water-soluble bio-oil fraction. The evaporation of water would necessarily also evaporate a large proportion of the water-soluble bio-oil fraction having boiling points similar to that of water. Any impurities in the original water used for the precipitation of bio-oil would also have been concentrated into the final residual after evaporation, rendering the coke yields from the subsequent pyrolysis of solid residual unreliable. Based on the above consideration, no attempt was made to concentrate the water-soluble fraction for pyrolysis. Instead, the coke yield from the water-soluble bio-oil fraction was calculated as:

$$\mathrm{Coke}_{\mathrm{water-solube}} = \frac{(\mathrm{Coke}_{\mathrm{Bio\text{-}oil}} - \mathrm{Coke}_{\mathrm{L\text{-}LDO}} \times \mathrm{wt\%}_{\mathrm{L\text{-}LDO}} - \mathrm{Coke}_{\mathrm{H\text{-}LDO}} \times \mathrm{wt\%}_{\mathrm{H\text{-}LDO}})}{1 - \mathrm{wt\%}_{\mathrm{L-LDO}} - \mathrm{wt\%}_{\mathrm{H-LDO}}}$$

where Coke is the coke yield from each fraction on the basis of "per gram of feedstock" and wt% is the weight percent of the fraction in the original bio-oil. L-LDO is the light lignin-derived oligomers fraction. H-LDO is the heavy lignin-derived oligomers fraction. It is obvious that the calculated coke yield for the water-soluble fraction would also include the coke formed from the interactions among the water-soluble and water-insoluble fractions.

Figure 4-1 summarises the experimental flow diagram for the bio-oil separation,

the bio-oil pyrolysis and the product quantification and characterisation.

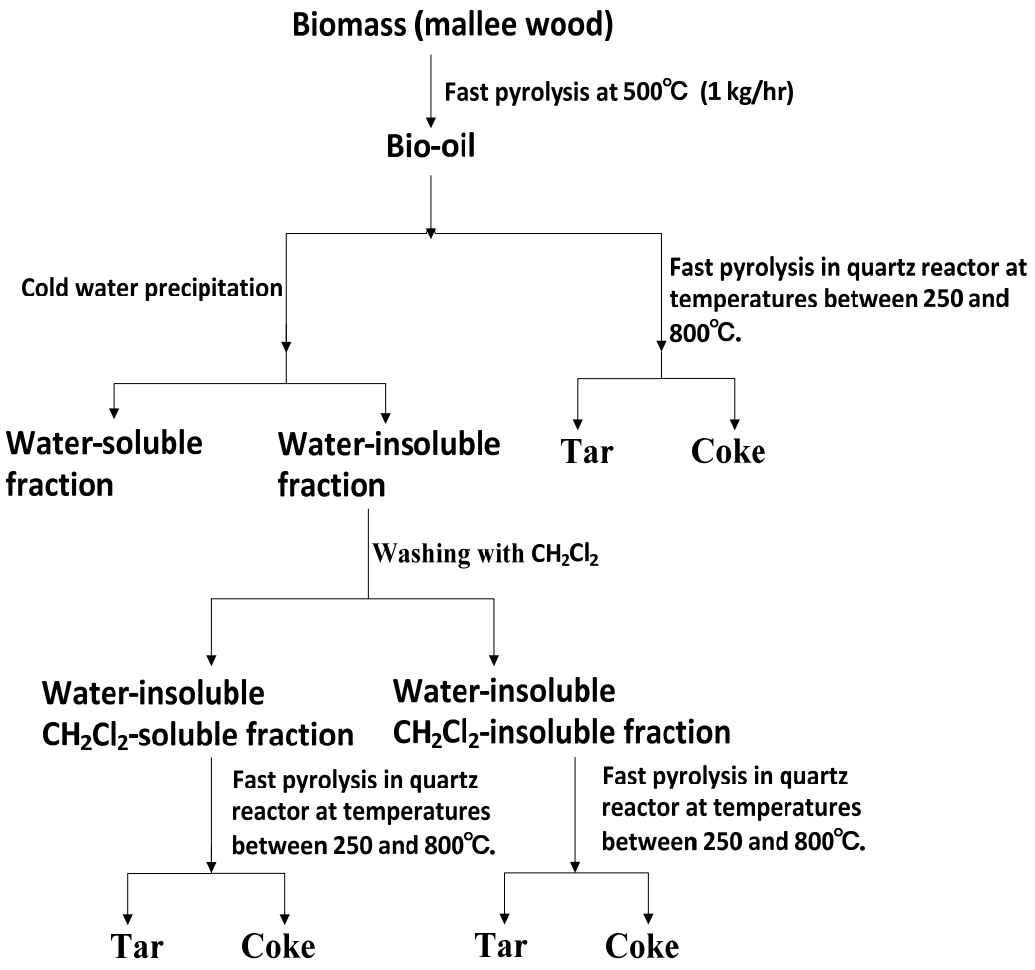

Figure 4-1. A flow chart of the types of experiments including the preparation of bio-oil, the separation of bio-oil fractions and the pyrolysis of bio-oil and its fractions.

4.2.2. Characterization of tar

In this study, the UV-fluorescence spectra of tars were recorded using a Perkin-Elmer LS50B spectrometer. The details have been described in Section 2.6.1, ***Chapter 2***. Briefly, tar solutions were diluted with CH_3OH to record their synchronous spectra with a constant energy difference of -2800 cm^{-1} between the excitation and emission monochromators. The fluorescence intensity was then

expressed on the basis of "per gram of bio-oil". Furthermore, the differences in fluorescence intensity between the tars produced from the pyrolysis of bio-oil and those from the lignin-derived oligomers under the same pyrolysis conditions were calculated on the basis of "per gram of bio-oil" [16-18].

When the synchronous fluorescence intensities were expressed on the basis of "per gram of bio-oil", the intensities of tars from the pyrolysis of bio-oil could serve as a semi-quantitative reflection of the "yield" of the aromatic species during pyrolysis. Therefore the fluorescence spectroscopy could be used to trace the formation and evolution of aromatic ring systems during pyrolysis.

4.3 Results and discussion

Figure 4-2 presents the coke yields from the pyrolysis of bio-oil, light lignin-derived fraction and heavy lignin-derived oligomers fraction as a function of temperature between 250 and 800 °C. It should be noted that the coke yields are shown in Figure 4-2 as accumulative. It is clear that all bio-oil fractions, both water-soluble and water-insoluble, could contribute to the formation of coke. While the coke yields from the light lignin-derived oligomers and heavy lignin-derived oligomers fractions were determined experimentally (details given below) and expressed on the basis of "per g of bio-oil", the "coke yield" from the water-soluble fraction was calculated as the difference between the coke yield of bio-oil and that of the water-insoluble (including light lignin-derived oligomers and heavy lignin-derived oligomers) under the same pyrolysis conditions. Therefore, the calculated coke yield of the water-soluble fraction also includes the coke formed due to the interactions among the water-soluble and water-insoluble fractions.

Figure 4-2 shows that coke can be formed over a wide range of temperatures from temperatures below 250 °C to temperatures over 800 °C in this study. The coke yield from the pyrolysis of bio-oil shows a maximum at around 350 °C. Obviously, the reactions dominant and responsible for coke formation at 800 °C would be drastically different from those at temperatures below 250 °C. Therefore, the

discussion in what follows will be divided into two temperature ranges.

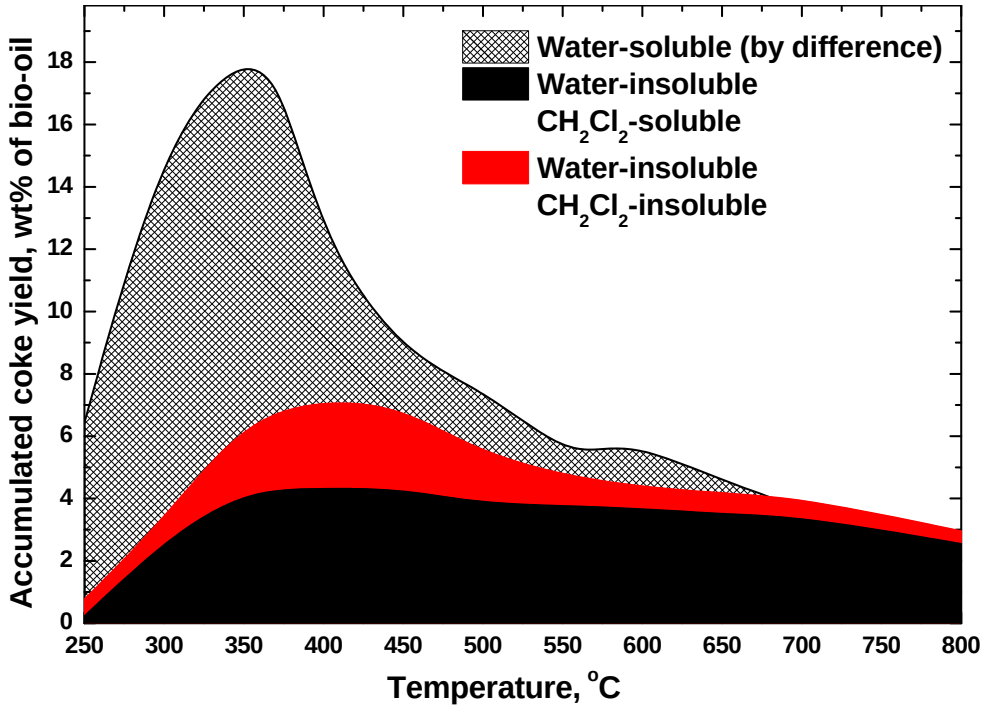

Figure 4-2. Coke yields from the pyrolysis of bio-oil and its fractions as functions of pyrolysis temperature (250 to 800 °C).

This fraction contains mainly lignin-derived materials particularly oligomers. Therefore in this paper this fraction is termed as lignin-derived oligomers fraction [10, 19]. This observation is in good agreement with the previous studies on the identification of the different fractions of bio-oil [13-15, 19-21].

4.3.1 Coke formation during the pyrolysis of bio-oil at high temperature (> 450 °C)

Figure 4-3 shows the coke yields from the pyrolysis of water-insoluble bio-oil fractions (including the CH_2Cl_2-soluble light lignin-derived oligomers fraction and the CH_2Cl_2-insoluble heavy lignin-derived oligomers fraction) at temperatures between 450 and 800 °C. These coke yields were those determined experimentally and are expressed on the basis of the "feedstock", i.e. on the basis of the pyrolysis substrate fed into the fluidised-bed/fixed-bed reactor. In other words, these results

directly show the capacity of each individual feedstock in the formation of coke during pyrolysis.

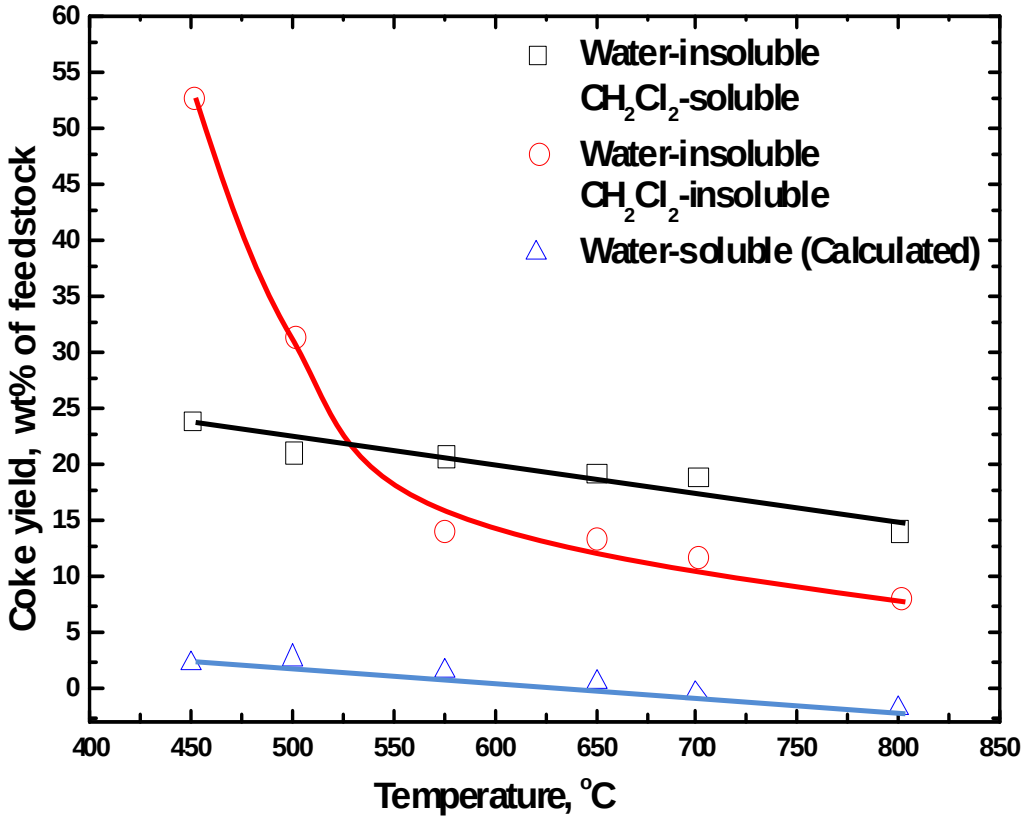

Figure 4-3. Coke yields from the pyrolysis of lignin-derived oligomers and water-soluble fraction as functions of pyrolysis temperature (450 to 800 °C).

The data in Figure 4-3 indicate that the coke yield from the light lignin-derived oligomers was significant (~25 wt% at 450 °C) and showed much less sensitivity to increasing temperature than that from the heavy lignin-derived oligomers fraction. This can be understood by considering that the light lignin-derived oligomers fraction is relatively stable with significant aromatic structures. These structures appear to polymerise easily to form coke.

The heavy lignin-derived oligomers could also form a large amount of coke at 450 °C (Figure 4-3), which then decreased rapidly with increasing temperature. In fact, this heavy lignin-derived oligomers fraction contains lignin (and possibly cellulose/hemicellulose) structures that have undergone limited extents of thermal decomposition when the bio-oil was prepared from the pyrolysis of wood at 500 °C.

The heavy lignin-derived oligomers fraction could also contain the products from the re-polymerisation of reactive species in the bio-oil vapour as the vapour was cooled down to condense as the liquid bio-oil when the original bio-oil was prepared. In either case, the heavy lignin-derived oligomers fraction would contain structures that are thermally instable and can be further decomposed as it is heated up. In other words, the partially decomposed structures (from lignin or other wood components in wood) would further decompose to form structures approaching those in the light lignin-derived oligomers fraction. It is thus noteworthy that the coke yields from both light lignin-derived oligomers and heavy lignin-derived oligomers fractions showed similar stability at temperatures above 600 °C. This provides a plausible explanation for the decreases in the coke yield from heavy lignin-derived oligomers with increasing temperature from 450 °C to 600 °C in Figure 4-3.

The water-soluble fraction (including the interactions) has much lower tendency (Figure 4-3) to form coke than the water-insoluble (light lignin-derived oligomers plus heavy lignin-derived oligomers) fractions when the pyrolysis temperature was higher than 450 °C. The water-soluble fraction is dominated by light species from the pyrolysis of wood, especially those from cellulose/hemicelluloses. Compared with the water-insoluble fractions, much lower concentration of aromatic structures, especially larger ones, were in the water-soluble fraction [12]. It thus appears that the observed coke yield at elevated temperatures (> 450 °C) is largely related to the concentration of aromatics species which serve as good precursors for coke formation. These results in Figure 4-3 indicate that, when these light species in the water-soluble fraction were heated up rapidly to elevated temperatures (> 450 °C) as they mixed with the hot sand particles in the reactor, the evaporation and thermal decomposition were the dominant processes, producing little coke (Figure 4-3).

In fact, at high temperatures (> 700 °C), the calculated yields for the water-soluble fraction were even negative. This is believed to be due to the "self-gasification" of coke by the species in the bio-oil. The bio-oil contained a significant amount (~ 20 wt%) of water. The thermal decomposition of bio-oil, especially the light water-soluble species, would also produce significant amounts of water and other reactive species such as CO_2. Therefore, the coke formed from the pyrolysis of bio-oil at elevated temperatures (> 700 °C) could be gasified by steam and these

reactive species (e.g. CO_2) as soon as the coke was formed. Alternatively, the reforming of coke-forming species (including those from lignin-derived species in light lignin-derived oligomers and heavy lignin-derived oligomers) in the gas phase could have been intensified at high temperatures to reform the coke-forming species directly into light gases. In either case, the net result is that the coke-forming tendency of the light lignin-derived oligomers and heavy lignin-derived oligomers fractions was effectively reduced. Therefore, the data in Figure 4-3 serve to provide evidence that the formation of coke from various species in the bio-oil may not be additive.

4.3.2 Coke formation during the pyrolysis of bio-oil at low temperatures (< 450 °C)

Figure 4-4 presents the coke yields (on the basis of the feedstock fed into the reactor) from the pyrolysis of light lignin-derived oligomers fraction and heavy lignin-derived oligomers fraction at temperatures between 250 and 450 °C. While the bio-oil was produced from the pyrolysis of wood at 500 °C, reheating the bio-oil (Figure 4-2) and/or its water-insoluble fraction (Figure 4-4) to 250 °C (much lower than the temperature the oil was produced) could produce substantial amounts of coke. This coke formation was clearly due to the re-polymerisation of bio-oil components. The coke yields from the pyrolysis of both lignin-derived oligomers fractions increased with increasing temperature from 250 °C to 400 °C (Figure 4-4). These results therefore indicate that the increases in temperature in this range intensified the polymerisation reactions.

While bio-oil contains some concentrations of radicals even at room temperature, these radicals are largely stable and at very low concentrations. The formation of additional coke with increasing temperature in the range of 250 to 450 °C must have originated from additional bond breakage, creating additional radicals, which could recombine to result in coke formation. The data in Figure 4-4 thus indicate that the lignin-derived oligomers fractions, frequently believed to be relatively stable, could generate enough radicals to result in up to 50% of its mass (heavy lignin-derived

oligomers) turning into coke at 350 to 400 °C.

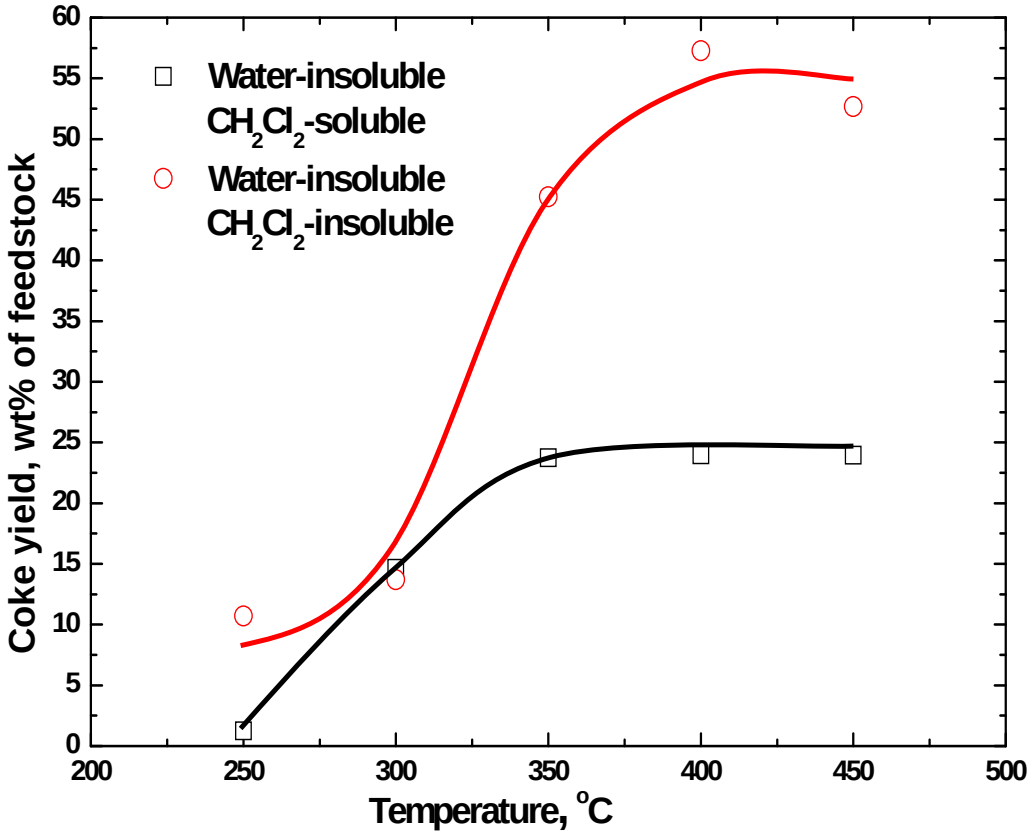

Figure 4-4. Coke yields from the pyrolysis of lignin-derived oligomers as functions of pyrolysis temperature (250 to 450 °C).

The most important observation in Figure 4-2 is the significant difference between the coke yields from the pyrolysis of whole bio-oil and those from the pyrolysis of lignin-derived oligomers fractions in the low temperature range (< 450 °C). The difference is due to the presence of the water-soluble fraction in the bio-oil, playing a substantial role in the formation of coke during the pyrolysis of bio-oil at low temperatures.

Two possible routes of coke formation involving the water-soluble species might be conceptualised. The first one is the coke formation directly from the species in the water-soluble fraction. The second one is the coke formation through the interactions among the species in the water-soluble and water-insoluble fractions (light

lignin-derived oligomers plus heavy lignin-derived oligomers) during the pyrolysis of bio-oil.

In the water-soluble fraction of bio-oil, besides a small portion of small aromatic species (normally with a single ring, e.g. phenols), the main species had originated from the decomposition of cellulose/hemicellulose during the pyrolysis of biomass [12]. In this study, levoglucosan, the single most abundant organic compound in the bio-oil (about 6~7 wt%), was pyrolysed at 400 °C in the fluidised-bed/fixed-bed reactor under otherwise the same experimental conditions as those for the pyrolysis of bio-oil. 15 wt% of levoglucosan turned into solid (coke) which was not soluble in $CHCl_3$+CH_3OH. Kawamoto et al.[22] also reported that substantial amounts of CH_3OH-insoluble solid can be formed from the pyrolysis of levoglucosan at temperatures between 300 and 400 °C. It can thus be concluded that coke can be formed from the species in the water-soluble fraction during the pyrolysis of bio-oil at temperatures between 250 and 450 °C.

In addition to levoglucosan, other species such as furans and cyclic ketones in the water-soluble fraction may form coke in this temperature range. Because the water-soluble fraction contains numerous compounds with a wide range of functionalities, it was impractical to quantify the yield of coke from each individual species under our experimental conditions. This means that no direct evidence could be obtained to prove/disprove if all the coke formation during the pyrolysis of bio-oil could be accounted for by the coke yield of each individual species or if the interactions have contributed to the formation of substantial amounts of coke. However, indirect evidence was obtained to emphasise the importance of the interactions among the species in the water-soluble and water-insoluble fractions to the formation of coke. This will be discussed below.

4.2.3 The importance of interaction to coke formation during the pyrolysis of bio-oil

Figure 4-5 show the differences between the synchronous spectra of the tars produced from the pyrolysis of bio-oil and those from the pyrolysis of lignin-derived oligomers fractions at temperatures between 250 and 800 °C. The majority of larger aromatic ring systems that can be detected by the fluorescence spectroscopy in the bio-oil were in the water-insoluble fraction with the water-soluble fraction containing negligibly small amounts of larger aromatic ring systems. This is in good agreement with the literature [12]. It was surprised to note in Figure 4-5A that less aromatic ring systems were released from the pyrolysis of bio-oil than from the pyrolysis of lignin-derived oligomers fractions, resulting in the negative fluorescence intensity difference. In other words, the presence of the water-soluble fraction in the bio-oil has hindered the release of aromatic ring systems in the water-insoluble fraction. Since the large aromatic ring system might not be decomposed to gases at these low temperature (250 to 400 °C) [12], the aromatic ring systems not released due to the presence of the water-soluble fraction must have turned into coke during the pyrolysis of bio-oil. In the absence of the water-soluble fraction, these aromatic ring systems would have been released as tar, as is in the case of the pyrolysis of the water-insoluble fractions. The data in Figure 4-5A show that the additional amount of such aromatic ring systems turning into coke increased with increasing temperature from 250 to 300 °C to reach a maximum before it decreased with further increasing temperature from 300 to 450 °C. This trend of the additional amount of aromatic ring systems turning into coke is in good agreement with the trend in Figure 4-2 showing the coke yield due to the water-soluble fraction displaying a maximum around 300 °C. Therefore, the data in Figure 4-5A provide indirect but clear evidence that the water-soluble fraction interacted with the water-insoluble fraction to form additional coke during the pyrolysis of bio-oil at low temperatures.

The nature of the interactions among the water-soluble and water-insoluble fractions is believed to be radical reactions: the radicals were generated and then recombined to form bigger molecules (coke). Therefore the extents of such interactions would clearly change with temperature. At low temperatures (e.g. 250 °C), the interactions were limited by the amount of radicals that can be generated

at low temperatures. At high temperatures (e.g. > 400 °C), while significant amounts of radicals can be generated, the thermal breakdown of both coke precursors and the newly formed coke became dominant to limit the amount of coke that can be formed from such interactions.

At very high temperatures (> 500 °C), the thermal decomposition became the dominant reactions, diminishing the amount of coke that can be formed. Accompanying the thermal decomposition would be the formation of additional aromatic ring systems. The data in Figure 4-5B indicate that the pyrolysis of the water-soluble and water-insoluble fractions co-existing in the bio-oil has produced more aromatic ring systems as tar than the pyrolysis of water-insoluble fraction alone. It is clear that the pyrolysis of the water-soluble fraction has contributed to the formation of aromatic ring systems, in good agreement with our previous observation that the pyrolysis of cellulose-derived species (which could be the main source of water-soluble species) at higher temperature (> 700°C) resulted in the formation of aromatics [12].

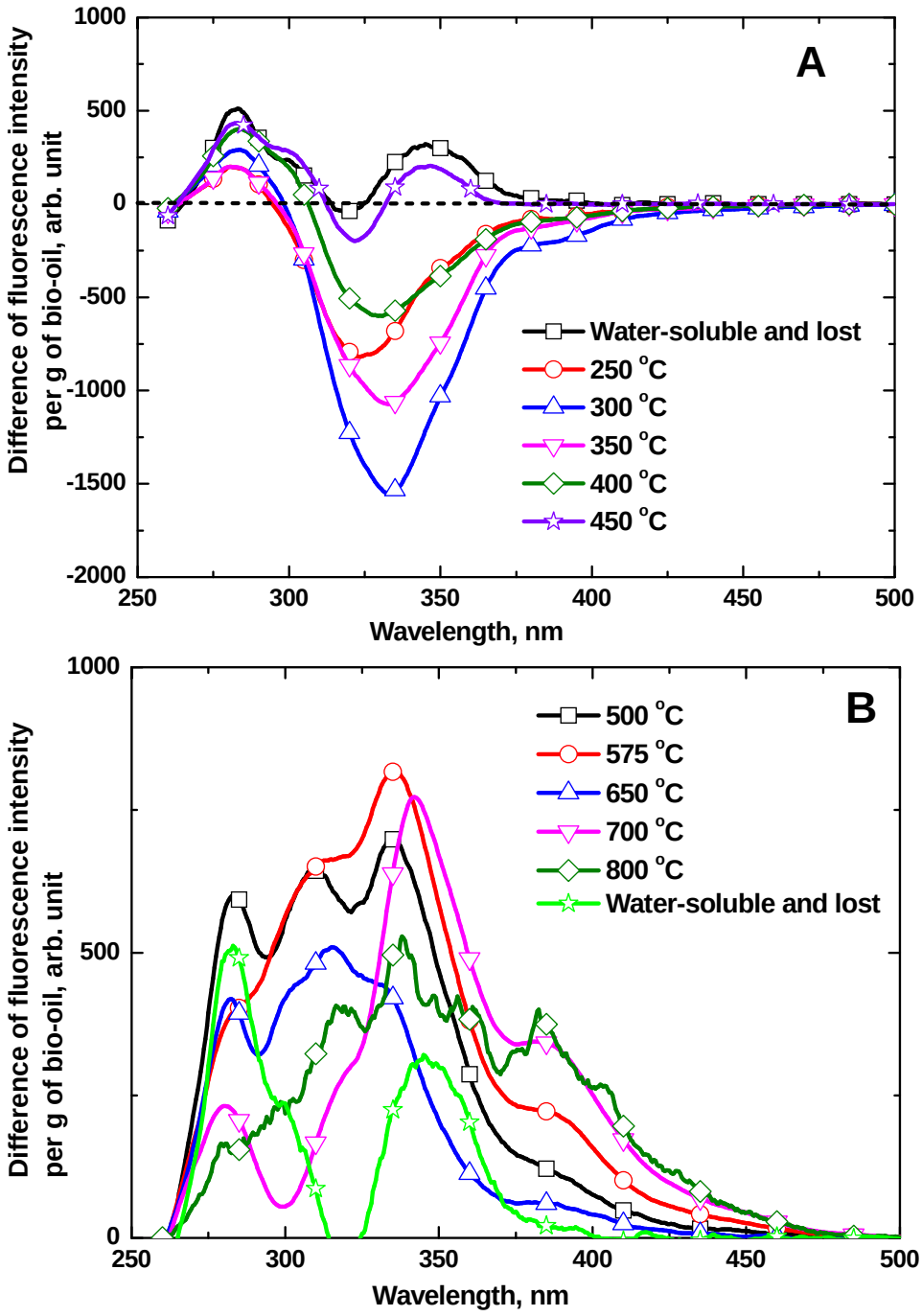

Figure 4-5. Differences of constant energy (-2800 cm-1) synchronous spectra of the tars produced from the pyrolysis of bio-oil and those form the pyrolysis of lignin-derived oligomers at temperatures (A) between 250 and 450°C, (B) between 500 and 800°C.

4.4 Conclusions

The bio-oil produced from the pyrolysis of mallee wood at 500 °C at fast heating rates in a 1 kg/hr fluidised-bed reactor has been pyrolysed again in a bench-scale two-stage fluidised-bed/fixed-bed reactor at temperatures between 250 and 800 °C. The pyrolysis of the lignin-derived oligomers, separated from the same bio-oil, has given information about the formation of coke from lignin-derived oligomers during the pyrolysis of bio-oil. This study has also gained insights into the interactions between the species in water-soluble fraction (mainly cellulose/hemicellulose-derived species) and lignin-derived oligomers in the formation of coke during the re-pyrolysis of bio-oil. Our results indicate that, besides the coke formation directly from the species in the water-soluble fraction, significant portions of lignin-derived oligomers in the bio-oil could turn/polymerise into coke during the pyrolysis at relatively low temperatures e.g. 250-400 °C. This process can be enhanced by the presence of cellulose/hemicellulose-derived species in the bio-oil, which are reactive and produce radicals to enhance the polymerisation reactions. The interactions were suppressed with increasing temperature (e.g. > 450 °C) due to the intensified decomposition. Self-gasification of coke by the water in the bio-oil and the water (and other species) formed during the re-pyrolysis of bio-oil at high temperature (e.g. > 700 °C) may decrease the observed yield of coke.

4.5 References

[1] D. Chiaramonti, A. Oasmaa, Y. Solantausta, Power generation using fast pyrolysis liquids from biomass, Renewable and Sustainable Energy Reviews, 11 (2007) 1056-1086.

[2] S. Iborra, G. Huber, Synthesis of transportation fuels from biomass: chemistry, catalysts, and engineering, Chemical reviews, 106 (2006) 4044-4098.

[3] D.C. Elliott, A. Oasmaa, Catalytic hydrotreating of black liquor oils, Energy & Fuels, 5 (1991) 102-109.

[4] X. Li, R. Gunawan, C. Lievens, Y. Wang, D. Mourant, S. Wang, H. Wu, M. Garcia-Perez, C.-Z. Li, Simultaneous catalytic esterification of carboxylic acids and acetalisation of aldehydes in a fast pyrolysis bio-oil from mallee biomass, Fuel, 90 (2011) 2530-2537.

[5] G. van Rossum, B.M. Güell, R.P.B. Ramachandran, K. Seshan, L. Lefferts, W.P.M. Van Swaaij, S.R.A. Kersten, Evaporation of pyrolysis oil: Product distribution and residue char analysis, AIChE Journal, 56 2200-2210.

[6] R.P.B. Ramachandran, G. van Rossum, W.P.M. van Swaaij, S.R.A. Kersten, Evaporation of biomass fast pyrolysis oil: Evaluation of char formation, Environmental Progress & Sustainable Energy, 28 (2009) 410-417.

[7] A. Sanna, K. Ogbuneke, J.M. Andrésen, Bio-coke from upgrading of pyrolysis bio-oil for co-firing, fuel, 88 (2009) 2340-2347.

[8] D. Wang, S. Czernik, D. Montane, M. Mann, E. Chornet, Biomass to hydrogen via fast pyrolysis and catalytic steam reforming of the pyrolysis oil or its fractions, Industrial & Engineering Chemistry Research, 36 (1997) 1507-1518.

[9] S. Czernik, R. French, C. Feik, E. Chornet, Hydrogen by catalytic steam reforming of liquid byproducts from biomass thermoconversion processes, Industrial & Engineering Chemistry Research, 41 (2002) 4209-4215.

[10] M. Garcia-Perez, A. Chaala, H. Pakdel, D. Kretschmer, C. Roy, Characterization of bio-oils in chemical families, Biomass and Bioenergy, 31 (2007) 222-242.

[11] C. Lievens, D. Mourant, M. He, R. Gunawan, X. Li, C.-Z. Li, An FT-IR spectroscopic study of carbonyl functionalities in bio-oils, fuel, 90 (2011) 3417-3423.

[12] Y. Wang, X. Li, D. Mourant, R. Gunawan, S. Zhang, C.-Z. Li, Formation of aromatic structures during the pyrolysis of bio-oil, Energy & Fuels, 26 (2012) 241-247.

[13] B. Scholze, D. Meier, Characterization of the water-insoluble fraction from pyrolysis oil (pyrolytic lignin). Part I. PY-GC/MS, FTIR, and functional groups, Journal of Analytical and Applied Pyrolysis, 60 (2001) 41-54.

[14] R. Bayerbach, D. Meier, Characterization of the water-insoluble fraction from fast pyrolysis liquids (pyrolytic lignin). Part IV: Structure elucidation of oligomeric molecules, Journal of Analytical and Applied Pyrolysis, 85 (2009) 98-107.

[15] R. Bayerbach, V.D. Nguyen, U. Schurr, D. Meier, Characterization of the water-insoluble fraction from fast pyrolysis liquids (pyrolytic lignin): Part III. Molar mass characteristics by SEC, MALDI-TOF-MS, LDI-TOF-MS, and Py-FIMS, Journal of Analytical and Applied Pyrolysis, 77 (2006) 95-101.

[16] C.-Z. Li, K.D. Bartle, R. Kandiyoti, Vacuum pyrolysis of maceral concentrates in a wire-mesh reactor, fuel, 72 (1993) 1459-1468.

[17] C.-Z. Li, K.D. Bartle, R. Kandiyoti, Characterization of tars from variable heating rate pyrolysis of maceral concentrates, fuel, 72 (1993) 3-11.

[18] C.-Z. Li, C. Sathe, J.R. Kershaw, Y. Pang, Fates and roles of alkali and alkaline earth metals during the pyrolysis of a Victorian brown coal, fuel, 79 (2000) 427-438.

[19] M. Garcia-Perez, S. Wang, J. Shen, M. Rhodes, W.J. Lee, C.-Z. Li, Effects of temperature on the formation of lignin-derived oligomers during the fast

pyrolysis of mallee woody biomass, Energy & Fuels, 22 (2008) 2022-2032.

[20] C.A. Mullen, A.A. Boateng, Characterization of water insoluble solids isolated from various biomass fast pyrolysis oils, Journal of Analytical and Applied Pyrolysis, 90 (2010) 197-203.

[21] B. Scholze, C. Hanser, D. Meier, Characterization of the water-insoluble fraction from fast pyrolysis liquids (pyrolytic lignin): Part II. GPC, carbonyl goups, and 13C-NMR, Journal of Analytical and Applied Pyrolysis, 58-59 (2001) 387-400.

[22] H. Kawamoto, M. Murayama, S. Saka, Pyrolysis behavior of levoglucosan as an intermediate in cellulose pyrolysis: polymerization into polysaccharide as a key reaction to carbonized product formation, Journal of Wood Science, 49 (2003) 469-473.

Chapter 5

Catalytic Steam Reforming of Cellulose-derived Compounds using a Char-Supported Iron Catalyst

5.1 Introduction

Biomass gasification is an attractive method to produce synthesis gas [1-4]. However, there are many obstacles that need to be resolved before this process can become a viable commercial renewable energy technology. One of the most significant problems is the existence of tar in the product gas [4, 5]. Among many tar removal techniques, catalytic reforming is widely accepted as an efficient and economical option to convert tar into syngas [6-12].

Many catalysts have been investigated for tar reforming [5, 6, 13, 14]. Dolomites were used for tar elimination with high activity and low cost. However, as a result of fragility, they are very soft and quickly eroded in fluidised beds [15]. Although zeolites and olivine are inexpensive, they can be deactivated easily by coke deposition [16, 17]. Nordgreen et al. [18, 19] used elemental and metallic iron as catalysts for tar reforming during gasification of biomass in a fluidised bed. However, iron can be deactivated rapidly by coke in the absence of hydrogen. With high activity for converting tar to syngas, Ni-based catalysts have been widely used in biomass gasification [5, 6]. Nevertheless, Ni-based catalysts are expensive and hardly regenerated, limiting the use for industrial application [6].

Among these catalysts, the char or char-supported iron catalysts have shown adequate catalytic activities and have high economic feasibility for reforming tar during the gasification of biomass [14]. The further development of a tar reforming technology based on the char or char-supported catalysts requires a better understanding of the reactions involved. For example, the possible interactions among various species in the bio-oil/bio-volatiles on the catalyst surface remain largely unknown. In particular, little is known about how these interactions might affect the notorious coke formation on catalyst surface, which could deactivate the catalyst [13, 14].

Cellulose is one of the major chemical components of plant biomass, contributing a large portion of final products from the thermal treatments of biomass. For example, as a liquid product form the pyrolysis of biomass, bio-oil contains many cellulose-derived compounds such as aldehydes, ketones, acids, furfurals and

anhydrosugars [20, 21]. With well-defined chemical structure, cellulose has received much attention from studies on biomass utilisation. For example, the pyrolysis and/or gasification behaviour of cellulose has been a topic of intensive research to assist in understanding the corresponding behaviour of biomass [21-26]. However, insufficient knowledge exists about the catalytic steam reforming of cellulose-derived tar using a char-supported iron catalyst. This knowledge is non-negligible to understand the overall reactions occurring in the catalytic steam reforming of biomass/bio-oil using a char-supported catalyst.

Aromatic compounds, with single-ring to multiple-ring structures, constitute the tar from the gasification of biomass along with other oxygen-containing hydrocarbons [6, 27, 28]. These aromatic compounds, especially those with large aromatic structures, are more stable than other compounds in the tar, and prone to form large molecules such as coke during reforming. Therefore, the formation/evolution of various large/complex aromatic ring systems during the catalytic reforming process is especially important, requiring particular attention.

This study forms part of our ongoing efforts to understand the catalytic reforming of biomass/bio-oil tar using a char-supported iron catalyst. Cellulose was pyrolysed at 500 °C followed by the *in-situ* catalytic steam reforming using char-supported iron as a catalyst at different temperatures between 500 °C and 850 °C. Ultraviolet (UV) fluorescence spectroscopy was used to trace the evolution of aromatic ring systems during the reforming process. Gas chromatography- mass spectrometry (GC-MS) was used to quantify the evolution of light compounds in the tars. To gain a further understanding of the roles played by the char-supported iron in the reforming process, the fresh and used catalyst char structures were characterised by Fourier transformed Raman spectroscopy.

5.2 Experimental section

5.2.1Catalyst preparation

Char-supported iron was prepared for this study. The procedures were detailed in Section 2.4, ***Chapter 2***. Briefly, pulverised (ranging from 106 to 150 μm) raw coal (Loy Yang brown coal) was firstly mixed in an aqueous solution of 0.2M H_2SO_4 with a ratio of the acid solution to coal of 30:1 by mass and stirred in an argon atmosphere for 24 hour. The slurry was then filtered and washed with de-ionized water until the pH value of the filtrates was constant (4.5–5.0). After drying, the acid-washed coal (H-form coal) was then impregnated with 3 wt% Fe by ion-exchanging with corresponding $FeCl_3$ solution. The treated coal is termed as the Fe-loaded coal.

A one-stage fluidised-bed/fixed-bed reactor (Figure 2-2) [29, 30] was used to prepare the catalysts at 800 °C. About 25 grams of Fe-loaded coal were firstly loaded into the quartz reactor followed by 15 min argon purging before it was heated at about 10 °C/min to the desired temperature with 0.5 L/min of argon flow. The reactor was then held for 15 min at 800 °C with additional 0.21 L/min of steam. At the end of 15 min, the reactor was lifted out of the furnace to be cooled down to room temperature with the continuous argon flow. The fresh char-supported iron catalyst was then collected and stored in a freezer (about -10 °C) until required for the reforming experiments.

5.2.2. Pyrolysis/reforming experiments

The pyrolysis and reforming of cellulose were carried out in a novel two-stage fluidised-bed/fixed-bed quartz reactor (Figure 5-1) [13, 14]. The details of the experiment system and operating procedures can be found in Section 2.3 and 2.5, ***Chapter 2*** (Figure 2-1 and Figure 2-3). Briefly, the bottom part of the reactor acted as a fluidised-bed pyrolyser while the top part was used as a fixed-bed catalytic volatile reformer. The cellulose (α-cellulose, Sigma-Aldrich) particles were entrained in a feeder with argon (1 L/min) and fed into the fluidised bed at 100 mg/min via the injection probe. Steam was injected at the middle part of the reactor, which was controlled by an HPLC pump. In any catalytic reforming experiment, about 1 gram

of catalyst was pre-loaded into the top part of the reactor and the reforming section was conducted at different temperatures between 500 and 850 °C. The bottom part, where cellulose pyrolysis took place, was kept at 500 °C. Tar was collected by a series of three tar traps containing a mixture of HPLC-grade chloroform and methanol (80:20 by volume) at the reactor outlet (Section 2.3, 2.5, ***Chapter 2***) [14, 15, 25].

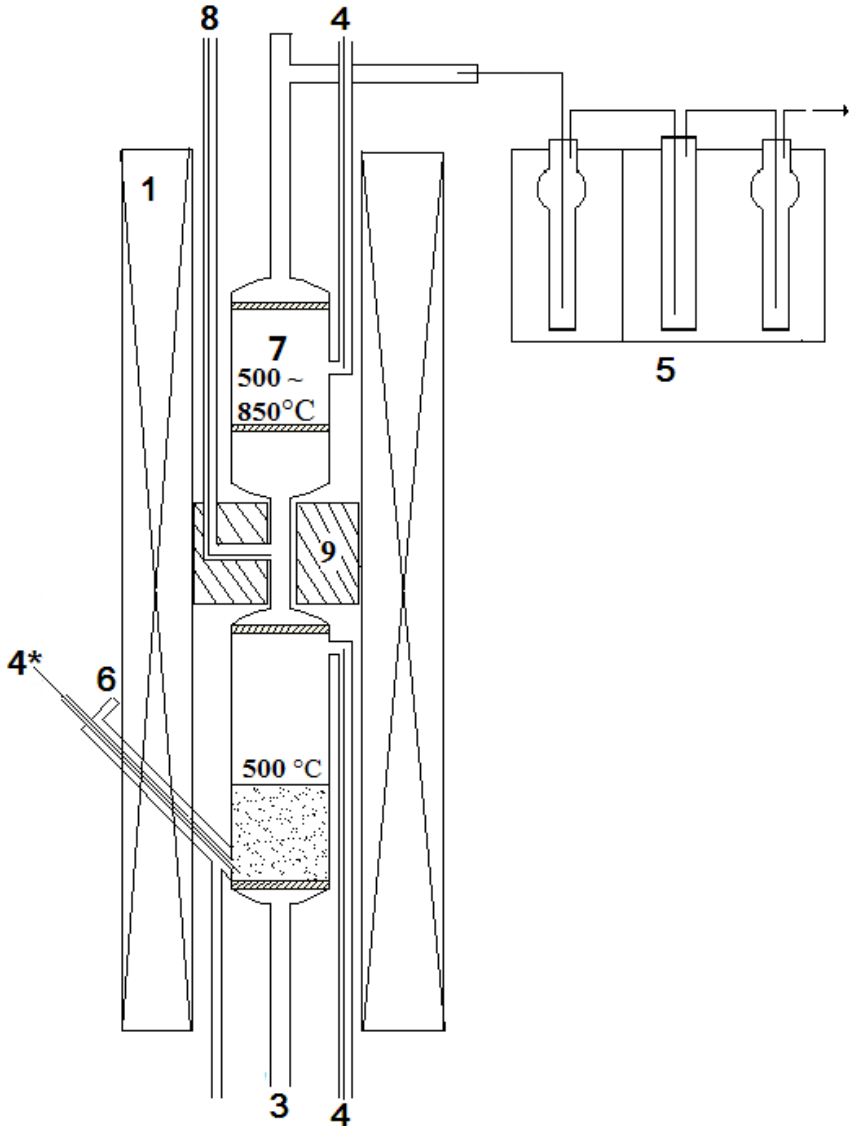

Figure 5-1. A schematic diagram of the two-stage fluidised-bed/fixed-bed reactor system. 1, furnace; 2, cellulose feeding tube; 3, fluidising gas inlet 4, thermocouples; 5, tar trap system; 6, cooling tube; 7, catalyst room (catalytic reforming process); 8, steam injection probe; 9, insulation materials (kaowool). (*) This thermocouple was used to measure the temperature in the fluidised bed and would be replaced by a

feeding probe after the target temperature was reached.

To study the effects of steam on the catalyst char structure alone, blank experiments were conducted. The only difference between the reforming experiment and blank experiment is the introduction of cellulose. In other words, all the experimental conditions were identical, except there was no feeding of cellulose during blank experiment.

5.2.3. Tar and catalyst characterisation

In this study, the UV-fluorescence spectra of tars were recorded using a Perkin-Elmer LS50B spectrometer. The detail procedure can be found Section 2.6.1, ***Chapter 2***. Tar Samples were analysed using an Agilent GC-MS with a capillary column (INNOWax). The details of the instrument and procedures can be found in Section 2.6.2, ***Chapter 2***.

Spent catalysts (about 0.2 g) were mixed in a mixture of HPLC-grade chloroform and methanol (80:20 by volume) and stirred for 24 hours. UV-fluorescence spectroscopy and GC-MS were used to analyse the solution to determine species removed from the spent catalyst.

The structural features of fresh and spent catalysts were characterized by using a Perkin–Elmer Spectrum GX FT-Raman spectrometer. A detailed description of the instrument and sample preparation can be found in Section 2.7, ***Chapter 2.*** The Raman spectra, ranging from 800 to 1800 cm^{-1}, were deconvoluted into 10 Gaussian bands using the GRAMS/32 AI software, and a detailed discussion of the assignment of Raman bands can be found in in Section 2.7, ***Chapter 2.***

5.3 Results and discussion

5.3.1 Tar yields from the pyrolysis, steam reforming and catalytic steam reforming of cellulose-derived compounds

Figure 5-2 shows the tar yields from the pyrolysis and the reforming of cellulose as a function of the pyrolysis/reforming temperature in the top stage when the bottom stage was kept at 500 °C. As expected, all the tar yields decreased with increasing temperature because of the enhanced cracking at higher temperatures. The tar yields from pyrolysis and the non-catalytic steam reforming show more similarities than that from catalytic steam reforming of cellulose. Therefore, the effects of extra steam without catalysts on tar reforming were not significant, which is in agreement with our previous study on the reforming of mallee wood biomass [13, 14]. However, the tar yield had a 3~4 % decrease from pyrolysis to non-catalytic steam reforming at low temperatures (e.g. 500 and 550 °C); the small decrease of tar yield due to the additional steam supplied might be a result of intensified hydrolysis of tars, especially larger molecules by the added water in non-catalytic steam reforming process.

The most obvious and important finding is the lower tar yield, particularly at the lower temperatures (< 700 °C), from catalytic steam reforming of cellulose. Clearly, the iron-char catalyst showed a good effect on tar reduction even at low temperatures.

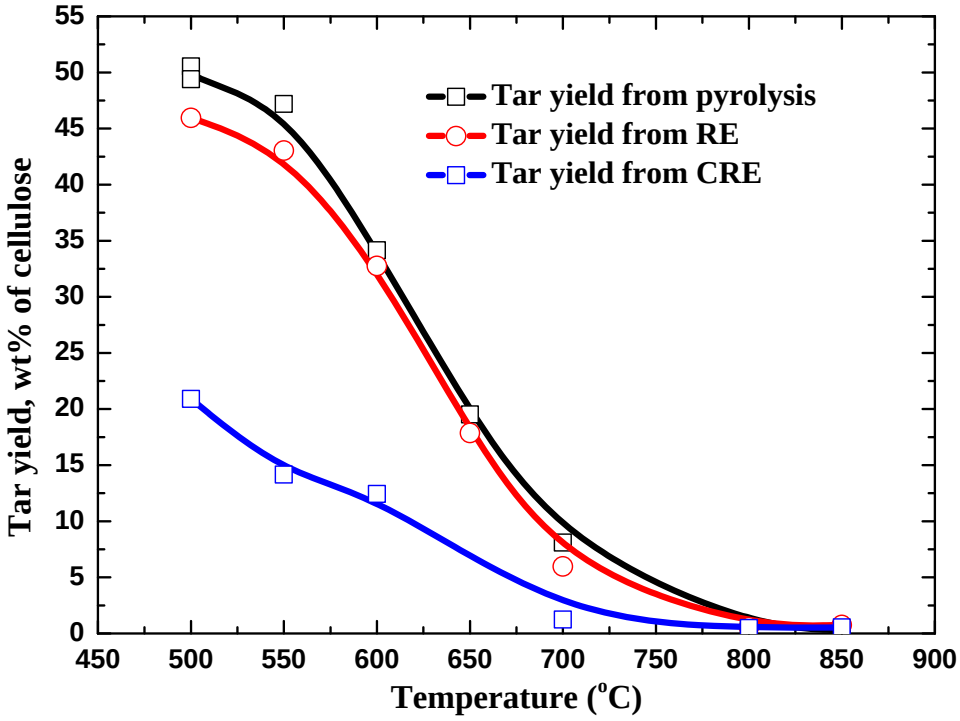

Figure 5-2. Tar yield from cellulose as a function of the pyrolysis/steam reforming (RE) and catalytic steam reforming (CRE) temperature (500-850 °C). The data on the pyrolysis of cellulose were taken from ***Chapter 3***.

5.3.2 Formation of aromatic structures during the reforming of cellulose-derived compounds

The data in Figure 5-2 showed the char-supported iron catalyst to be active at temperature as low as 500 °C in reforming the tar. To further understand the catalytic reforming reactions, efforts were made to understand the evolution of aromatic structures during reforming.

The fluorescence synchronous spectra of tars are shown in Figure 5-3 and Figure 5-4. It should be noted that the fluorescence intensity in Figure 5-3 was multiplied by the tar yield to express the intensity on the basis of "per gram of cellulose", and, thus is a reflection of the "yields" of aromatic structural compounds.

Compared with our previous UV-fluorescence analysis of the tars from biomass pyrolysis/reforming [13, 14, 31-33], the low intensities of the tar samples from the pyrolysis/reforming of cellulose indicate that limited amounts of aromatic ring systems were formed from the pyrolysis and reforming of cellulose under the present experimental conditions (< 850 °C) . In particular, the intensities were found to be very low for the tars produced from cellulose pyrolysis/reforming at low temperatures (500 to 600 °C). This indicates that lowly conjugated or unconjugated compounds, such as furfurals and sugars, are the main products produced from cellulose under these conditions.

It was initially suspected that some aromatic compounds might have been adsorbed on the catalyst surface. The spent catalysts were then washed with a mixture of HPLC-grade chloroform and methanol (80:20 by volume). UV-fluorescence spectroscopy and GC-MS were used to analyse the solutions to determine species removed from the spent catalyst by washing.

However, the negligible fluorescence intensities of the catalyst-washed solutions indicate that the physical adsorption of large aromatic ring systems by the catalyst was very limited. There was no obvious peak observed in the chromatogram of catalyst-washed solutions. Therefore, the amount of species physically absorbed on the spent catalysts is negligible.

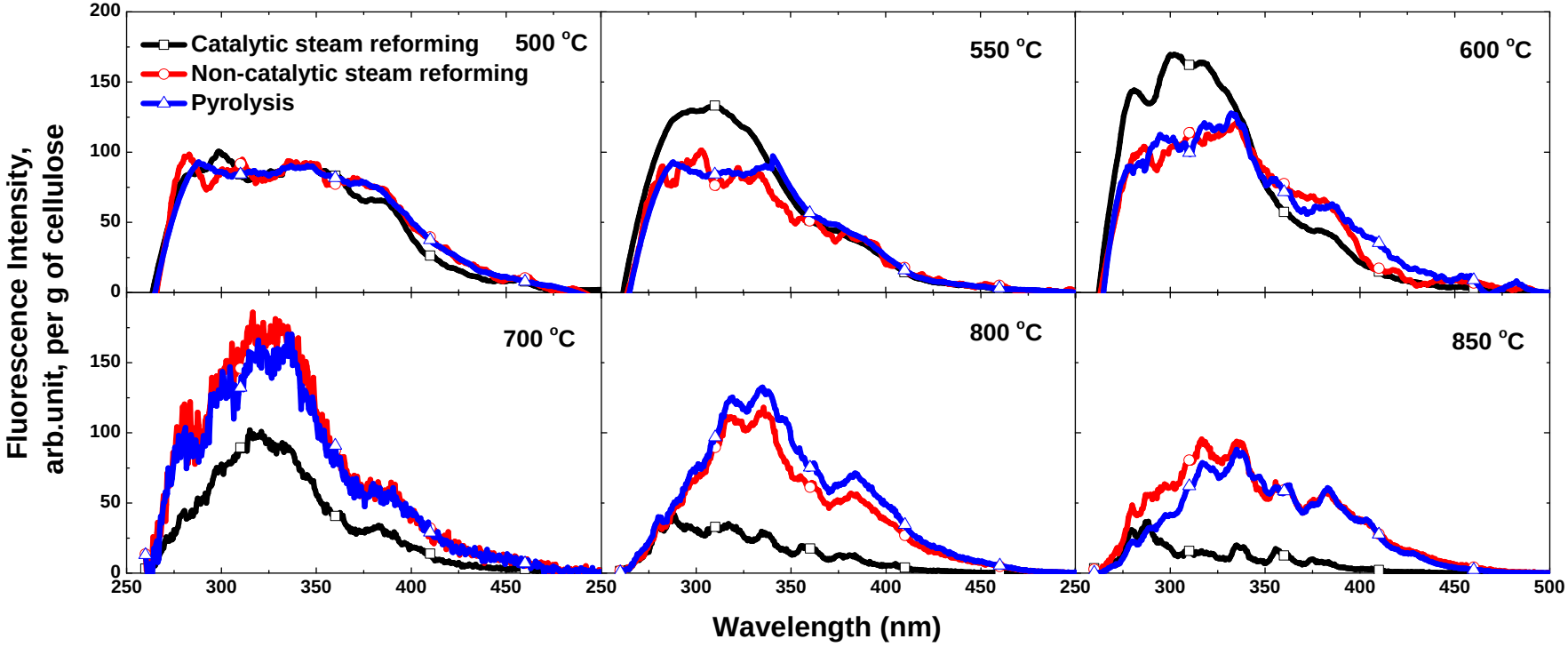

Figure 5-3. Constant energy (-2800 cm^{-1}) synchronous spectra of the tars produced from the pyrolysis, steam reforming and catalytic steam reforming of cellulose at temperatures between 500 and 850 °C.

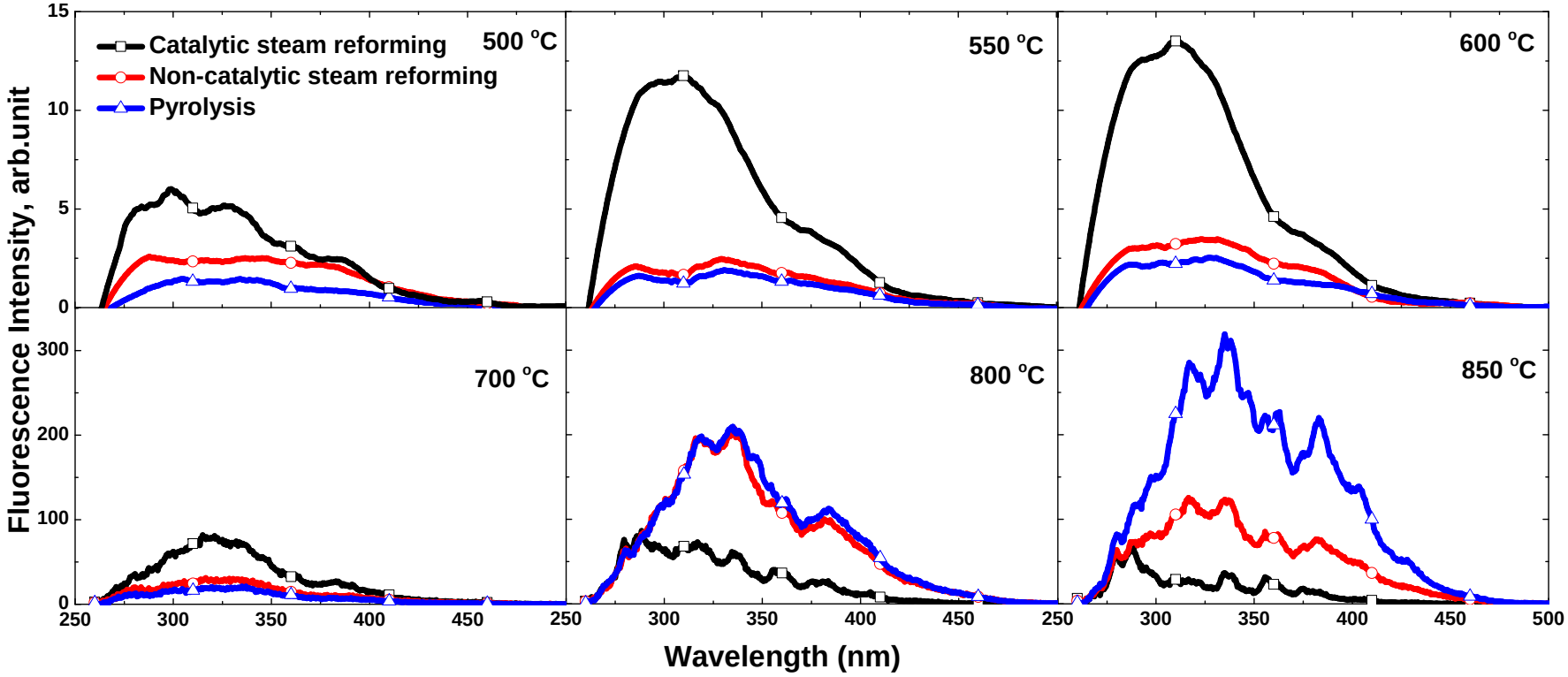

Figure 5-4. Constant energy (-2800 cm-1) synchronous spectra (4ppm methanol solution) of the tars produced from the pyrolysis, non-catalytic reforming and catalytic reforming of cellulose at temperatures between 500 and 850 °C.

A few observations can be made with the data in Figure 5-3 and Figure 5-4. Firstly, the use of catalyst in reforming at 500 °C and 600 °C actually led to increases in the fluorescence intensities (i.e. the yields of aromatic ring systems). Similar observation was made before with the reforming of mallee wood [14]. The increases in the fluorescence intensities are believed to be mainly due to the enhanced dehydration of sugar structures, leading to the formation of aromatic structures. Secondly, the reforming was greatly enhanced by the catalyst at temperatures higher than 700 °C. The use of a catalyst resulted in significant decreases in the observed fluorescence intensity. Compared with the non-catalytic reforming and pyrolysis, the catalyst appeared to be particularly effective for the reforming of large aromatic ring systems (with wavelengths longer than 300 nm). Some observed small aromatic ring systems (with wavelengths shorter than 300 nm) may have been the products of partial reforming of larger aromatic ring systems. If so, the smaller aromatic ring systems were able to escape from the reforming reactions on the catalyst surface. This would in turn, again, indicate (or in agreement with the above statement) that the catalyst was not particularly effective for the reforming of small aromatic ring systems. The small aromatic ring systems are likely to have lower propensity to form coke and thus represent low troubles for the use of its product synthesis gas (e.g. in a gas engine), than the larger ones.

5.3.3 Changes in the composition of light components in tars during the reforming of cellulose-derived compounds

Figure 5-5 shows the GC-MS total ion chromatograms of the tar from pyrolysis, non-catalytic steam reforming and catalytic steam reforming of cellulose at temperatures between 500 and 850 °C. In terms of types of compounds found in the tars, no obvious qualitative differences among pyrolysis and non-catalytic steam reforming of cellulose could be identified from the GC-MS results (Figure 5-5 and Table 5-1). With UV-fluorescence data (Figure 5-3), both set of results indicate that the effect of extra steam without catalyst was very limited on the reforming of cellulose-derived compounds, both large and small molecules.

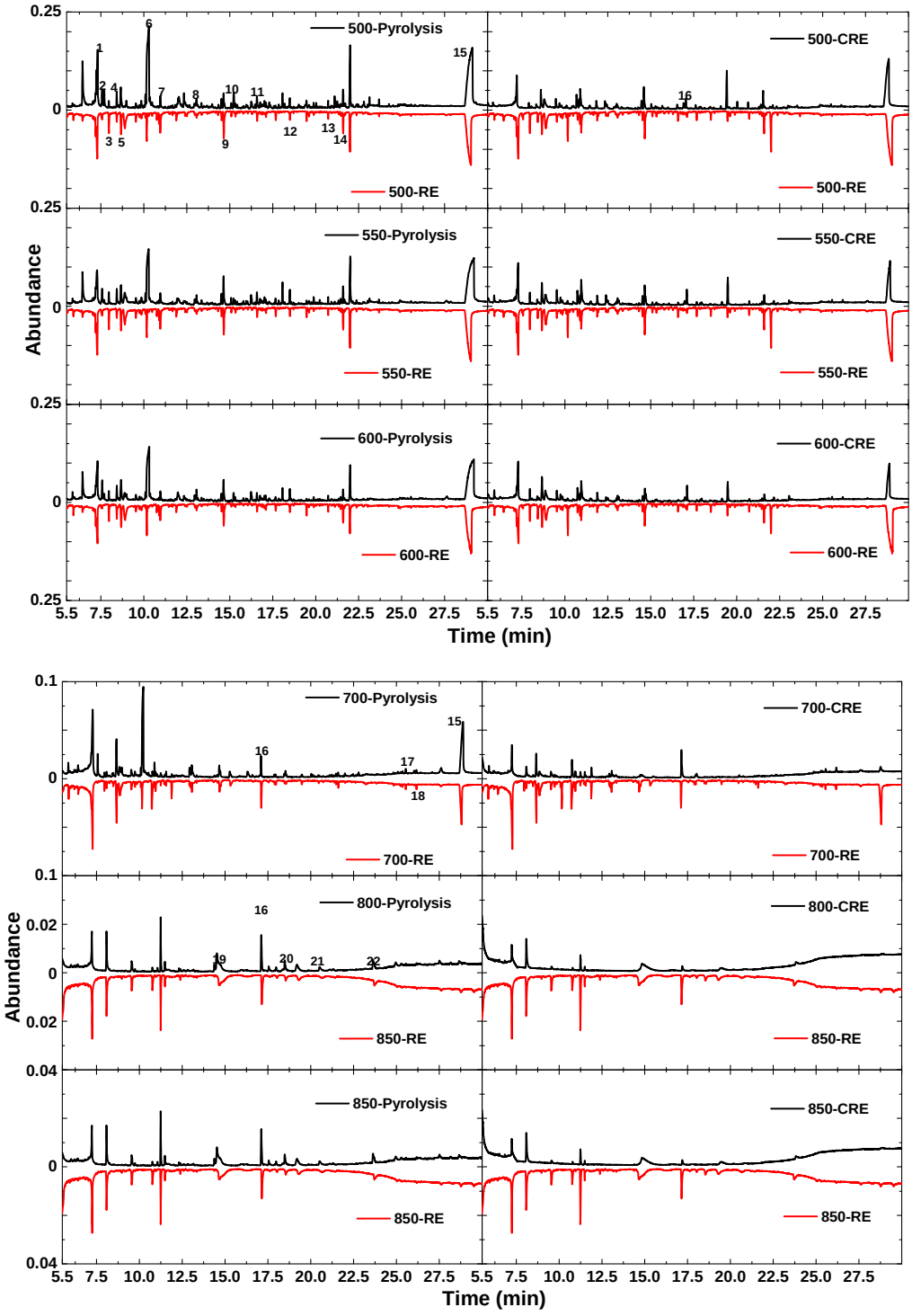

Figure 5-5. GC-MS total ion chromatograms of the tars produced from the pyrolysis, non-catalytic reforming and catalytic reforming of cellulose at different temperatures (500-850 °C).

Table 5-1. Main chemical compounds in tars determined by GC-MS

No.	Tentative identification	No.	Tentative identification
1	1,1,3-Trimethoxy propane 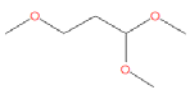	12	Pentanedioic acid 2-oxo-dimethyl ester 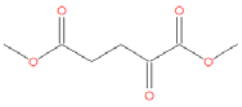
2	4-Methoxy-2-butanone 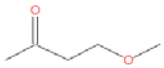	13	1,4:3,6-Dianhydro-α-d-glucopyranose 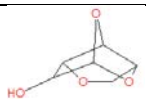
3	Dimethoxy-tetrahydorfuran 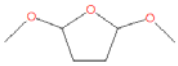	14	5-Hydroxymethyl-furfural (HMF) 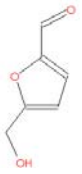
4	Dimethoxy-acetic acid-methyl ester 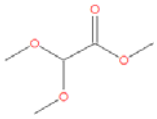	15	1,6-Anhydro-β-D-glucopyranose (Levoglucosan) 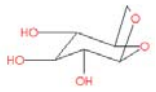
5	1-Hydroxy-2-propanone 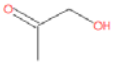	16	Phenol 
6	1,1,2-Trimethoxy-ethane 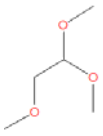	17	1,4-Benzenediol 
7	Furfural 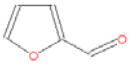	18	1,3-Benzenediol (Resorcinol) 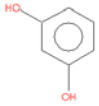
8	2-Ethyl-1,3-dioxolane 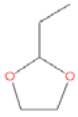	19	Naphthalene 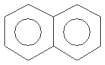
9	2-Hydorxy-2-cyclopenten-1-one 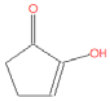	20	2-Furanmethanol 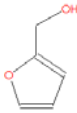
10	3-Methyl-1,2-cyclopentaanedione 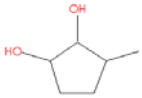	21	2,3-Dihydro-benzofuran 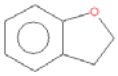
11	1,2,4-Cyclopentanetrione 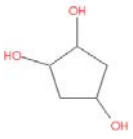	22	Phenanthrene 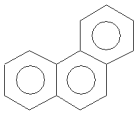

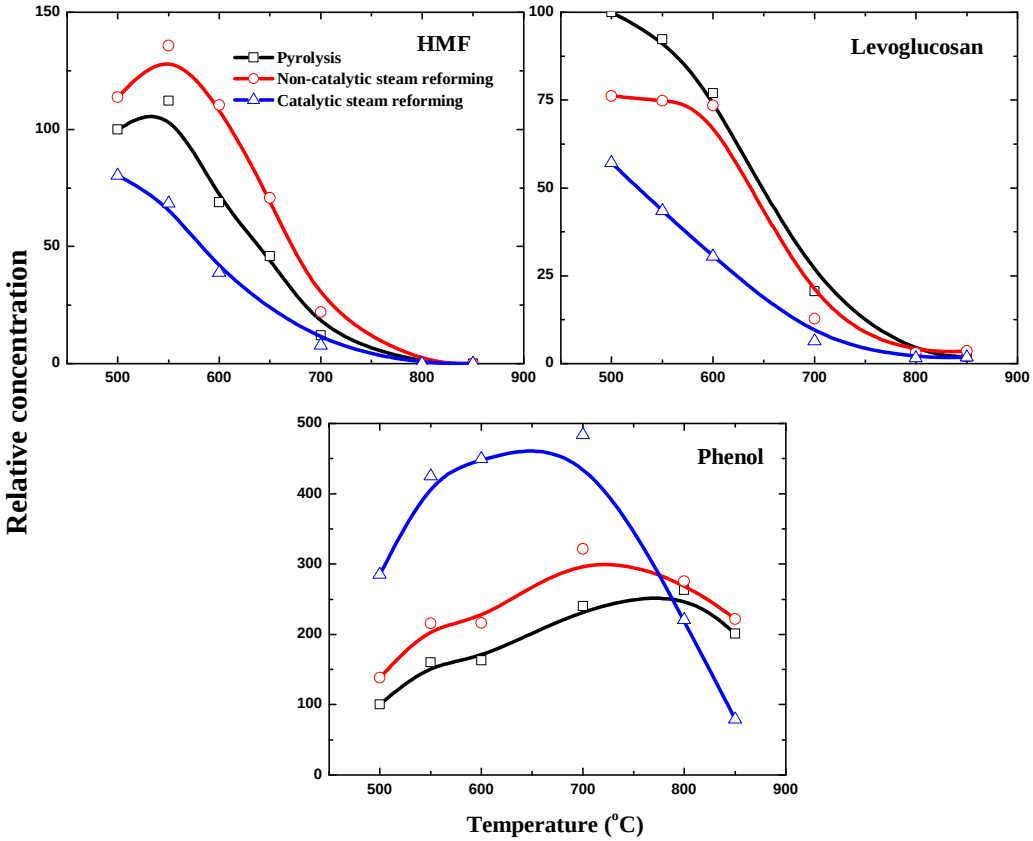

Figure 5-6. Relative concentration (set the one from pyrolysis of cellulose at 500 °C as 100%) of some selected compounds in tars produced from pyrolysis, non-catalytic reforming and catalytic reforming of cellulose at different temperatures (500-850 °C).

From the comparison of the chromatograms of the catalytic reforming tars with those from Pyrolysis/non-catalytic reforming of cellulose, only few peaks have obvious changes including the presence and the abundance at low temperatures (500-600 °C), and the differences became more obvious with an increasing temperature.

Levoglucosan is well known as the most abundant sugar compound from pyrolysis of cellulose, which can be further degrade to some lower molecular weight compound such as HMF [21, 24, 25]. Aromatic compounds can be formed during pyrolysis of cellulose, particularly at high temperatures. Phenol is a typical compound with single aromatic ring which presents in the tar at temperature as low as 500 °C. To gain further insight into involved reactions, these three compounds HMF, levoglucosan and phenol were quantified by peaks area integration, and their

relative concentrations in function of temperature are shown in Figure 5-6. In the pyrolysis or non-catalytic steam reforming of cellulose, the concentrations of HMF reached a maximum at 550°C and then decreased significantly at the higher reaction temperatures, indicating that the formation and conversion of HMF occurred in parallel. During the catalytic steam reforming, the concentration of HMF was relatively lower and decreased monotonously with the reaction temperatures, suggesting the conversion of HMF into some other compounds are dominant. Char was used as catalyst support in this study, processing of which with sulfuric acid may create hydroxyl group, the bronsted acid sites, on its surface. The acidic sites could catalyse the dehydration of sugar and/or sugar oligomers to HMF and also could catalyse the polymerisation of HMF on the acidic sites. The detailed reaction pathways for HMF over the char-based catalyst have not yet been clear.

The concentration of levoglucosan in tars from the pyrolysis is higher than that from non-catalytic steam reforming where extra water was present, especially at the relatively lower temperatures such as at 500°C. The extra water can affect the formation of levoglucosan from cellulose in three ways: change the pyrolysis routes of cellulose-derived compounds, lead to the hydrolysis of levoglucosan and the reforming of levoglucosan into gaseous products. The use of catalyst significantly facilitates the reforming of levoglucosan, as shown in Figure 5-6.

Phenol can be formed from the aromatisation of sugars at high temperature. Interestingly, the abundance of phenol increased drastically below 700°C in the presence of catalyst and meanwhile the abundance of the sugars such as levoglucosan decreased significantly. It is possible that levoglucosan was transformed into phenol with the aid of the catalyst. The further increase of reaction temperatures to 850°C result in a substantial decrease of phenol abundance. The disappearance of phenol at this high temperature is understandable as phenol can be reformed into gaseous products.

In addition, it is found that the sugars such as levoglucosan, sugars derivatives such as HMF are easier to be reformed than the phenolics such as phenol when comparing their final abundance at 850°C.

5.3.4 Changes in the structural features of iron-char catalyst

Figure 5-7 shows the total Raman peak areas in the region of 800 ~ 1800 cm^{-1} of the fresh and spend catalysts. The catalysts used in the steam reforming process at lower temperatures (< 700 °C) showed somewhat higher total peak areas than the fresh one. According to the results from UV and GC-MS analysis, this observation may indicate the absorption of O-containing groups into the catalyst structure after being used for catalytic reforming of cellulose-derived compounds at these temperatures (500 to 600 °C). The temperature was not high enough to remove these O-containing functional groups. With increasing temperature, the reactive O-containing groups in the cellulose-derived compounds were depleted, and the steam reforming/gasification of the small aromatics in the chars were enhanced, both resulting in the decreases of the total peak areas of these catalysts used at higher temperatures (≥ 700 °C) catalytic steam reforming.

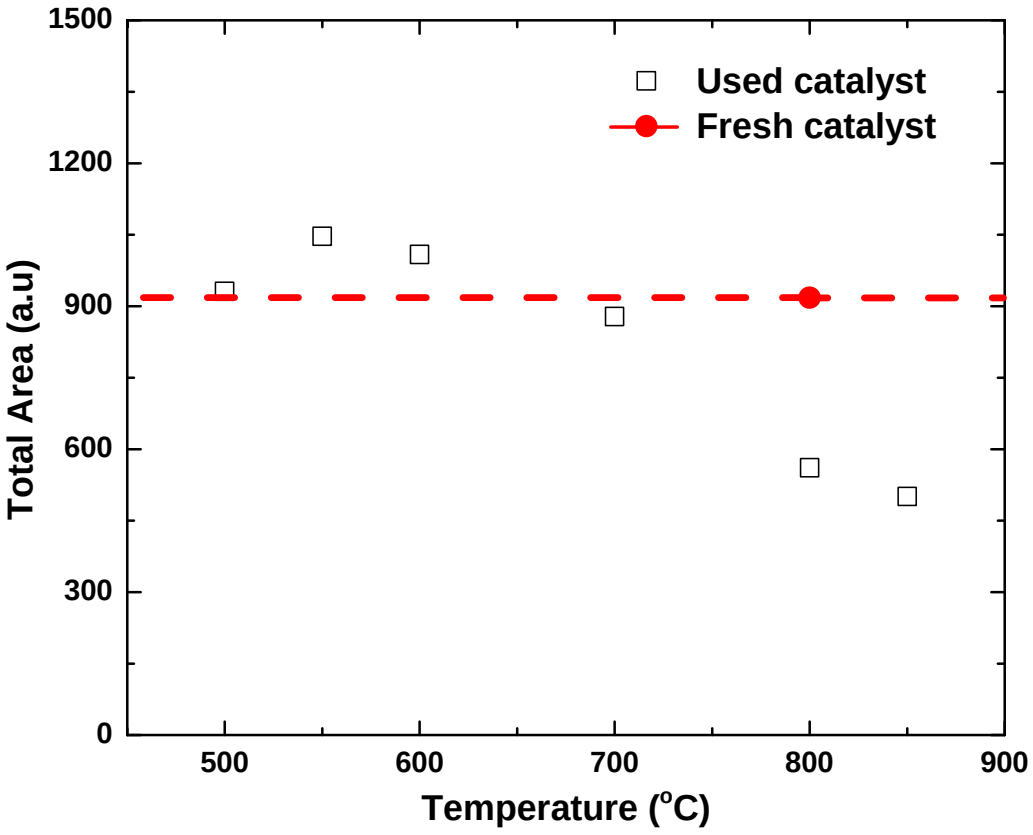

Figure 5-7. Total Raman peaks area (800-1800 cm^{-1}) of chars used as catalysts in the steam reforming of cellulose tar at different temperatures (500-850 °C).

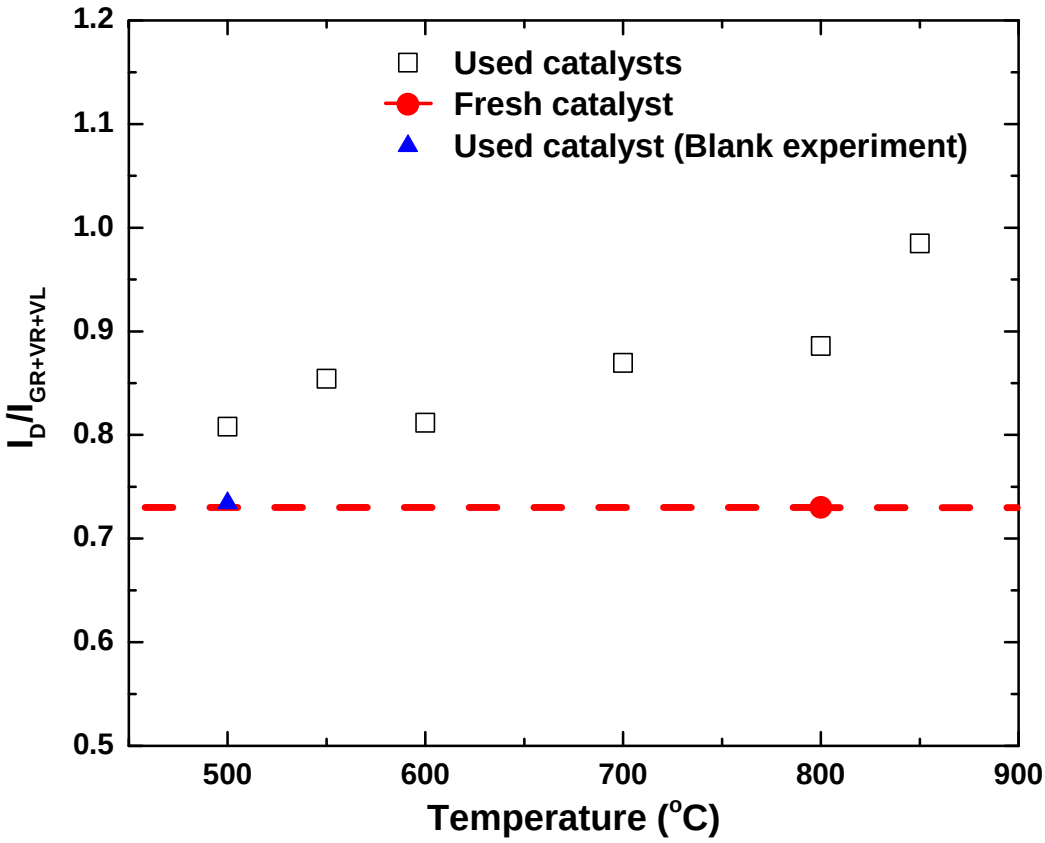

Figure 5-8. The ratio of $I_D/I_{(GR+VL+VR)}$ of chars used as catalysts in the steam reforming of cellulose tar at different temperatures (500-850 °C).

Raman spectra of different chars were curve fitted using ten Gaussian bands, and the representative of each band can be found in Section 2.7, ***Chapter 2***. Figure 5-8 shows the band area ratio $I_D/I_{GR+VL+VR}$ as a function of different catalytic reforming temperature. The ratios $I_D/I_{GR+VL+VR}$ of chars increased after being used. The reasons for these increases may be different between low and high temperature catalytic reforming of cellulose-derived compounds.

At lower temperatures (500-600 °C), considering the limited steam activity, the direct consumption of small aromatic ring systems by steam gasification would have been limited (the similar ratios between used catalyst from blank experiment and fresh catalyst in Figure 5-8). However, part of the cellulose-derived compounds, especially high polarity compounds (e.g. levoglucosan) could be adsorbed on the catalyst surface (the decrease of such compounds can be seen in Figure 5-5). The subsequent dehydration of these compounds bonded with char could form new ring

structures to increase the portion of larger aromatic ring systems. In other words, the regeneration of aromatic ring systems might not only increase the larger ring systems but also decrease the small ring system simultaneously. Both phenomena contributed to the increases in the $I_D/I_{GR+VL+VR}$ ratio.

At higher temperatures (700-850 °C), as shown in Figure 5-8, the $I_D/I_{GR+VL+VR}$ ratio increased with increasing temperature. Besides the enhanced steam gasification of small aromatics, the conversion/rearrangement of small aromatic rings into large aromatic structures was activated by radicals from the enhanced cracking of the cellulose-derived compounds (e.g. H radicals) at high temperatures. The radicals may have been generated on the catalyst surface or generated in the gas phase and then adsorbed onto the catalyst surface.

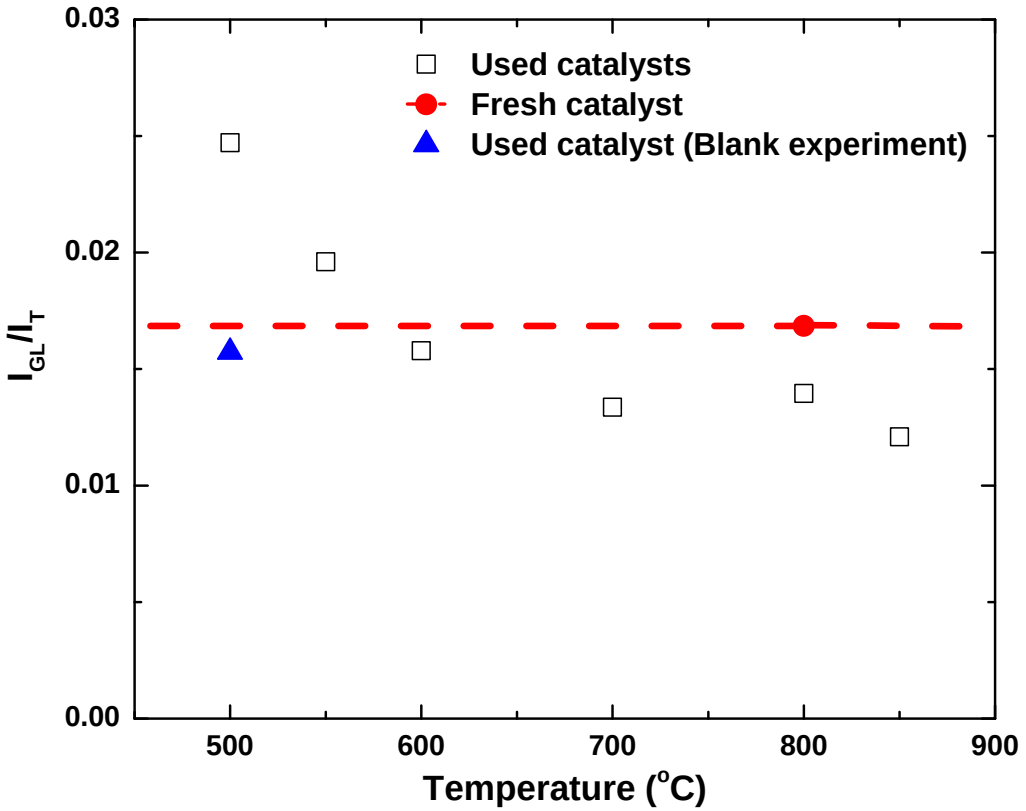

Figure 5-9. The ratio of I_{GL}/I_T of chars used as catalysts in the steam reforming of cellulose tar at different temperatures (500-850 °C). (Blank experiment: No feedstock)

Figure 5-9 shows the band intensity ratio I_{GL}/I_T as a function of different catalytic reforming temperatures. This ratio I_{GL}/I_T reflects the portion of carbonyl groups in the char [34]. At low temperatures (500-550°C), many O-containing compounds could be formed and adsorbed on the catalyst during catalytic reforming of cellulose-derived compounds, resulting in the increases in the I_{GL}/I_T with decreasing temperature.

5.4 Conclusions

The cellulose-derived compounds from the pyrolysis of pure cellulose at 500 °C have been reformed in-situ using a char-supported iron catalyst with steam at temperatures between 500 and 850 °C. The product tars were quantified and characterised with ultraviolet fluorescence spectroscopy and gas chromatography-mass spectrometry. Our results indicate that steam alone has minimum effects on reforming of tars in the absence of a catalyst. At low temperatures (< 700 °C), the catalytic steam reforming showed better effects on the conversion of non-aromatics (e.g. sugars), particularly large molecules than the conversion of aromatic structures. The dehydration of sugar compounds could be enhanced by the catalyst. Various aromatic ring systems can be formed at high temperatures (≥ 700 °C), and the catalyst was effective on their reforming with steam. To gain further understanding on reactions occurred on the catalyst, the char structural features of catalyst were obtained. The information indicated that O-containing groups in the cellulose-derived compounds were easily absorbed on the catalyst at lower temperatures (< 700 °C).

5.5 References

[1] S. Iborra, G. Huber, Synthesis of transportation fuels from biomass: chemistry, catalysts, and engineering, Chemical reviews, 106 (2006) 4044-4098.

[2] P. McKendry, Energy production from biomass (part 1): overview of biomass, Bioresource Technology, 83 (2002) 37-46.

[3] M.M. Yung, W.S. Jablonski, K.A. Magrini-Bair, Review of Catalytic Conditioning of Biomass-Derived Syngas, Energy & Fuels, 23 (2009) 1874-1887.

[4] A.V. Bridgwater, The technical and economic feasibility of biomass gasification for power generation, Fuel, 74 (1995) 631-653.

[5] M.A. Caballero, J. Corella, M.P. Aznar, J. Gil, Biomass gasification with air in fluidized bed. Hot gas cleanup with selected commercial and full-size nickel-based catalysts, Industrial and Engineering Chemistry Research, 39 (2000) 1143-1154.

[6] Z. Abu El-Rub, E.A. Bramer, G. Brem, Review of Catalysts for Tar Elimination in Biomass Gasification Processes, Industrial & Engineering Chemistry Research, 43 (2004) 6911-6919.

[7] C.M. Kinoshita, Y. Wang, J. Zhou, Effect of reformer conditions on catalytic reforming of biomass-gasification tars, Industrial and Engineering Chemistry Research, 34 (1995) 2949-2954.

[8] P. Simell, E. Kurkela, P. Ståhlberg, J. Hepola, Catalytic hot gas cleaning of gasification gas, Catalysis Today, 27 (1996) 55-62.

[9] S. Rapagnà, N. Jand, P.U. Foscolo, Catalytic gasification of biomass to produce hydrogen rich gas, International Journal of Hydrogen Energy, 23 (1998) 551-557.

[10] J. Corella, M.-P. Aznar, J. Gil, M.A. Caballero, Biomass Gasification in

Fluidized Bed: Where To Locate the Dolomite To Improve Gasification?, Energy & Fuels, 13 (1999) 1122-1127.

[11] R. Zhang, R.C. Brown, A. Suby, K. Cummer, Catalytic destruction of tar in biomass derived producer gas, Energy Conversion and Management, 45 (2004) 995-1014.

[12] J. Han, H. Kim, The reduction and control technology of tar during biomass gasification/pyrolysis: An overview, Renewable and Sustainable Energy Reviews, 12 (2008) 397-416.

[13] Z. Min, M. Asadullah, P. Yimsiri, S. Zhang, H. Wu, C.-Z. Li, Catalytic reforming of tar during gasification. Part I. Steam reforming of biomass tar using ilmenite as a catalyst, Fuel, 90 (2011) 1847-1854.

[14] Z. Min, P. Yimsiri, M. Asadullah, S. Zhang, C.Z. Li, Catalytic reforming of tar during gasification. Part II. Char as a catalyst or as a catalyst support for tar reforming, Fuel, 90 (2011) 2545-2552.

[15] J. Delgado, M.P. Aznar, J. Corella, Calcined Dolomite, Magnesite, and Calcite for Cleaning Hot Gas from a Fluidized Bed Biomass Gasifier with Steam: Life and Usefulness, Industrial & Engineering Chemistry Research, 35 (1996) 3637-3643.

[16] K.S. Seshadri, A. Shamsi, Effects of Temperature, Pressure, and Carrier Gas on the Cracking of Coal Tar over a Char−Dolomite Mixture and Calcined Dolomite in a Fixed-Bed Reactor, Industrial & Engineering Chemistry Research, 37 (1998) 3830-3837.

[17] S. Rapagnà, N. Jand, A. Kiennemann, P.U. Foscolo, Steam-gasification of biomass in a fluidised-bed of olivine particles, Biomass and Bioenergy, 19 (2000) 187-197.

[18] T. Nordgreen, T. Liliedahl, K. Sjöström, Elemental Iron as a Tar Breakdown Catalyst in Conjunction with Atmospheric Fluidized Bed Gasification of Biomass: A Thermodynamic Study, Energy & Fuels, 20 (2006) 890-895.

[19] T. Nordgreen, T. Liliedahl, K. Sjöström, Metallic iron as a tar breakdown catalyst related to atmospheric, fluidised bed gasification of biomass, Fuel, 85 (2006) 689-694.

[20] M. Garcia-Perez, A. Chaala, H. Pakdel, D. Kretschmer, C. Roy, Characterization of bio-oils in chemical families, Biomass and Bioenergy, 31 (2007) 222-242.

[21] P.R. Patwardhan, D.L. Dalluge, B.H. Shanks, R.C. Brown, Distinguishing primary and secondary reactions of cellulose pyrolysis, Bioresource Technology, 102 (2011) 5265-5269.

[22] T. Yoshida, Y. Matsumura, Gasification of Cellulose, Xylan, and Lignin Mixtures in Supercritical Water, Industrial & Engineering Chemistry Research, 40 (2001) 5469-5474.

[23] H.C. Yoon, P. Pozivil, A. Steinfeld, Thermogravimetric Pyrolysis and Gasification of Lignocellulosic Biomass and Kinetic Summative Law for Parallel Reactions with Cellulose, Xylan, and Lignin, Energy & Fuels, 26 (2011) 357-364.

[24] P.R. Patwardhan, J.A. Satrio, R.C. Brown, B.H. Shanks, Influence of inorganic salts on the primary pyrolysis products of cellulose, Bioresource Technology, 101 (2010) 4646-4655.

[25] D.K. Shen, S. Gu, The mechanism for thermal decomposition of cellulose and its main products, Bioresource Technology, 100 (2009) 6496-6504.

[26] D.K. Shen, S. Gu, Pyrolytic behaviour of cellulose in a fluidized bed reactor, Cellulose Chemistry and Technology, 44 (2010) 79-87.

[27] J. Han, The reduction and control technology of tar during biomass gasification/pyrolysis: An overview, Renewable & Sustainable Energy Reviews, 12 (2008) 397-416.

[28] T.A. Milne, N. Abatzoglou, R.J. Evans, Biomass Gasifier “Tars”: Their Nature, Formation, and Conversion, in, NERL, Golden, CO, USA, 1998.

[29] D.M. Quyn, H. Wu, C.-Z. Li, Volatilisation and catalytic effects of alkali and alkaline earth metallic species during the pyrolysis and gasification of Victorian brown coal. Part I. Volatilisation of Na and Cl from a set of NaCl-loaded samples, fuel, 81 (2002) 143-149.

[30] D.M. Quyn, H. Wu, J.-i. Hayashi, C.-Z. Li, Volatilisation and catalytic effects of alkali and alkaline earth metallic species during the pyrolysis and gasification of Victorian brown coal. Part IV. Catalytic effects of NaCl and ion-exchangeable Na in coal on char reactivity, Fuel, 82 (2003) 587-593.

[31] M. Garcia-Perez, X.S. Wang, J. Shen, M.J. Rhodes, F. Tian, W.-J. Lee, H. Wu, C.-Z. Li, Fast Pyrolysis of Oil Mallee Woody Biomass: Effect of Temperature on the Yield and Quality of Pyrolysis Products, Industrial & Engineering Chemistry Research, 47 (2008) 1846-1854.

[32] D. Mourant, Z. Wang, M. He, X.S. Wang, M. Garcia-Perez, K. Ling, C.-Z. Li, Mallee wood fast pyrolysis: Effects of alkali and alkaline earth metallic species on the yield and composition of bio-oil, Fuel, 90 (2011) 2915-2922.

[33] Y. Wang, X. Li, D. Mourant, R. Gunawan, S. Zhang, C.-Z. Li, Formation of Aromatic Structures during the Pyrolysis of Bio-oil, Energy & Fuels, 26 (2012) 241-247.

[34] X. Li, J.-i. Hayashi, C.-Z. Li, FT-Raman spectroscopic study of the evolution of char structure during the pyrolysis of a Victorian brown coal, fuel, 85 (2006) 1700-1707.

Chapter 6

Evolution of Aromatic Structures during the Reforming of Bio-oil: Importance of the Interactions among Bio-oil Components

6.1 Introduction

Bio-oil, a complex mixture of chemical compounds produced from the pyrolysis of biomass, will play an increasingly important role in the global energy market. As was explained in ***Chapter 1,*** it can be upgraded into liquid transport biofuels or reformed into syngas [1-4].

Among the numerous possible applications for bio-oil, the catalytic steam reforming of bio-oil could become an efficient process to produce syngas or hydrogen [5-9]. However, many obstacles still exist before this technology route can be commercialised. For example, the incomplete reforming of bio-oil would produce tarry materials that can contaminate the product gas, increasing its propensity to form coke and deactivate catalysts [10, 11].

Bio-oil contains multiple compounds possessing various complex aromatic ring systems originating from the thermal decomposition of biomass components (e.g. lignin, cellulose and hemicellulose) and the interactions among the intermediates from these components during pyrolysis [12, 13].

In ***Chapter 3*** and ***Chapter 4***, the results have shown that drastic changes in aromatic ring systems occurred during the pyrolysis of bio-oil. These changes strongly influence the formation of tar and coke [14]. Insufficient knowledge exists about the evolution/formation of aromatic ring systems during the steam reforming of bio-oil. In particular, the evolution of aromatic structures is the result of a whole array of gas-phase reactions involving active species/intermediates such as radicals. A bio-oil contains reactive functional groups that vary with the feedstock composition (e.g. the relative proportion and structures of cellulose, hemi-cellulose and lignin) [15]. These reactive functional groups are largely responsible for the formation of radicals and thus contribute to the evolution of aromatic ring systems [14]. Our previous studies have shown that the origins of many species or families of compounds could be traced back to the key components of biomass such as lignin, cellulose and hemi-cellulose [15-17]. It is also possible to separate lignin-derived oligomers from other bio-oil components [14, 16, 18, 19]. Therefore, a study to trace the evolution of aromatic structures from lignin-derived species and from other

bio-oil species could give same detailed insights into the reaction mechanism of aromatic structures during the reforming of bio-oil. Moreover, comparison of aromatic structures from different families of bio-oil would give great insight into the importance of the interactions among bio-oil components to the evolution of aromatic ring systems during the reforming of bio-oil.

Continuing to understand the evolution/formation of aromatic ring systems during the reforming of bio-oil, this study aims to study the catalytic/non-catalytic steam reforming of bio-oil at different temperatures between 500 and 850 °C. Char-supported iron catalysts [20] were used in this study due to their great potential of commercial applications. To gain further insight into the reactions, the lignin-derived oligomers separated from bio-oil were also reformed under similar conditions but in isolation from other bio-oil components. Ultraviolet (UV) fluorescence spectroscopy was used to trace the development of aromatic ring systems during the reforming process. FT-Raman spectroscopy was used to characterise the changes in the char structures of the char-supported iron catalyst.

6.2 Experimental section

6.2.1 Samples and catalyst preparation

The preparation of bio-oil and its lignin-derived oligomers fraction were detailed in Section 2.2, ***Chapter 2***. The procedures for preparation of char-supported iron catalysts can be found in Section 2.4, ***Chapter 2***.

6.2.2 Pyrolysis/Reforming experiments

The pyrolysis and reforming of bio-oil and lignin-derived oligomers were carried out in a novel two-stage fluidised-bed/fixed-bed quartz reactor (Figure 6-1) [20, 21]. The details of the experiment system and operating procedures can be found in Section 2.3 and 2.5, ***Chapter 2*** (Figure 2-1 and Figure 2-3). In comparison to reforming experiments of cellulose in ***Chapter 5***, both the top and bottom stages of

the reactor were operated at the same temperature, the experiments were conducted in the temperature range of 500 °C to 850 °C during the reforming of bio-oil or its lignin-derived oligomers fraction. Steam was injected from the bottom part of the reactor, which was controlled by a HPLC pump. The flow rate of steam/water was 15 vol% of the total gas flow rate. It would be adjusted to correspond to the change of total gas flow rate, therefore the gas residence time inside the top stage of the reactor remained roughly constant even when the reactor temperature was increased.

The bio-oil was fed into the reactor via an air-cooled injection probe, with the help of argon carrier gas (0.21 L/min), at a rate of 100 mg/min using a syringe pump equipped with a 20 ml stainless steel syringe. The solid feedstock (lignin-derived oligomers fraction) particles were entrained in a feeder with argon (1 L/min) and fed into the fluidised bed at 100 mg/min via a cold water-cooled injection probe injection probe.

In any catalytic reforming experiment, about 1 gram of catalyst was pre-loaded into the top part of the reactor and the reforming section was conducted at different temperatures between 500 and 850 °C. Tar was collected by a series of three tar traps containing a mixture of HPLC-grade chloroform and methanol (80:20 by volume) at the reactor outlet (Section 2.3, 2.5, ***Chapter 2*****)** [14, 15, 25].

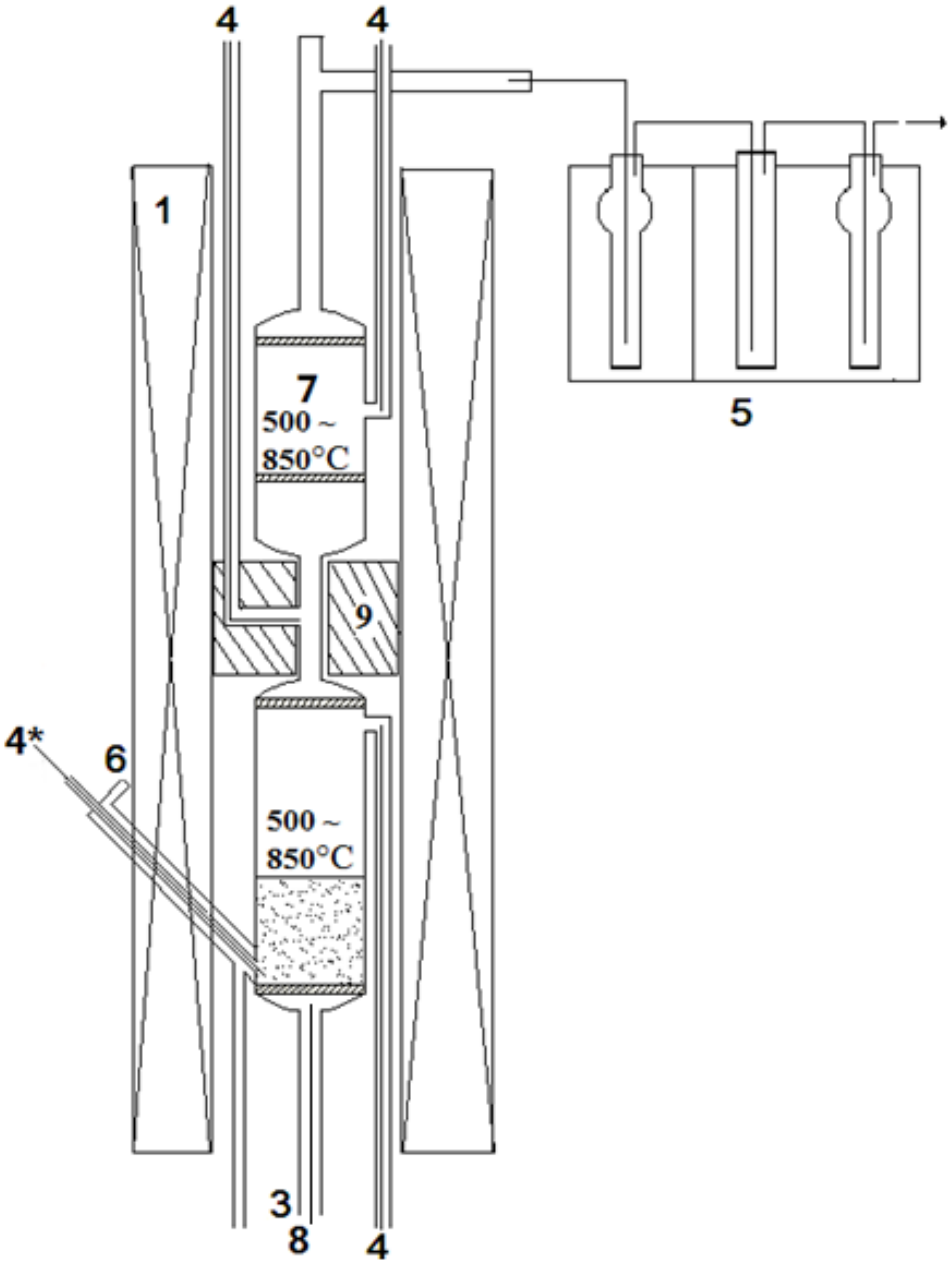

Figure 6-1. A schematic diagram of the two-stage fluidised-bed/fixed-bed reactor system. 1, furnace; 2, feeding tube; 3, fluidising gas inlet 4, thermocouples; 5, tar trap system; 6, cooling tube; 7, catalyst room (catalytic reforming process); 8, steam injection probe; 9, insulation materials (kaowool). (*) This thermocouple was used to measure the temperature in the fluidised bed and would be replaced by a feeding probe after the target temperature was reached.

To study the effects of steam on the catalyst char structure alone, blank experiments were conducted. The only difference between the reforming experiment

and blank experiment is the introduction of feedstock. In other words, all the experimental conditions were identical, except there was no feeding of feedstock during blank experiment.

6.2.3 Tar and catalysts characterisation

In this study, a Perkin-Elmer LS50B spectrometer was used to record the UV-fluorescence spectra of tars. The detail procedures can be found Section 2.6.1, ***Chapter 2***.

Spent catalysts (about 0.2 g) were mixed in a mixture of HPLC-grade chloroform and methanol (80:20 by volume) and stirred for 24 hours. UV-fluorescence spectroscopy and GC-MS were used to analyse the solution to determine species removed from the spent catalyst. However, the negligible fluorescence intensities of the catalyst-washed solutions indicate that the physical adsorption of large aromatic ring systems by the catalyst was very limited. There was no obvious peak observed in the chromatogram of catalyst-washed solutions. Therefore, the amount of species physically absorbed on the spent catalysts is negligible.

The structural features of fresh and spent catalysts were characterized by using a Perkin–Elmer Spectrum GX FT-Raman spectrometer. A detailed description of the instrument and sample preparation can be found in Section 2.7, ***Chapter 2.*** The Raman spectra, ranging from 800 to 1800 cm^{-1}, were deconvoluted into 10 Gaussian bands using the GRAMS/32 AI software, and a detailed discussion of the assignment of Raman bands can be found in in Section 2.7, ***Chapter 2.***

6.3 Results and discussion

6.3.1 Evolution of aromatic ring systems during the steam reforming of bio-oil and its lignin-derived compounds

6.3.1.1 Reforming of lignin-derived oligomers

Figure 6-2 shows the tar yields from lignin-derived oligomers as a function of the pyrolysis/reforming temperatures between 500 and 850 °C. Part of the data from the pyrolysis of lignin-derived oligomers was taken from ***Chapter 3***. The enhanced cracking is the main reason for the decreases in tar yield with increasing temperature during pyrolysis and reforming. Compared with the tar yields from the pyrolysis of lignin-derived oligomers, decreases in the tar yield were achieved from non-catalytic steam reforming, which were further reduced by the catalytic steam reforming at the same temperatures. The difference in the tar yield between reforming and pyrolysis of lignin-derived oligomers was reduced with increasing temperature.

The lignin-derived oligomers contain various aromatic ring systems, including large ring systems (more than two rings) with varied functional groups [14, 16, 18]. At low temperatures (e.g. < 700 °C), the thermal cracking of lignin-derived oligomers, particularly, its larger aromatic systems, was insufficient. However, the extra steam might enhance the cracking through free radical reactions such as H donation, and this reaction can be further enhanced via catalyst (***Chapter 5***). At high temperatures (e.g. > 700 °C), the formation of PAHs through condensation of small aromatic rings and radical reactions (e.g. Diels-Alder-type reaction) became dominated. These PAHs were stable and not easily reformed by steam without catalyst, thus, resulting in the similar tar yields between pyrolysis and non-catalytic steam reforming of lignin-derived oligomers, and smaller yields for the catalytic steam reforming of lignin-derived oligomers (Figure 6-2).

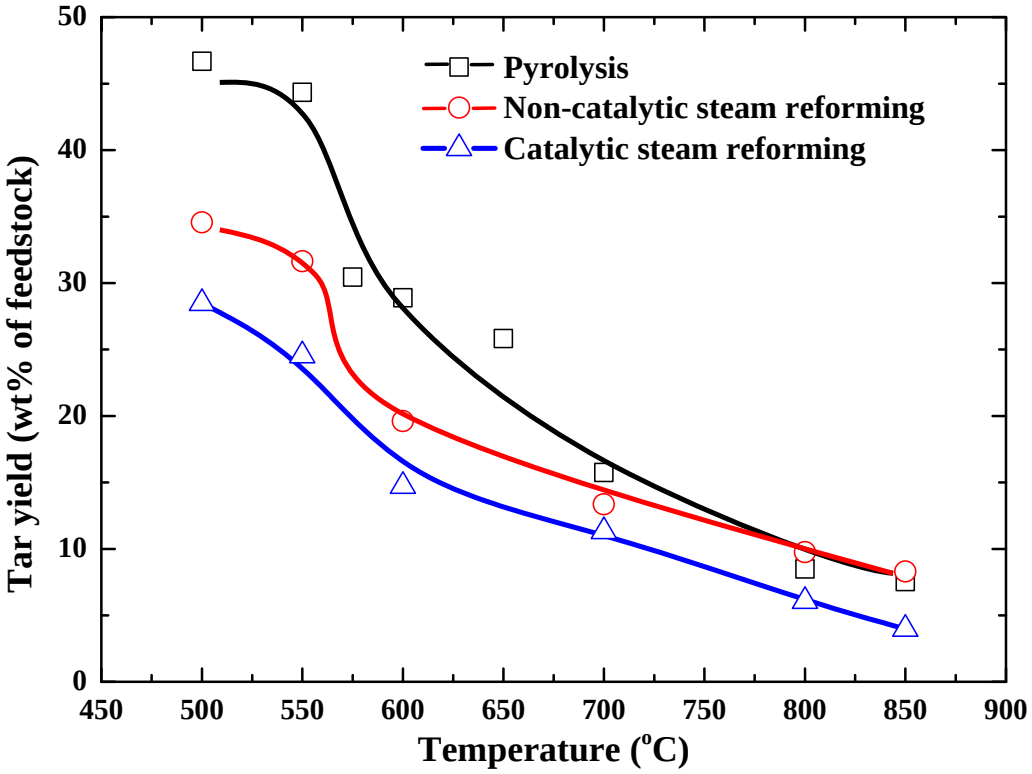

Figure 6-2. Tar yields from lignin-derived oligomers as functions of the pyrolysis, non-catalytic steam reforming and catalytic steam reforming temperature (500-850 °C).

Figure 6-3 presents the synchronous spectra of these tars. The fluorescence intensity is expressed on the basis of "per g of lignin-derived oligomers" to be a reflection of the "yield" of lager aromatic ring systems [14]. The lignin-derived oligomers contain various aromatic ring systems, including large ring systems (more than two rings) with varied functional groups [14, 16, 18]. At low temperatures (e.g. < 700 °C), the thermal cracking of lignin-derived oligomers, particularly, its larger aromatic systems, was insufficient. However, the extra steam might enhanced the cracking through hydrolysis of them, and this reaction can be further enhanced via catalyst (***Chapter 5***). At high temperatures (e.g. > 700 °C), the formation of PAHs through condensation of small aromatic rings and radical reactions (e.g. Diels-Alder-type reaction) became dominated. These PAHs were stable and not easily reformed by steam without catalyst, thus, resulting in the similar tar yields between pyrolysis and non-catalytic steam reforming of lignin-derived oligomers, and smaller yields for the catalytic steam reforming of lignin-derived oligomers

(Figure 6-2). Therefore, the changes observed in the fluorescence intensity show great similarities with that of the tar yields in Figure 6-3.

The shape of the spectra can qualitatively show the aromatic ring size distribution [14]. Similar shapes of the spectra of these tars from the pyrolysis and from the reforming of lignin-derived oligomers at identical temperatures can be observed. This indicates no obvious selectivity to the aromatics from the catalytic steam reforming of lignin-derived oligomers using char-supported iron as a catalyst. The result is in agreement with our previous study for biomass tar reforming [20, 21].

6.3.1.2 Reforming of bio-oil

Figure 6-4 shows the tar yields from bio-oil as a function of the pyrolysis/reforming temperatures between 500 and 850 °C. Part of the data from the pyrolysis of bio-oil has been shown and discussed in ***Chapter 3*** [14]. As expected, the tar yields decreased with increasing temperature. Unlike the obvious differences in the tar yield from the pyrolysis and the non-catalytic steam reforming of lignin-derived oligomers, the extra steam only contributed the effect of further reducing tars from the non-catalytic steam reforming of bio-oil at 500 and 550 °C. It is known that bio-oil contains large portion of water (about 19 wt %), and the cracking of bio-oil constituents may form even more water (e.g. dehydration of some sugar compounds). At low temperatures, the extra steam could enhance the hydrolysis of the organic vapours with the increased contact with steam. However, with increasing temperature, more water could be formed, and "self-reforming" became more effective resulting in similar tar yields between the pyrolysis and the non-catalytic steam reforming of bio-oil. In comparison, the tar yields were further reduced in the whole range of temperatures (500 to 850 °C) by catalytic steam reforming.

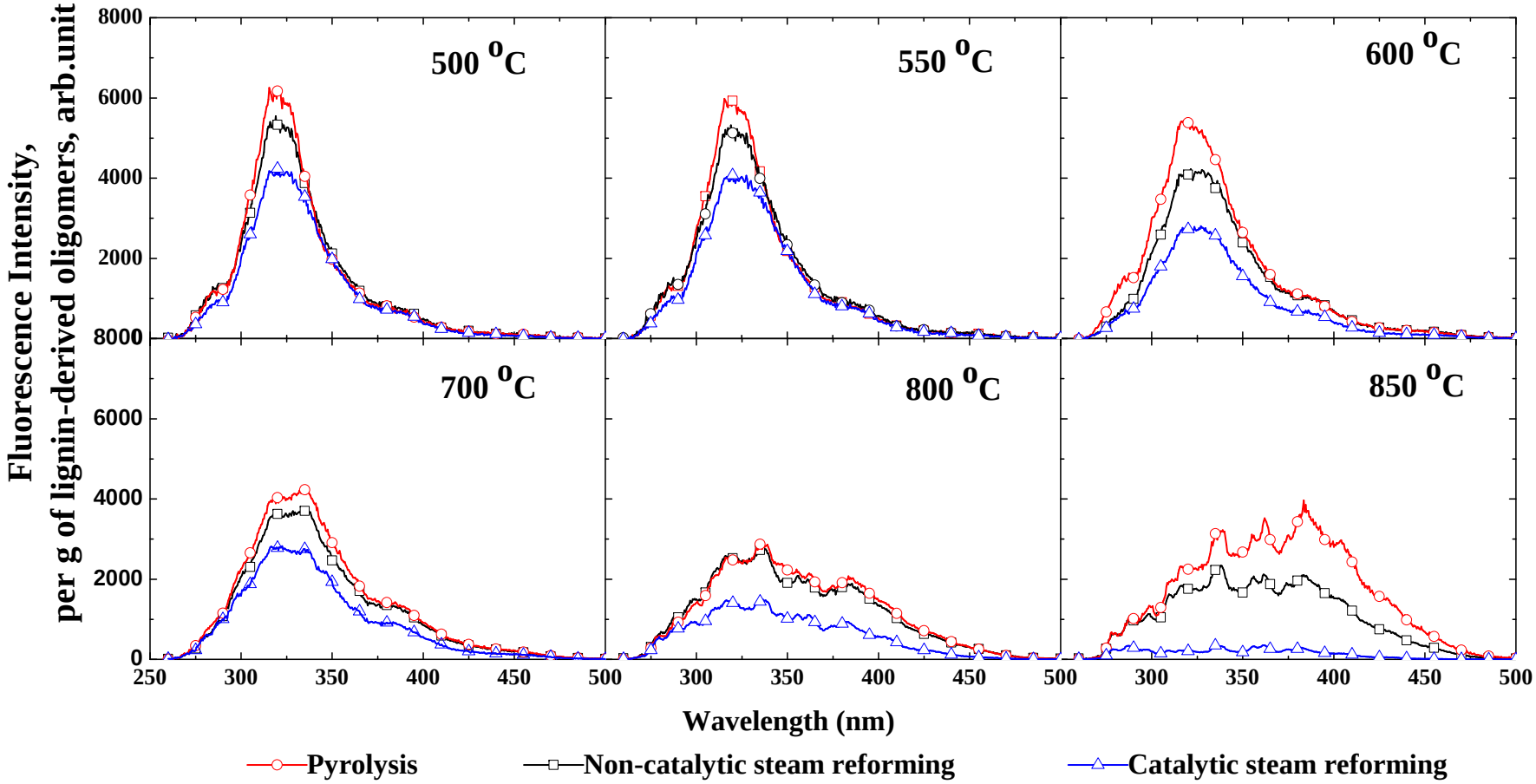

Figure 6-3. Constant energy (-2800 cm^{-1}) synchronous spectra (per g of lignin-derived oligomers) of the tars produced from the pyrolysis, non-catalytic steam reforming and catalytic steam reforming of lignin-derived oligomers at temperatures between 500 and 850 °C.

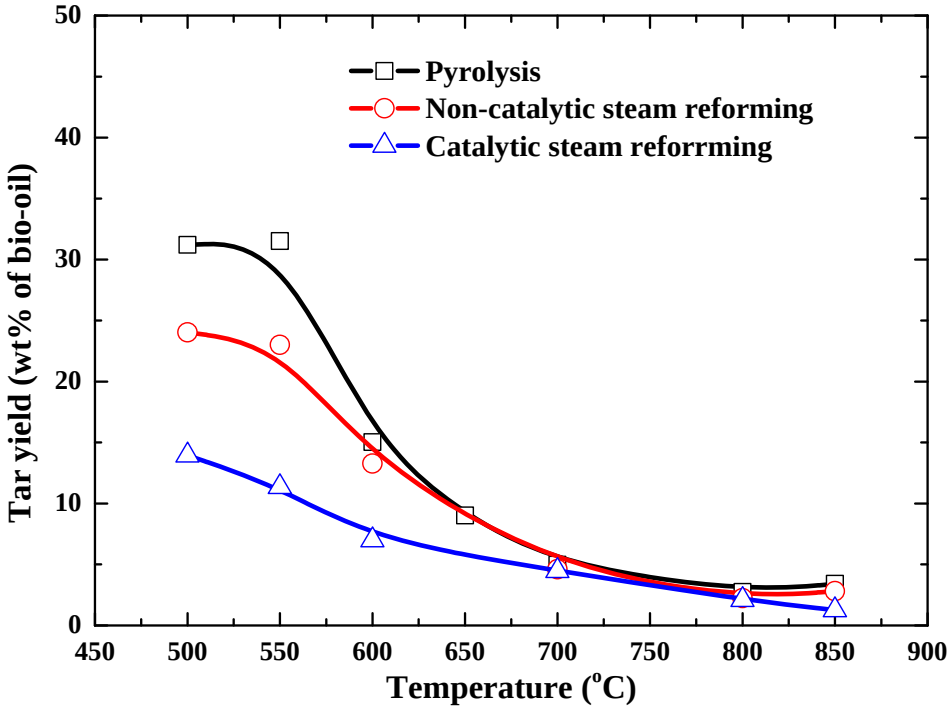

Figure 6-4. Tar yields from bio-oil as functions of the pyrolysis, non-catalytic steam reforming and catalytic steam reforming temperatures (500-850 °C).

The effect of non-catalytic and catalytic steam reforming on reducing aromatic ring systems can be observed from the fluorescence spectra in Figure 6-5. Generally, the decreasing tar yields from the non-catalytic steam reforming and catalytic steam reforming are similar between bio-oil and lignin-derived oligomers, under the experimental conditions used in this study.

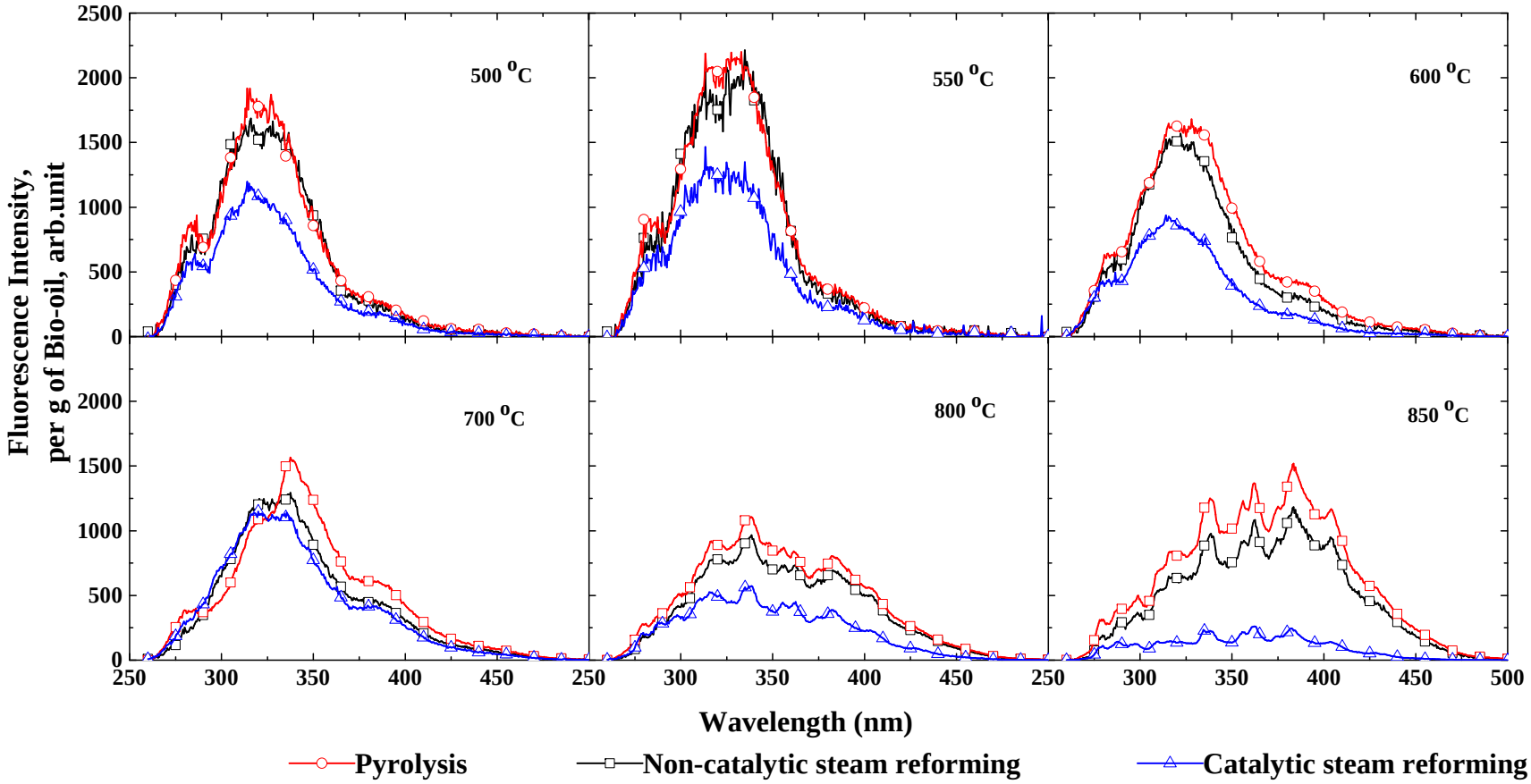

Figure 6-5. Constant energy (-2800 cm^{-1}) synchronous spectra (per g of bio-oil) of the tars produced from the pyrolysis, non-catalytic steam reforming and catalytic steam reforming of bio-oil at temperatures between 500 and 850 °C.

6.3.2 Comparison between the reforming of bio-oil and that of its lignin-derived oligomers

Lignin-derived oligomer fraction contains the majority of large (≥ 2 fused rings) aromatic ring systems in the bio-oil. It showed great similarities during non-catalytic/catalytic steam reforming to the bio-oil from above discussion. However, a large portion of non-aromatic compounds (mainly degraded from cellulose and hemicellulose) in the bio-oil could react with lignin-derived oligomers during the pyrolysis of bio-oil [14]. Consequently, the effects of cellulose/hemicellulose-derived compounds and their interactions with lignin-derived oligomers on the evolution of aromatic ring systems during the reforming of bio-oil are important to be understood. To judge the importance of these interactions during non-catalytic and catalytic steam reforming of bio-oil, calculations based on the data obtained from the UV-fluorescence spectroscopy of the tars produced from bio-oil and lignin-derived oligomers were carried out.

Firstly, a factor reflecting the sole performance of steam or catalyst on the evolution of the aromatics was calculated by dividing the intensity of the tar from the non-catalytic or catalytic steam reforming of lignin-derived oligomers with that from the pyrolysis of lignin-derived oligomers at same temperatures at each wavelength (equation 1).

$$Factor_{\text{steam or catalyst}} = \frac{\text{Intensity of the tar from RE or CRE of lignin-derived oligomers}}{\text{Intensity of the tar from pyrolysis of lignin-derived oligomers}} \quad (1)$$

Where RE means non-catalytic steam reforming and CRE means catalytic steam reforming.

By multiplying this factor with the intensity of the tar from the pyrolysis of bio-oil, it is possible to predict the intensity of the tar from the non-catalytic or catalytic steam reforming of bio-oil at each wavelength (equation 2).

$$\text{Intensity}_{\text{predicted}} = \text{Factor} * \text{Intensity of the tar from pyrolysis of bio-oil} \quad (2)$$

This prediction is based on the assumption that there is no interaction between lignin-derived oligomers and the cellulose/hemicellulose-derived compounds with the introduction of steam or catalyst. Therefore, information about any occurring interactions can be obtained by comparing the predicted results with the corresponding experimental results.

6.3.2.1 Interactions during the non-catalytic reforming of bio-oil

Figure 6-6 shows the synchronous spectra of the tars from the non-catalytic steam reforming of bio-oil at temperatures between 500 and 850 °C and the corresponding predicted spectra based on those of lignin-derived oligomers. Although the experimental and predicted results show great similarities, it can be observed that some differences exist between these spectra at higher temperatures (≥ 600 °C).

At 500 and 550 °C, the spectra from experimental and predicted results are almost identical, indicating the limited effects of interactions on the evolution of aromatic ring systems with the extra steam supply. At these temperatures, the extra steam could not effectively enhance the cracking of cellulose/hemicellulose-derived compounds to form more radicals, and no more aromatics were formed directly by these compounds reacting with steam (***Chapter 5***).

At 600 and 700 °C, the spectra of experimental results show slightly higher intensity at wavelengths < 350 nm, but slightly lower intensity at wavelengths >350 nm, indicating that more aromatics with 1-3 rings but fewer ones with >3 rings are present in the tars obtained from the actual experiments. At these temperatures, very limited amounts of aromatics were formed from reactions between cellulose/hemicellulose-derived compounds and steam (***Chapter 5***). But, the enhanced steam reactivity could make cellulose/hemicellulose-derived compounds to form more radicals. These radicals could then improve the cracking of large aromatic structures into smaller ones (e.g. via ring opening by H radical), or prevent the large aromatic ring systems from forming from the nascent volatiles.

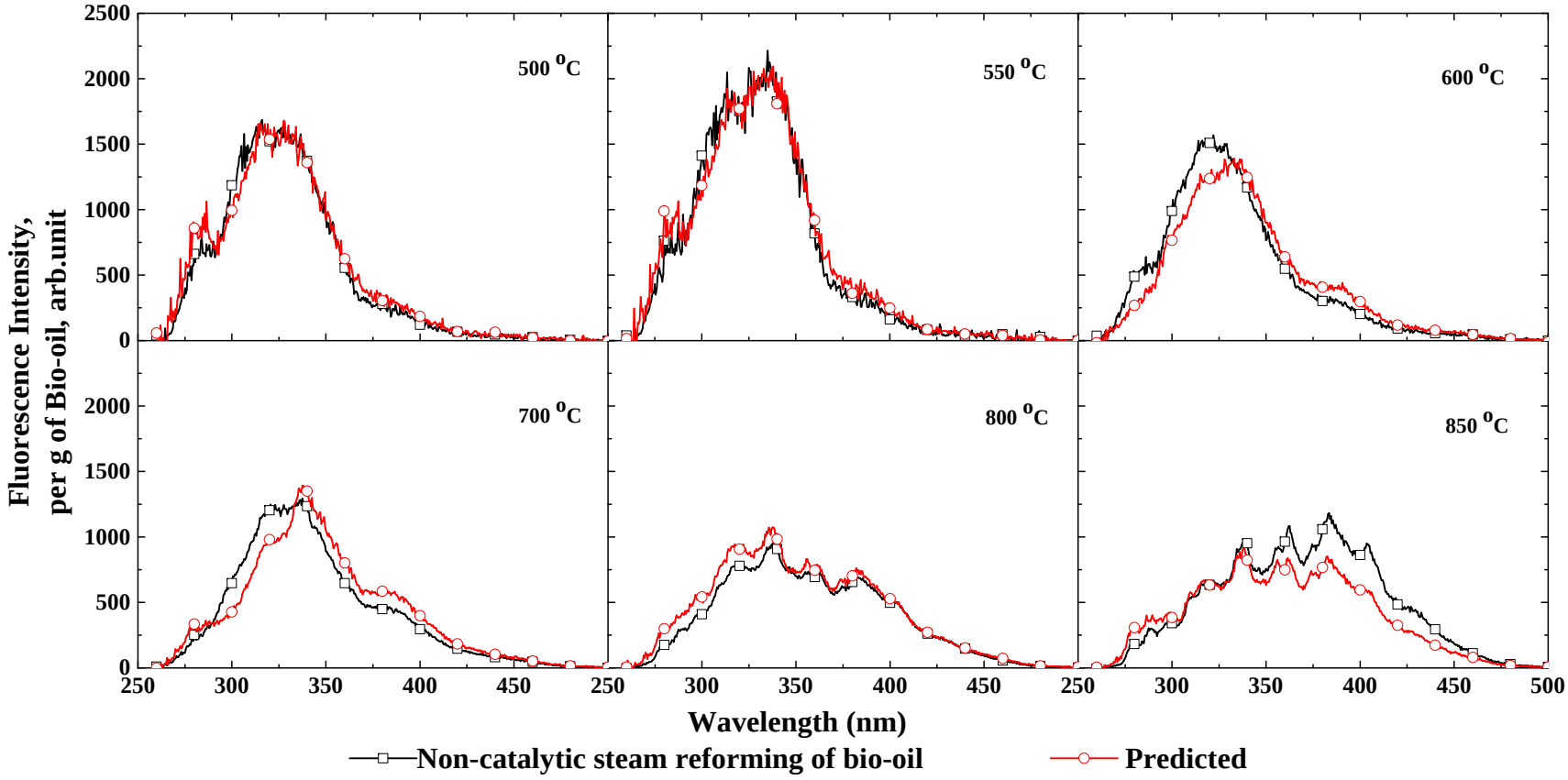

Figure 6-6. Constant energy (-2800 cm^{-1}) synchronous spectra (per g of bio-oil) of the tars produced from the non-catalytic steam reforming of bio-oil and their predicted spectra (calculated using equations 1 and 2) at temperatures between 500 and 850 °C.

With increasing temperature, more aromatic ring systems could be formed from cellulose/hemicellulose-derived compounds. However, the steam reforming of aromatics, especially of smaller ones, was intensified. Therefore, the additional but relatively smaller aromatic ring systems from cellulose/hemicellulose-derived compounds could be reformed at 800 °C, resulting in slightly lower intensities from experimental result at wavelengths <350 nm. In comparison, additional very large aromatic ring systems from cellulose/hemicellulose-derived compounds could be formed at 850 °C, which were stable under steam reforming, resulting in higher intensities at wavelengths >350 nm.

6.3.2.2 Interactions during the catalytic reforming of bio-oil

Figure 6-7 shows the synchronous spectra of the tars from the catalytic steam reforming of bio-oil at temperatures between 500 and 850 °C and the corresponding predicted spectra based on those of lignin-derived oligomers. The obvious contrast to the non-catalytic reforming results (Figure 6-6) is the difference between the experimental and predicted spectra at low temperatures (500 and 550 °C).

At 500 and 550 °C, the predicted intensities at wavelengths (> 350 nm) are higher than that from experiments, indicating that the presence of cellulose/hemicellulose-derived compounds could suppress the formation of larger aromatic ring systems during the catalytic steam reforming of bio-oil. As is discussed in ***Chapter 5***, although the char-support iron catalyst could enhance the formation of small aromatic ring systems (e.g. single ring) during reforming of cellulose-derived compounds in steam, the yields of aromatics were very low. More importantly, the presence of catalyst improved the conversion of cellulose-derived compounds to enrich the amount of radicals. Therefore, during the catalytic steam reforming of bio-oil, with abundant radicals from reforming of cellulose/hemicellulose-derived compounds, the formation of larger aromatic ring systems (> 350 nm) could be suppressed either by cracking into smaller ones or combination into further larger ones such as coke. However, at 500 and 550°C, the cracking of larger aromatic ring systems is very limited. Additionally, there is no obvious difference in intensities at

wavelengths around 325 nm between them, indicating no more single rings in the experimental results. Therefore, the most possible suppression way is the combination of aromatic ring systems to form coke.

At 600 and 700 °C, the further enhanced catalytic steam reforming of cellulose/hemicellulose-derived compounds not only formed relatively smaller aromatic ring systems but also released more radicals, resulting in obvious dissimilarity between the experimental and predicted spectra at wavelengths lower than 350 nm.

At even higher temperatures (800 and 850 °C), the additional very large aromatic structures could be contributed directly from cellulose/hemicellulose-derived compounds.

6.3.3 Changes in the char structural features of char-supported iron catalyst

Figure 6-8 shows the total Raman peak area in the region of 800 ~ 1800 cm^{-1} of the char-supported catalysts. It can be seen, at temperatures < 700 °C, the catalysts after catalytic steam reforming of bio-oil have higher total Roman peak area than those after catalytic steam reforming of lignin-derived oligomers. This can be taken as an indication that there were higher concentrations of O-containing radicals (or other reactive species) during the reforming of the former than that of the latter. These O-containing radicals/species are due to the reforming/cracking of abundant reactive O-containing structures derived from cellulose/hemi-cellulose.

At temperatures > 800 °C, these O-containing structures derived from cellulose/hemi-cellulose must have been rapidly cracked/reformed to light gases including CO, CO_2 and H_2. In other words, their rapid cracking/reforming minimised their chance to interact with the char-supported catalysts. This results in a slightly lower total peak area of used catalysts than that of the fresh one.

Raman spectra of different chars were curve fitted using ten Gaussian bands, and the representative of each band can be found elsewhere [22, 23]. Figure 6-9 shows the band intensity ratio $I_D/I_{GR+VL+VR}$ as a function of different catalytic steam reforming temperature. The $I_D/I_{GR+VL+VR}$ ratios of chars after have been used as catalysts were larger than that of fresh catalyst.

At lower temperatures (500-600 °C), the direct consumption of small aromatic ring systems by steam gasification was limited. However, the species from thermal cracking of bio-oil and lignin-derived oligomers could be adsorbed on the catalyst surface. Subsequently, these compounds bonded with char, possibly forming new aromatic ring structures to increase the portion of larger aromatic ring systems via many reactions, such as dehydration and free radical reactions. The regeneration of aromatic ring systems would increase the larger ring systems at the expense of decrease the smaller ring systems, resulting in the increase in the $I_D/I_{GR+VL+VR}$ ratios than the fresh catalyst.

At higher temperatures (700-850 °C), the $I_D/I_{GR+VL+VR}$ ratio increased with increasing temperature. Besides the enhanced steam gasification of small aromatics, the small aromatic rings could be rearranged into large aromatic rings activated by radicals from enhanced cleavage. In addition, the large aromatics, such as nascent coke, could condense on the catalyst surface to increase the portion of large aromatic ring systems.

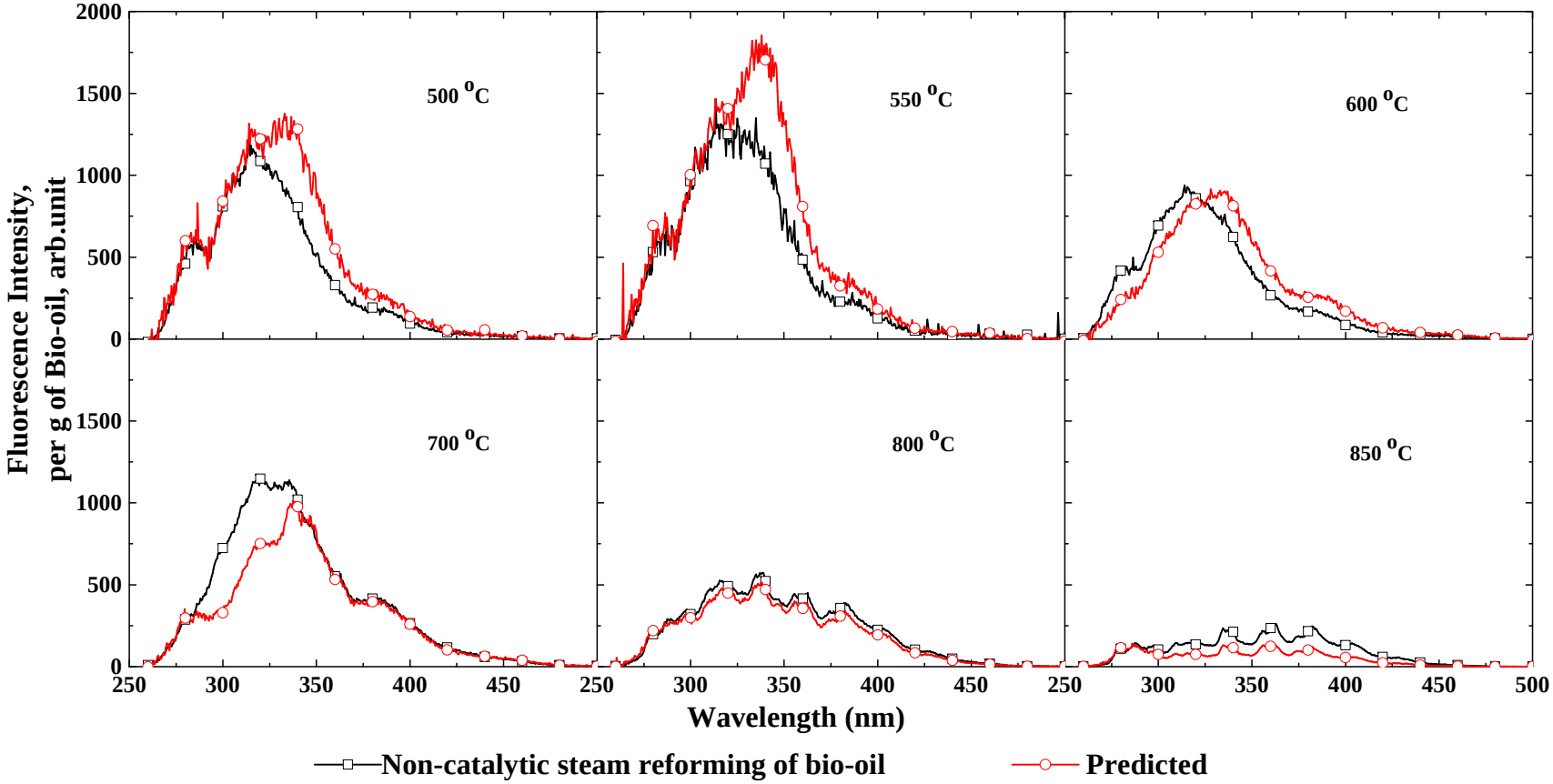

Figure 6-7. Constant energy (-2800 cm^{-1}) synchronous spectra (per g of bio-oil) of the tars produced from the catalytic steam reforming of bio-oil and their predicted spectra (calculated using equations 1 and 2) at temperatures between 500 and 850 °C.

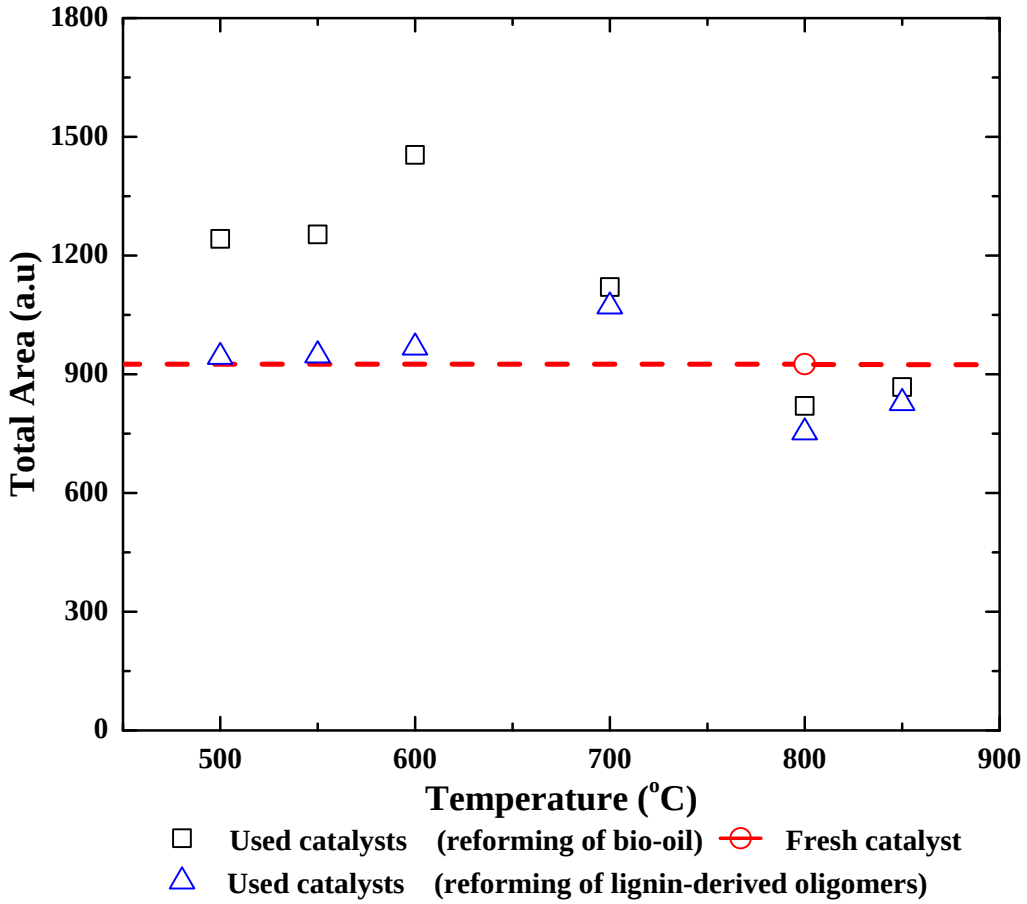

Figure 6-8. Total Raman peaks area (800 -1800 cm^{-1}) of chars after being used in the steam reforming of bio-oil and lignin-derived oligomers at different temperatures (500-850 °C).

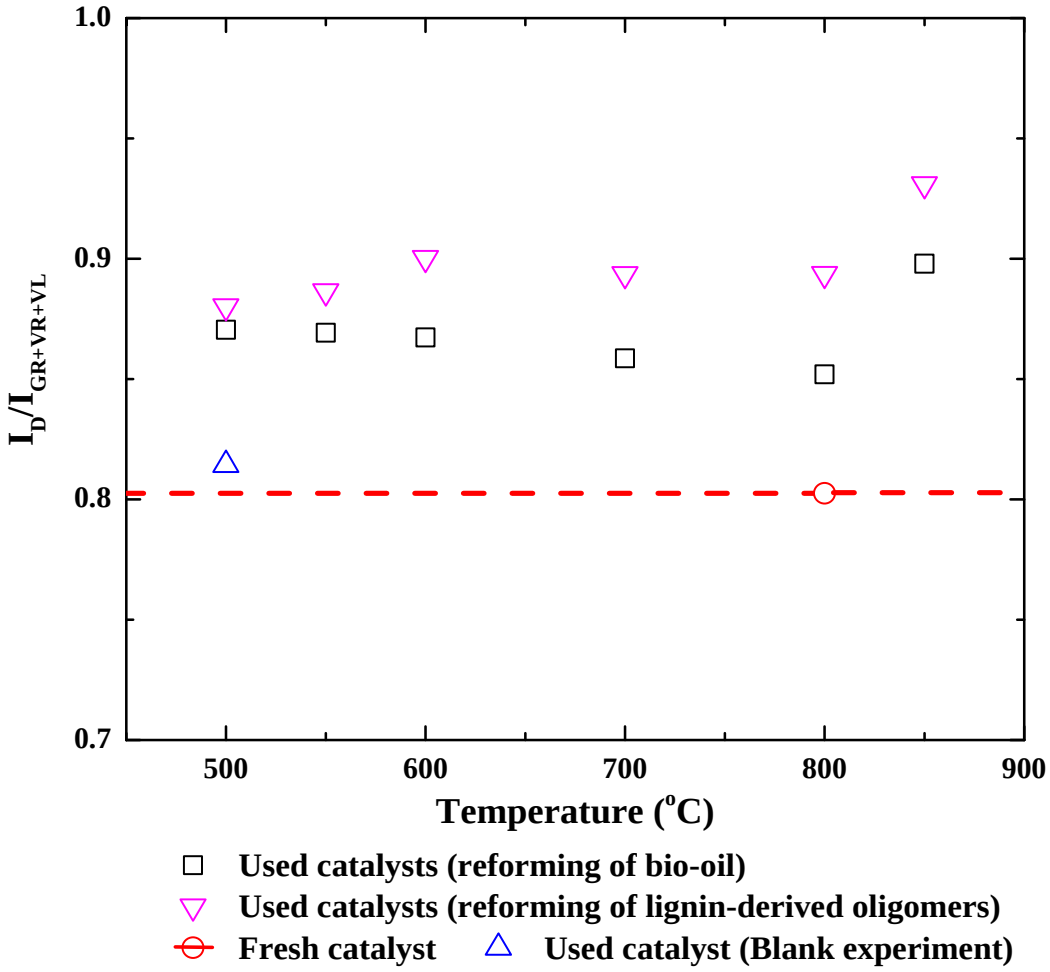

Figure 6-9. The ratio of $I_D/I_{(GR+VL+VR)}$ of chars used as catalysts in the steam reforming of bio-oil and lignin-derived oligomers at different temperatures (500-850 °C). (Blank experiment: No feedstock)

6.4 Conclusions

The pyrolysis, steam reforming and catalytic steam reforming of mallee wood bio-oils and its lignin-derived oligomers were conducted in a quartz reactor at various temperatures (500 to 850 °C). The product tars were quantified and characterised with ultraviolet fluorescence spectroscopy. The lignin-derived oligomers, containing the majority of larger aromatic ring systems in the bio-oil, showed similarities with the bio-oil in many aspects during the reforming process. However, the differences in the evolution of aromatics were presented in the further quantitative process. The results from this study indicate that catalyst showed better performance on reduction of aromatics, particularly the larger ones, during steam reforming of the bio-oil at lower temperatures (< 700 °C). With the information of the changes in the char structures of the catalyst, the results indicated that more radicals could be formed from cellulose/hemicellulose-derived compounds, and these radicals could easily react with larger aromatics. Meanwhile, more coke formed from the lignin-derived oligomers could reduce the activity of the catalyst. With an increasing temperature (> 700°C), the influence of the interaction became weaker during the catalytic steam reforming of the bio-oil.

6.5 References

[1] D. Chiaramonti, A. Oasmaa, Y. Solantausta, Power generation using fast pyrolysis liquids from biomass, Renewable and Sustainable Energy Reviews, 11 (2007) 1056-1086.

[2] S. Iborra, G. Huber, Synthesis of transportation fuels from biomass: chemistry, catalysts, and engineering, Chemical reviews, 106 (2006) 4044-4098.

[3] D.C. Elliott, A. Oasmaa, Catalytic hydrotreating of black liquor oils, Energy & Fuels, 5 (1991) 102-109.

[4] X. Li, R. Gunawan, C. Lievens, Y. Wang, D. Mourant, S. Wang, H. Wu, M. Garcia-Perez, C.-Z. Li, Simultaneous catalytic esterification of carboxylic acids and acetalisation of aldehydes in a fast pyrolysis bio-oil from mallee biomass, Fuel, 90 (2011) 2530-2537.

[5] D. Wang, S. Czernik, D. Montané, M. Mann, E. Chornet, Biomass to hydrogen via fast pyrolysis and catalytic steam reforming of the pyrolysis oil or its fractions, Industrial and Engineering Chemistry Research, 36 (1997) 1507-1518.

[6] M.P. Aznar, J. Corella, J. Delgado, J. Lahoz, Improved steam gasification of lignocellulosic residues in a fluidized bed with commercial steam reforming catalysts, Industrial and Engineering Chemistry Research, 32 (1993) 1-10.

[7] J.R. Galdámez, L. García, R. Bilbao, Hydrogen production by steam reforming of bio-oil using coprecipitated ni−al catalysts. Acetic Acid as a Model Compound, Energy & Fuels, 19 (2005) 1133-1142.

[8] S. Czernik, R. French, C. Feik, E. Chornet, Hydrogen by catalytic steam reforming of liquid byproducts from biomass thermoconversion processes, Industrial and Engineering Chemistry Research, 41 (2002) 4209-4215.

[9] R.M. Navarro, M.A. Peña, J.L.G. Fierro, Hydrogen production reactions from carbon feedstocks: Fossil fuels and biomass, Chemical reviews, 107 (2007) 3952-3991.

[10] A.G. Gayubo, B. Valle, A.T. Aguayo, M. Olazar, J. Bilbao, Pyrolytic lignin removal for the valorization of biomass pyrolysis crude bio-oil by catalytic transformation, Journal of Chemical Technology & Biotechnology, 85 132-144.

[11] T.A. Milne, N. Abatzoglou, R.J. Evans, Biomass gasifier "tars": their nature, formation, and conversion, in, NERL, Golden, CO, USA, 1998.

[12] D. Mohan, C.U. Pittman, P.H. Steele, Pyrolysis of wood/biomass for bio-oil: a critical review, Energy & Fuels, 20 (2006) 848-889.

[13] D. Mourant, Z. Wang, M. He, X.S. Wang, M. Garcia-Perez, K. Ling, C.-Z. Li, Mallee wood fast pyrolysis: Effects of alkali and alkaline earth metallic species on the yield and composition of bio-oil, Fuel, 90 (2011) 2915-2922.

[14] Y. Wang, X. Li, D. Mourant, R. Gunawan, S. Zhang, C.-Z. Li, Formation of aromatic structures during the pyrolysis of bio-oil, Energy & Fuels, 26 (2012) 241-247.

[15] M. He, D. Mourant, R. Gunawan, C. Lievens, X.S. Wang, K. Ling, J. Bartle, C.-Z. Li, Yield and properties of bio-oil from the pyrolysis of mallee leaves in a fluidised-bed reactor, Fuel. In Press.

[16] M. Garcia-Perez, S. Wang, J. Shen, M. Rhodes, W.J. Lee, C.-Z. Li, Effects of temperature on the formation of lignin-derived oligomers during the fast pyrolysis of mallee woody biomass, Energy & Fuels, 22 (2008) 2022-2032.

[17] M. Garcia-Perez, X.S. Wang, J. Shen, M.J. Rhodes, F. Tian, W.-J. Lee, H. Wu, C.-Z. Li, Fast Pyrolysis of Oil Mallee Woody Biomass: Effect of temperature on the yield and quality of pyrolysis products, Industrial & Engineering Chemistry Research, 47 (2008) 1846-1854.

[18] C.A. Mullen, A.A. Boateng, Characterization of water insoluble solids isolated from various biomass fast pyrolysis oils, Journal of Analytical and Applied Pyrolysis, 90 (2011) 197-203.

[19] B. Scholze, D. Meier, Characterization of the water-insoluble fraction from

pyrolysis oil (pyrolytic lignin). Part I. PY-GC/MS, FTIR, and functional groups, Journal of Analytical and Applied Pyrolysis, 60 (2001) 41-54.

[20] Z. Min, P. Yimsiri, M. Asadullah, S. Zhang, C.Z. Li, Catalytic reforming of tar during gasification. Part II. Char as a catalyst or as a catalyst support for tar reforming, Fuel, 90 (2011) 2545-2552.

[21] Z. Min, M. Asadullah, P. Yimsiri, S. Zhang, H. Wu, C.-Z. Li, Catalytic reforming of tar during gasification. Part I. Steam reforming of biomass tar using ilmenite as a catalyst, Fuel, 90 (2011) 1847-1854.

[22] X. Li, J.-i. Hayashi, C.-Z. Li, Volatilisation and catalytic effects of alkali and alkaline earth metallic species during the pyrolysis and gasification of Victorian brown coal. Part VII. Raman spectroscopic study on the changes in char structure during the catalytic gasification in air, fuel, 85 (2006) 1509-1517.

[23] X. Li, J.-i. Hayashi, C.-Z. Li, FT-Raman spectroscopic study of the evolution of char structure during the pyrolysis of a Victorian brown coal, Fuel, 85 (2006) 1700-1707.

Chapter 7

Conclusions and recommendations

7.1 Introduction

The purpose of the study is to gain fundamental understanding on the chemical behaviour of bio-oil in its pyrolysis and reforming processes. The product tar and coke from the bio-oil and its components were quantified, and the chemical compositions of the product tar were analysed. Many possible reactions, including the interactions among different bio-oil components, were presented to explain the evolution of the bio-oil during pyrolysis or reforming processes. Char-supported catalysts were used for the reforming of bio-oil with steam. Characterizations of fresh and used catalysts were analysed and discussed. The main conclusions from the present study are listed below.

7.2 Conclusions

7.2.1 Formation of aromatic structures during the pyrolysis of bio-oil

- The majority of larger (≥ 2 rings) aromatic ring systems as detected by UV-fluorescence spectroscopy are in the lignin-derived oligomers.
- Significant portions of aromatic ring systems in the bio-oil could turn/polymerise into solids not soluble in $CHCl_3$+CH_3OH during the pyrolysis at relatively low temperatures e.g. 350-400 °C.
- The presence of cellulose/hemicellulose-derived species in the bio-oil could enhance the polymerisation reactions at lower temperatures.
- The pyrolysis of cellulose-derived species in the bio-oil at high temperatures (e.g. > 700 °C) tended to form additional very large aromatic ring systems.

7.2.2 Formation of coke during the pyrolysis of bio-oil

- The coke formation can directly from the bio-oil and its different fractions, such as species in the water-soluble and lignin-derived oligomers.

- Significant portions of lignin-derived oligomers in the bio-oil could turn/polymerise into coke during the pyrolysis at relatively low temperatures e.g. 250-400°C. This process can be enhanced by the presence of cellulose/hemicellulose-derived species in the bio-oil, which are reactive and produce radicals to enhance the polymerisation reactions.
- The interactions between the species in the water-soluble fraction and lignin-derived oligomers were suppressed with increasing temperature (e.g. > 450°C) due to the intensified decomposition.
- Self-gasification of coke by the water in the bio-oil and the water (and other species) formed during the re-pyrolysis of bio-oil at high temperature (e.g. > 700°C) may decrease the observed yield of coke.

7.2.3 Catalytic steam reforming of cellulose-derived compounds using a char-supported iron catalyst

- Without catalyst, there is no obvious effect on reforming cellulose-derived tars with extra steam.
- At low temperatures (< 700 °C), compared with aromatic structural systems, the catalytic steam reforming showed better effects on the conversion of non-aromatics (e.g. sugars), particularly large molecules. The dehydration of sugar compounds could be enhanced by the catalytic reforming process.
- Various aromatic ring systems can be formed at high temperatures (≥ 700 °C) from cellulose, and the catalyst was effective on reforming of them with steam.
- O-containing groups in the cellulose-derived compounds were more easily absorbed on the catalyst at lower temperatures (< 700 °C).

7.2.4 Evolution of aromatic structures during the reforming of bio-oil: Importance of the interactions bio-oil components

- The lignin-derived oligomers, containing the majority of larger aromatic ring systems in the bio-oil, showed similarities with the bio-oil in many aspects during the reforming process.
- Compared with the reforming of lignin-derived oligomers, catalyst showed better performance on reduction of aromatics, particularly the larger ones, during steam reforming of the bio-oil at lower temperatures (< 700 °C).
- During reforming of the bio-oil at lower temperatures (< 700 °C), radicals could be formed from cellulose/hemicellulose-derived compounds, which could easily react with larger aromatics originated from lignin. Meanwhile, more coke formed from the lignin-derived oligomers could reduce the activity of the catalyst as well.
- At higher temperatures (> 700°C), the influence of the interaction became weaker during the catalytic steam reforming of the bio-oil.

7.3 Recommendations

1. This study mainly focused on the effect of pyrolysis/reforming temperature on the evolution of chemical compositions of the bio-oil. Other parameters such as pressure, residence time and heating rate can be changed to study the influences of them on the thermal behaviour of bio-oil.

2. Catalytic hydrogenation of bio-oil is a potential way to upgrade bio-oil into chemicals and transportation fuels. The deactivation of catalysts by coke formation has been reported as a major problem in this process. From this study, it is clear that coke could be formed at temperature as low as about 250 °C during the pyrolysis of bio-oil. However, the introduction of H_2 during hydrogenation process may change the reaction pathway to form coke. Therefore, the understanding of involved reactions occurring during the hydrogenation of bio-oil is required.

Appendix I

Permission of Reproduction from

the Copyright Owner

Home | Create Account | Help

Title: Formation of Aromatic Structures during the Pyrolysis of Bio-oil

Author: Yi Wang, Xiang Li, Daniel Mourant, Richard Gunawan, Shu Zhang, and Chun-Zhu Li

Publication: Energy & Fuels

Publisher: American Chemical Society

Date: Jan 1, 2012

User ID

Password

Enable Auto Login

LOGIN

Forgot Password/User ID?

If you're a copyright.com user, you can login to RightsLink using your copyright.com credentials.

Already **a RightsLink user** or want to learn more?

PERMISSION/LICENSE IS GRANTED FOR YOUR ORDER AT NO CHARGE

This type of permission/license, instead of the standard Terms & Conditions, is sent to you because no fee is being charged for your order. Please note the following:

- Permission is granted for your request in both print and electronic formats, and translations.
- If figures and/or tables were requested, they may be adapted or used in part.
- Please print this page for your records and send a copy of it to your publisher/graduate school.
- Appropriate credit for the requested material should be given as follows: "Reprinted (adapted) with permission from (COMPLETE REFERENCE CITATION). Copyright (YEAR) American Chemical Society." Insert appropriate information in place of the capitalized words.
- One-time permission is granted only for the use specified in your request. No additional uses are granted (such as derivative works or other editions). For any other uses, please submit a new request.

BACK | CLOSE WINDOW